Tampereen yliopisto

Oona Katajisto

CALCINATION OF CALCIUM CARBONATE BASED MATERIALS IN ELECTRIC HEATED ROTARY KILN

Faculty of Engineering and Natural Sciences
Master of Science Thesis
November 2020

ABSTRACT

Oona Katajisto: Calcination of calcium carbonate based materials in electric heated rotary kiln
Master of Science Thesis
Tampere University
Master's Degree Programme in Mechanical Engineering
November 2020

Current activities to restrain climate change are evaluated to be insufficient to meet the international and national climate targets. Cement industry is one of the main CO_2 emitters in industry sector. Electrification and carbon capture and utilization or storage (CCUS) technologies are seen as potential solutions to reduce greenhouse gas emissions from heavy industries. Traditionally, heat required for cement and lime production is generated by combustion of fossil fuels.

This thesis focuses on potential and effects of deploying electric heating in rotary kilns used in lime and cement production. The thesis consists of two sections. In the first section, literature review is conducted. Lime and cement production processes are introduced. Calcination reaction, lime uses, kiln types and CO_2 emissions and emission reduction methods are discussed. Electric heated kiln concept and its advantages and downsides compared to traditional kiln technologies are presented. Additionally, heat transfer in electric heated kiln is studied. Literature review shows that the main difference of process conditions in the electric heated rotary kiln compared to traditional rotary kiln is high partial pressure of CO_2 in the kiln gases. The main advantages of electric heating are the reduction of energy related emissions, transformation of process emissions into usable product, and easier process control.

In the second section, controlled experiments with laboratory scale electric heated rotary kiln are performed. The objective is to study calcination in CO_2 rich gas atmosphere. Experiments are performed for three different calcium carbonate based materials. Calcination of the raw materials is studied in different gas atmospheres, temperatures and pressures. The results are analyzed with thermogravimetry, differential scanning calorimetry, reactivity measurements, and particle size and dry matter content measurements.

The performed experiments showed promising results for calcination degree and reactivity in CO_2 rich gas atmosphere. However, recarbonation and blockages in the rotary tube caused challenges that require more studying. Recarbonation occurred in experiments in CO_2 rich gas atmosphere both in slight positive pressure relative to atmospheric pressure and in vacuum. Recarbonation can be prevented with rapid cooling and change of gas atmosphere, however the technological solutions need to be studied and tested. Small scale of the kiln used in the experiments is a possible reason for the blockages but it requires confirmation from pilot scale experiments. Measurement range of CO_2 concentration of the gas analyzer used in the experiments was too narrow which affected the evaluation of direct capture potentials. Thus, a more comprehensive analysis of the kiln off-gases is suggested. In further experiments, sintering of the particles need to be considered as well. Additionally, further research on economic feasibility of electric heated rotary kiln is recommended.

Keywords: rotary kiln, electric heating, calcination

TIIVISTELMÄ

Oona Katajisto: Kalsiumkarbonaatti-pohjaisten materiaalien kalsinointi sähkölämmitteisessä kiertouunissa
Diplomityö
Tampereen yliopisto
Konetekniikan DI-tutkinto-ohjelma
Marraskuu 2020

Nykyisten ilmastonmuutosta rajoittavien toimien on arvioitu olevan riittämättömiä kansainvälisten ja kansallisten ilmastotavoitteiden saavuttamiseksi. Sementtiteollisuus on yksi suurimmista teollisuuden toimialan CO_2-päästöjen aiheuttajista. Sähköistäminen sekä hiilidioksidin talteenotto ja hyödyntäminen tai varastointi (CCUS) nähdään potentiaalisina ratkaisuina raskaan teollisuuden kasvihuonekaasupäästöjen vähentämiseen. Perinteisesti sementin ja kalkin valmistuksessa vaadittava lämpö on tuotettu polttamalla fossiilisia polttoaineita.

Tämä työ keskittyy sähkölämmityksen hyödyntämiseen kalkin ja sementin valmistuksessa käytettävissä kiertouuneissa sekä sen tuomiin mahdollisuuksiin ja vaikutuksiin. Työ koostuu kahdesta osasta. Ensimmäinen osuus keskittyy kirjallisuuskatsaukseen. Siinä esitellään kalkin ja sementin tuotantoprosessit. Käsiteltäviä asioita ovat kalsinointireaktio, kalkin käyttökohteet, uunityypit, hiilidioksidipäästöt ja päästövähennyskeinot. Osassa esitellään myös sähkölämmitteinen uunikonsepti ja pohditaan siihen liittyviä hyötyjä ja haasteita perinteiseen uuniin verrattuna. Lisäksi käsitellään sähkölämmitteisen uunin lämmönsiirtoa. Kirjallisuuskatsaus osoittaa, että suurin ero prosessiolosuhteissa sähkölämmitteisen ja perinteisen uunin välillä on hiilidioksidin osapaine uunin kaasuissa. Energiaan liittyvien päästöjen vähentyminen, prosessipäästöjen muuttaminen käyttökelpoiseksi tuotteeksi sekä helpompi prosessin ohjaus ovat sähkölämmityksen suurimpia hyötyjä.

Toisessa osassa esitellään laboratoriomittakaavan sähkölämmitteisellä kiertouunilla toteutetut kontrolloidut kokeet. Kokeiden tavoite on tutkia kalsinoitumista kaasuatmosfäärissä, jossa hiilidioksidin osapaine on korkea. Kokeet suoritettiin kolmelle eri kalsiumkarbonaatti-pohjaiselle materiaalille. Raaka-aineiden kalsinoitumista tutkittiin erilaisissa kaasuatmosfääreissä, lämpötiloissa ja paineissa. Tulosten analysointiin käytettiin termogravimetriaa, differentiaalista pyyhkäisykalorimetriaa, reaktiivisuusmittauksia sekä partikkelikoko- ja kuiva-ainepitoisuusmittauksia.

Suoritetut kokeet osoittavat lupaavia tuloksia kalsinoitumisasteelle ja reaktiivisuudelle kaasuatmosfäärissä, jossa hiilidioksidin osapaine on korkea. Rekarbonoituminen ja tukokset uunissa aiheuttivat kuitenkin ongelmia, jotka vaativat enemmän tutkimusta. Rekarbonoitumista tapahtui kokeissa, jotka suoritettiin hieman ilmanpainetta korkeammassa paineessa sekä kokeissa, jotka suoritettiin vakuumissa. Molemmissa tapauksissa hiilidioksidin osapaine uunin kaasuissa oli korkea. Rekarbonoitumista voidaan estää nopealla jäähdytyksellä ja kaasuatmosfäärin muutoksella, mutta tekniset ratkaisut vaativat vielä tutkimusta ja testausta. Tukosten muodostumiselle mahdollinen syy on uunin pieni koko, mikä pitää varmistaa pilotti-mittakaavan kokeilla. Kaasuanalysaattorin mittausalue hiilidioksidin pitoisuudelle oli liian kapea, mikä vaikutti hiilidioksidin suoran talteenoton mahdollisuuksien arviointiin. Näin ollen ehdotetaan kattavampaa analyysiä uunin poistokaasuista. Partikkeleiden sintraantuminen täytyy myös ottaa huomioon tulevissa kokeissa. Lisäksi jatkotutkimukseksi suositellaan sähkölämmitteisen kiertouunin taloudellisen kannattavuuden tarkastelua.

Avainsanat: kiertouuni, sähkölämmitys, kalsinointi

PREFACE

This Master's thesis is part of Decarbonate project which aim is to reduce CO_2 emissions in several industries by developing and commercializing carbon capture and utilization (CCU) technologies. The project is co-financed by Business Finland, VTT and partner companies.

I want to thank Eemeli Tsupari from VTT for excellent guidance and support in this thesis, and also Antti Pasanen from VTT for guidance with the experimental section. From Tampere University, I want to give thanks to Jukka Konttinen and Henrik Tolvanen for helpful advices and comments to this thesis. I am also grateful for all my colleagues at VTT who gave advices and support during this project.

Also, huge thanks goes to my friends, Vilja, Minna, Elina, Peppiina and Tiina - you made the whole journey worth remembering. Finally, I want to give the greatest thanks to my family and Jesse for always being supportive and encouraging.

Tampere, 4.11.2020

Oona Katajisto

CONTENTS

LIST OF FIGURES

LIST OF TABLES

LIST OF SYMBOLS AND ABBREVIATIONS

ASK	Annular shaft kiln
CCUS	Carbon capture and utilisation or storage
CRS	Central Receiver Systems
DSC	Differential scanning calorimetry
ECRA	European Cement Research Academy
EU ETS	The EU emissions trading system
GHG	Greenhouse gas
HPSK	High performance shaft kiln
IEA	International Energy Agency
IPCC	The Intergovernmental Panel on Climate Change
LEILAC	Low Emissions Intensity Lime and Cement
LRK	Long rotary kiln
MFSK	Mixed feed shaft kiln
OBASK	Annular shaft kiln with opposite burners
PFRK	Parallel flow regenerative lime kiln
PRK	Rotary kiln with pre-heater
RFG	Recycled flue gas
SNG	Synthetic natural gas
TG	Thermogravimetry
TGA	Thermogravimetric analysis
UNFCCC	United Nations Framework Convention on Climate Change
VOC	Volatile organic compounds
XRD	X-ray powder diffraction
P_{eq}	equilibrium partial pressure of CO_2
T	temperature

1. INTRODUCTION

Climate change is constantly raising increasing concern in societies. Many international and national strategies have been set to restrict human-induced changes in climate, one of which is Paris Agreement between the parties of United Nations Framework Convention on Climate Change (UNFCCC). The aim of the agreement is to limit global warming below 2 °C, preferably below 1.5 °C (United Nations 2015). Paris Agreement came into effect in November 2016 and to date 189 of 197 parties have ratified the agreement (UNFCCC 2020). Europe has also introduced a growth strategy called European Green Deal to make Europe climate-neutral in 2050 and to advance sustainable economy (European Commission 2019). Main actions to achieve the targets are development of clean and secure energy system in which the role of renewable energy sources is vital, supporting industry towards innovations and circular economy, and ensuring energy and recourse efficient building and renovating (European Commission 2019). Europe Union also promotes power, industry and aviation sector to invest in low-carbon technologies with the EU emissions trading system (EU ETS). EU ETS is a 'cap and trade' system which sets a limit for the total emissions released from installations and aircraft operators. EU ETS is one of the main actions of the European Union to reach the emission reduction targets. (European Commission 2015) National climate goals of Finland are also in accordance with the international and EU level goals. In the Government Programme (Valtioneuvosto 2019), a carbon neutral Finland in 2035 is set as a target, and climate law and emission reduction measures will be reformed to meet the target.

Despite several ongoing international and national projects to restrain climate change, The Intergovernmental Panel on Climate Change (IPCC) has evaluated in its special report (Rogelj *et al.* 2018, p. 159) that the planned actions are not enough to reach the goal of Paris Agreement and rapid greenhouse gas (GHG) emission reductions are needed. Industry sector is one of the main emitters of carbon dioxide (CO_2). In the European Green Deal communication (European Commission 2019) is recognized that the transition towards sustainable industry sector is too slow. According to Pales et al. (2019), direct CO_2 emissions from industry sector covered 24 % of global CO_2-emissions in 2017. The main industrial product for CO_2 emissions is cement which production caused 6.2 % of global CO_2-emissions in 2017 (Pales *et al.* 2019).

CO_2 emissions from lime and cement production can be divided into process emissions and energy related emissions. The process emissions from lime and cement production are generated in calcination of calcium carbonate ($CaCO_3$). Calcium carbonate occurs in nature in limestone. In this work, calcination refers to thermal decomposition of calcium carbonate into calcium oxide (CaO) and carbon dioxide. Calcination is carried out in cement plants and dedicated lime kilns in which the heat is traditionally generated by combustion of fossil fuels. Over 50 % of total CO_2-emissions are released from calcination and around 40 % originate from combustion. (Lehne & Preston 2018; CEMBUREAU 2018) In addition to cement, calcium oxide which in general is called lime is used in many applications. In this thesis the focus is on cement, lime mud (used in pulp production) and lime in the raw.

Actions to reduce CO_2 emissions have already been planned and put into practice. Examples of the actions already taken or under development in lime and cement industries are improvements in energy efficiency of the kilns and use of alternative fuels such as biomass and waste-derived fuels (Lehne & Preston 2018; CEMBUREAU 2018). In addition, more novel techniques are under development, one of which is indirect heating connected with carbon capture and utilization or storage (CCUS). Conventionally, limestone is heated directly with flame and flue gases generated by combustion of fuels. In an ongoing project called Low Emissions Intensity Lime and Cement (LEILAC) indirect heating of limestone is demonstrated. With indirect heating the emissions from calcination will be pure CO_2 and can relatively simply be captured as the flue gases from the combustion are kept separate. (LEILAC 2017) LEILAC project has showed promising results and consequently LEILAC 2 project is established to continue the research. In LEILAC 2, multiple fuel sources, particularly electricity, will be piloted and also retrofitting of an existing cement plant with the new indirectly heated kiln technology will be demonstrated. (CORDIS 2020) In recent report by International Energy Agency (IEA), ways to achieve clean energy systems with zero-emissions were presented and assessed. Energy and material efficiency and renewable energy sources are immediate options to reduce CO_2 emissions. Additionally, four critical technology opportunities were acknowledged: electrification of transport, industry and buildings sectors, development and implementation of CCUS systems, shift towards hydrogen and hydrogen-derived synthetic fuels, and use of more sustainable alternative fuels and feedstock such as bioenergy. (IEA 2020b)

This thesis is part of a larger project called Decarbonate which object is to commercialize new concepts of CCUS in various industries (Decarbonate 2020). In this thesis, the focus is on electric heated rotary kiln for lime and cement production. Heat will be generated

with electricity instead of fuel combustion to minimize energy-related emissions. Additionally, in LEILAC project the kiln is vertical whereas the kiln studied in this thesis is horizontal rotary kiln (LEILAC 2017). The objective of the thesis is to study calcination in electric heated rotary kiln, and recognize the advantages and challenges related to the technology to improve the kiln concept and design and recognize the further experiment needs. Research questions of the thesis are:

1. Which factors and mechanisms affect calcination reaction in rotary kiln?
2. What are the advantages of electric heated rotary kiln compared to traditional rotary kilns?
3. What are the challenges related to calcination in electric heated rotary kiln?
4. How does the calcination degree of the studied products achieved by the electric heated rotary kiln correspond to the present industrial lime based products?
5. How does the reactivity of the studied products calcined in the electric heated rotary kiln correspond to the reactivity of present industrial lime based products?

In Figure 1, the progression of the thesis, research methods and results are illustrated. Research methods used in this thesis are literature review and controlled experiments.

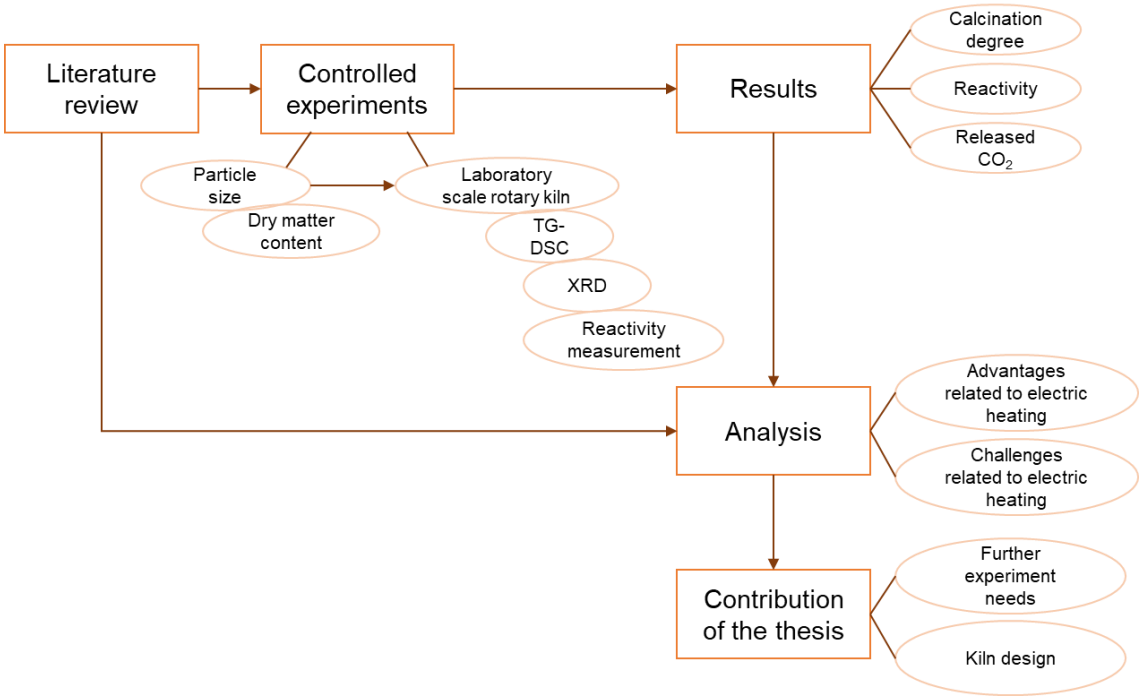

Figure 1. *Progression of the thesis, research methods and results*

Chapters 2 and 3 compose the theoretical background of the thesis. In chapter 2 production of lime and cement is discussed. First, the production processes of lime and cement are introduced. They are divided into separate subchapters as there are some major differences in the processes. In chapter 2.2 calcination reaction and the contributing factors are examined in more detail. In this chapter, the research question 1 is answered. Next, lime uses are presented. In this chapter as well, cement is discussed in separate subchapter and other main uses in other. Modern lime kiln types are introduced and horizontal and vertical kiln types are compared in chapter 2.4. Lastly, emissions and emission reduction methods are discussed. Electrification and CCUS technologies are highlighted by introducing them in separate subchapters. In chapter 3 the electric heated lime kiln concept is discussed. First, the concept is presented and advantages and downsides compared to traditional rotary kilns are examined. Research questions 2 and 3 are answered. In chapter 3.2 heat transfer in electric heated rotary kiln and challenges associated with it are discussed.

Controlled experiments are discussed in chapter 4. The controlled experiments are planned based on the results and observations from the literature review. Calcination is demonstrated with a laboratory scale electric heated rotary kiln. It is presented in more detail in chapter 4.1. Analytic methods such as thermogravimetry (TG), differential scanning calorimetry (DSC) and X-ray powder diffraction (XRD) are used in analysis. Additionally, measurements of reactivity, particle size and dry matter content are performed. All used analytic methods are discussed in chapter 4.2. Next, the test matrix for the experiments with laboratory scale rotary kilns is introduced. Lastly, parameters and boundaries of the experiments are discussed. In chapter 5, results of the experiments are presented and research questions 4 and 5 are answered. Calcination degree, reactivity and CO_2 content in the kiln of gases are all discussed in separate subchapter. Subchapter 5.4 consists of overall discussion of the results and their limitations. Based on the experiments with the laboratory scale rotary kiln and the results, answer is given to research question 3. Finally, in conclusions significance of the results and proposals for further research requirements are discussed.

2. PRODUCTION OF LIME AND CEMENT

Calcium oxide, generally called lime, is one of the earliest building materials, and nowadays it is widely utilized for different purposes. The raw material for lime products is naturally occurring limestone. The main component of limestone is calcite which consists of calcium carbonate. Earth's crust contains on average more than 4 % of calcium carbonate. (Stork *et al.* 2014; Kumar *et al.* 2007)

Some limestone deposits consist almost entirely of calcium carbonate containing impurities less than 5 % (Oates 1998). However, limestone deposits with high content of calcium carbonate are rare and usually the amount of impurities is in the range of 3–35 % (Stork *et al.* 2014; Kumar *et al.* 2007). Limestone deposits are found around the world but physical and chemical properties of the limestone vary between deposits from different locations (Piringer 2017, p. 91). In addition, there are other kinds of lime products such as magnesium containing dolomitic lime (also known as dolime, CaO•MgO). Raw material for dolomitic lime is dolomite ($CaCO_3$•$MgCO_3$). (Stork *et al.* 2014; Kumar *et al.* 2007) However, in this thesis only lime products derived from limestone are concerned.

The annual lime production was estimated by Apodaca (2020) to be approximately 424.6 Mt. The production by country in 2019 is presented in Figure 2. The Figure 2 only includes countries which lime production was over 2 Mt in 2019. China is by far the biggest producer of lime as its production covers over 70 % of the global production in 2019 (Apodaca 2020). Lime industry is located in the beginning of value chain, and thus lime market is significantly influenced by the industries which use lime as a raw material (Piringer 2017; Stork *et al.* 2014). In addition to large international lime producers, there are many small companies operating on local markets. This challenges the data gathering of lime production. (Dowling *et al.* 2015, p. 14) Limestone is also an important raw material in pulp and cement production but as lime is only an intermediate product in these processes it is not included in the data presented in Figure 2.

In the first section of this chapter, lime and cement production processes are discussed after which calcination reaction is studied in more detail in second section. Lime applications are discussed in third part which is divided into two sections, main uses and cement. In fourth section, different kiln types are presented. Lastly, CO_2 emissions generated in the lime and cement production and potential reduction techniques are examined.

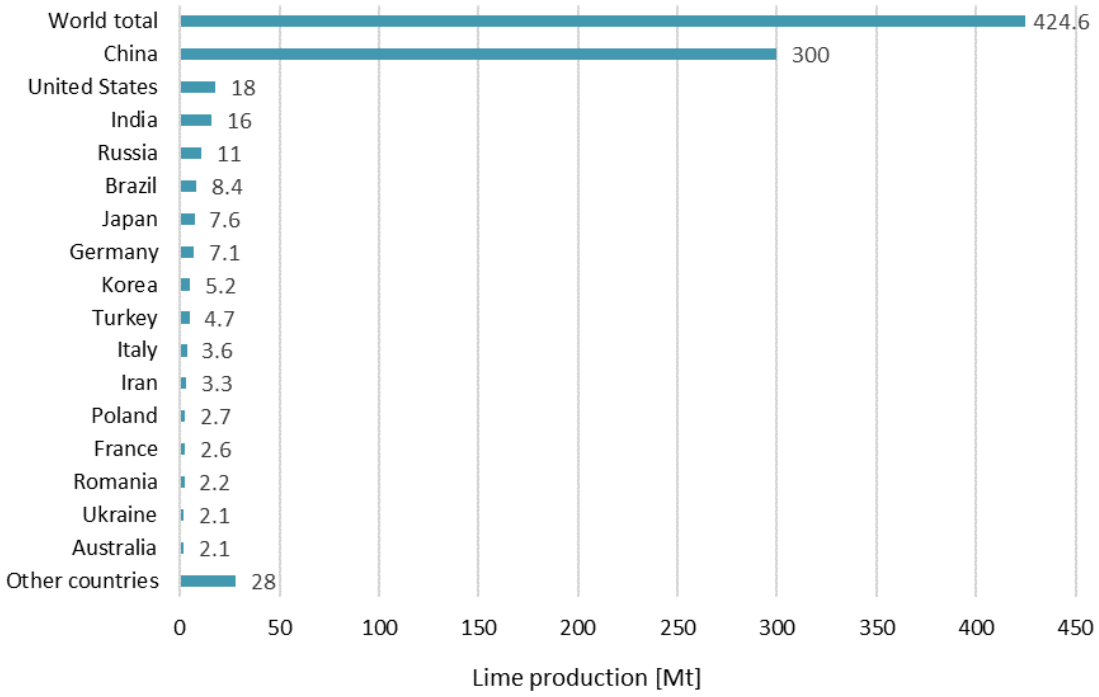

Figure 2. *Global lime production by country in year 2019, adapted from (Apodaca 2020)*

2.1 Production processes

Lime and cement production processes have some basic characteristics that are similar to both processes. However, there are also characteristics that considerably differentiate processes from each other. Thus, this chapter is divided into two sections. In the first subchapter lime production process is studied. Cement production process is discussed in second subchapter. Especially lime production process varies depending on the used lime kiln type and desired lime quality. Cement production process is more consistent. Here, the main characteristics of the production processes are presented. In case of cement the focus is on production of clinker which is one of the main raw materials of cement (CEMBUREAU 2018).

2.1.1 Lime production process

The production of lime starts with quarrying of limestone. First, topsoil and overburden covering the limestone are removed after which limestone can be quarried. (Stork *et al.* 2014, p. 12) After quarrying, the extracted rocks which diameter may be over 1 meter are transported to primary crusher to decrease the size of the grains. The function of primary crusher is based on either impact or compression. Limestone is crushed, milled and sieved until the desired grain size is achieved. The required grain size depends on

the lime kiln type. In some cases limestone is washed before calcination. (Stork *et al.* 2014, p. 13)

Next stage after limestone preparation is decomposition of calcium carbonate into calcium oxide (lime) and carbon dioxide. This process is called calcination. (Stork *et al.* 2014, p. 13) The following formula describes the calcination reaction:

$$CaCO_3(s) \leftrightarrow CaO(s) + CO_2(g). \quad (1)$$

S in the parenthesis refers to solid state and g to gas state. (Stork *et al.* 2014, p. 13) Calcination reaction is discussed in more detail in chapter 2.2. Calcination takes place in the lime kiln. There are two main types of kilns: vertical and horizontal kiln. (Stork *et al.* 2014, p. 13) Modern kiln types are examined in chapter 2.4. Traditionally, limestone is heated directly with flame and hot exhaust gases generated by burning fossil fuels in the kiln (Jiang *et al.* 2019, p. 3). After exiting the kiln, lime is cooled quickly to prevent the opposite reaction to calcination known as recarbonation (Eriksson *et al.* 2014, p. 205). In most cases calcination is incomplete and usually the calcination degree in industrial applications is approximately 95 %. However, the required degree depends on the application. (Stork *et al.* 2014)

The fine fraction of lime product contains impurities from both raw material and fuel, and it is separated from the lime product. After cooling lime is crushed and milled. The lime product is generally called quicklime. Quicklime is the most produced lime product. For some applications, quicklime is hydrated to produce calcium hydroxide $Ca(OH)_2$ which is also called hydrated lime. Hydration reaction formula can be described as followed:

$$CaO + H_2O \rightarrow Ca(OH)_2. \quad (2)$$

Hydration of quicklime is an exothermic reaction which means that thermal energy is released. Since hydration is inhibited in high temperatures, it does not occur in the kiln but after the cooling zone. Because quicklime easily reacts with the moisture in the air it is stored in dry conditions and with only limited exposure to air. (Stork *et al.* 2014) A schematic illustration of lime production process is presented in Figure 3.

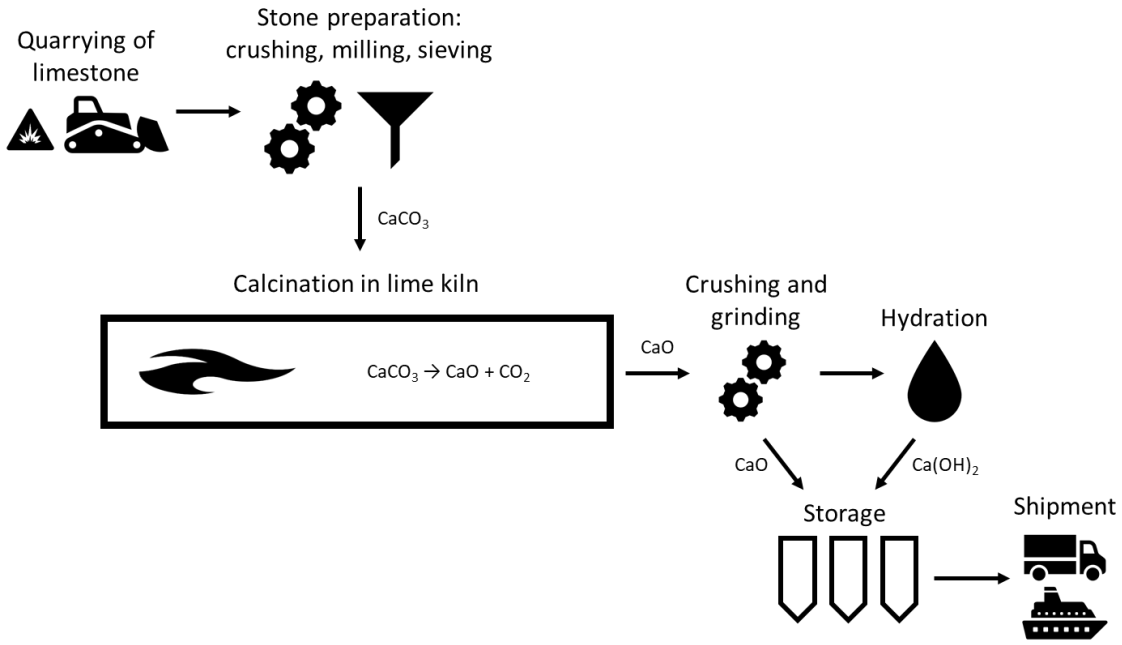

Figure 3. *Traditional lime production process, adapted from* (Stork *et al.* 2014)

2.1.2 Cement production process

Cement production partly differs from the lime production process. Additional mineral ingredients (iron oxide, alumina and silica) are needed to achieve the required composition of cement. Possible raw materials to form these compounds are iron ore, bauxite, shale, clay and sand for example. (CEMBUREAU 2018, p. 16) The mixture of limestone and other raw materials is called raw meal. The shares of the raw materials in raw meal have a significant effect on the quality of cement. It is also important that raw meal is ground into flowing powder before it enters the kiln. (Gao *et al.* 2016, p. 554-555) Before entering the kiln raw meal is preheated with exhaust gases from kiln in separate cyclones. The recovery of thermal energy from exhaust gases improves energy efficiency of the process. At modern cement mills next stage is pre-calciner. Raw meal enters a pre-calciner in which part of the limestone in raw meal is calcined into lime. (Gao *et al.* 2016, p. 555-556; CEMBUREAU 2018, p. 16) According to Gao *et al.* (2016, p. 556), the calcination rate of limestone in raw meal is approximately 80-90 % after the pre-calciner.

In the kiln, the lime reacts with other components in raw meal. Temperature in the kiln may reach 2000 °C to warm the raw meal up to 1450 °C. High temperature is needed to sinter the raw meal and form clinker. The product from the kiln is called clinker. (CEMBUREAU 2018, p. 17) The main mineral compounds of clinker are

- tricalcium silicate or alite: $3CaO \cdot SiO_2$ (C_3S),
- dicalcium silicate or belite: $2CaO \cdot SiO_2$ (C_2S),

- tricalcium aluminate or aluminate: $3CaO•Al_2O_3$ (C_3A) and
- tetracalcium aluminoferrite or ferrite: $4CaO•Al_2O_3•Fe_2O_3$ (C_4AF). (Finnsementti 2012, p. 15; Haimei 2011, p. 48)

After the kiln, clinker is cooled rapidly. Before mixed together with other raw materials of cement, such as gypsum, slag, power plant fly ash or limestone, clinker is ground into fine powder (Gao *et al.* 2016, p. 556; CEMBUREAU 2018, p. 17).

2.2 Calcination of limestone

As mentioned in previous chapter, calcination in this thesis refers to decomposition of limestone under high temperature. Calcination is an endothermic reaction i.e. energy is absorbed during the reaction. (García-Labiano *et al.* 2002; Valverde & Medina 2015; Eriksson *et al.* 2014). Reaction enthalpy of calcination is 178.8 kJ/mol (Barin & Knacke 1973). The mass of the CaO particle is theoretically 56 % of the parent $CaCO_3$ particle since the molar masses of the matters are 56 g/mol for CaO and 100 g/mol for $CaCO_3$ (Jiang *et al.* 2019; Stanmore & Gilot 2005).

The best fitting kinetic reaction models and rate-limiting processes for calcination have been studied and experimented widely. Ar & Doğu (2001) found that the best fitting model to their experimental data is shrinking core model with surface reaction rate controlling mechanism. They investigated calcination reaction of 10 different limestone samples with thermogravimetric analysis (TGA) method. Other tested models were film mass transfer control and product layer diffusion control models and the volume reaction model. All of them ended up in poor fitting to the experimental data. According to literature (Ar & Doğu 2001, p. 135; Jiang *et al.* 2019, p. 4; Kumar *et al.* 2007), in the shrinking core model the reaction is assumed to occur on the surface of the particle at first. As the reaction proceeds into the interior of the particle, particle size remains the same but the outer part around the unreacted core ($CaCO_3$) turns into a porous product layer (CaO) and the radius of the unreacted core decreases.

According to García-Labiano et al. (2002), the best fitting model varies between different limestone types as characteristics (such as porosity) of the limestone affect the calcination reactivity. In their calculations they used shrinking core model and changing grain size model. Changing grain size model states that limestone particles are comprised of non-porous spherical grains which have the same initial radius. As calcination occurs small grains of CaO form around the unreacted core grain. (García-Labiano *et al.* 2002) García-Labiano et al. (2002) also state that the rate-limiting process varies depending on the grain size.

It is generally stated on literature (Silcox *et al.* 1989; García-Labiano *et al.* 2002; Kumar *et al.* 2007; Eriksson *et al.* 2014; Jiang *et al.* 2019) that the temperature required for calcination is dependent on the partial pressure of CO_2. At a given temperature, the maximum partial pressure of CO_2 at which calcination is still possible is also called equilibrium partial pressure of CO_2 (Jiang *et al.* 2019). Different correlations for the relation between temperature and equilibrium partial pressure of CO_2 have been presented in literature. In Table 1, three different equations are presented in which P_{eq} represents the equilibrium partial pressure of CO_2 and T the temperature. The unit of pressure in the equation is standard atmosphere (atm). 1 atm = 101 325 Pa (Britannica Academic 2020). The unit of temperature is kelvin (K).

Table 1. *The relation between temperature and equilibrium partial pressure of CO_2*

Jiang et al. 2019, p. 6, according to Baker 1962	**Adapted from García-Labiano et al. 2002, p. 2388, according to Barin 1989**	**Silcox et al. 1989, p. 156**
$\log P_{eq} = 7.079 - {}^{8308}/_{T}$	$P_{eq} = 4.083 \times 10^{7} \times \exp\left({}^{-20474}/_{T}\right)$	$\ln P_{eq} = 17.74 - 0.0018T + 0.332 \ln T - {}^{22020}/_{T}$

These correlations are illustrated in Figure 4. The unit of temperature is converted into Celsius degrees (°C). The agreement is good when temperature is below 875 °C. With temperatures exceeding 875 °C the equilibrium partial pressure of CO_2 based on the equation presented by Jiang et al. (2019) according to Baker (1962) grows a little gentler compared to two others. It can be seen from Figure 4 that if the partial pressure of CO_2 in the kiln is decreased the temperature required for calcination is lower. At 1 atm partial pressure of CO_2 (e.g. 100 % CO_2 concentration at 1 atm), temperature required for calcination according to equations on Table 1 is 900.5 °C, 895.1 °C and 896.9 °C respectively. Higher temperatures compared to theory are usually required because the CO_2 released in calcination reaction may not instantly be evacuated from the surface of the particle, and thus the partial pressure of CO_2 is higher on the surface of the particles than in the kiln gases (Commandré *et al.* 2007, p. 474).

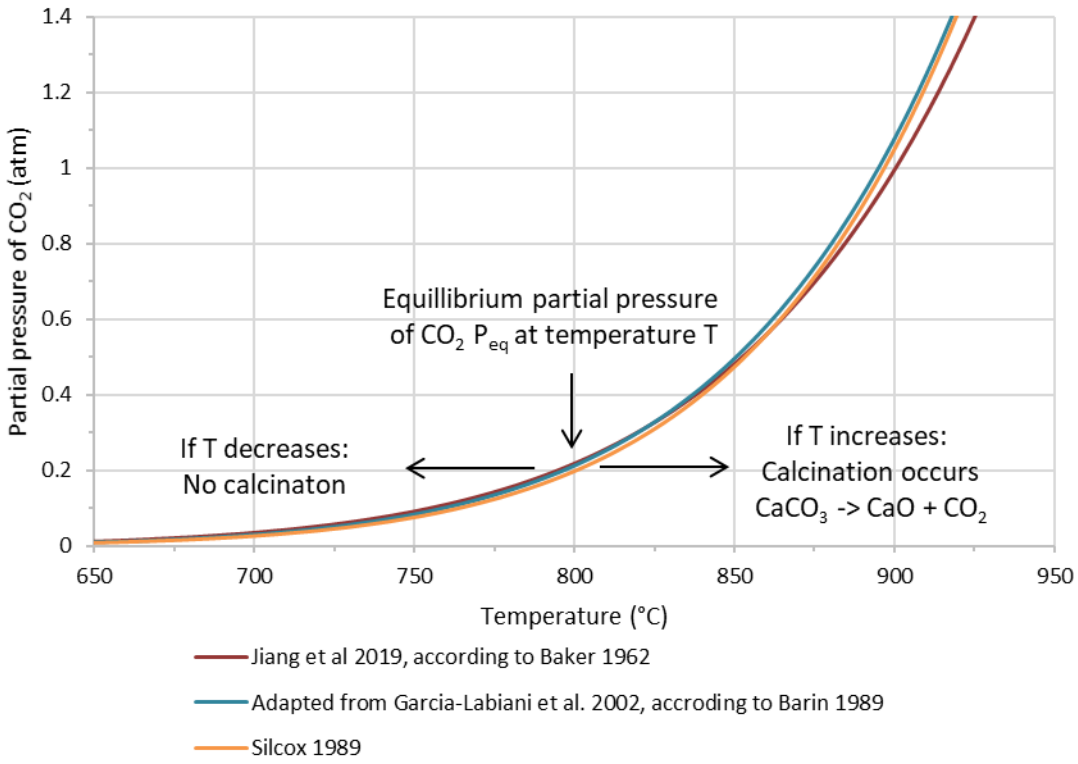

Figure 4. *The relation between temperature and equilibrium partial pressure of CO_2*

When partial pressure of CO_2 in the kiln approaches the equilibrium pressure calcination rate decreases. Calcination rate can be increased by lowering partial pressure of CO_2 or by increasing temperature. Partial pressure of CO_2 can be lowered by adding other gases to the kiln, such as air, steam or nitrogen. Particle size and shape affect the calcination rate as well. As the particle size decreases, calcination rate increases. (García-Labiano *et al.* 2002; Kumar *et al.* 2007; Jiang *et al.* 2019) In addition to partial pressure of CO_2, the total pressure of the kiln has an impact on the calcination rate as the experiments by García-Labiano *et al.* (2002) proved. In their experiment, they showed that calcination rate decreased when the total pressure increased even when CO_2 was not present in the gas atmosphere. This relation between calcination rate and total pressure has also been noticed by Dennis and Hayhurst (1987). Additionally, microstructure and surface morphology of limestone have a considerable influence on calcination rate (García-Labiano *et al.* 2002, p. 2384; Kumar *et al.* 2007, p. 611).

A reverse reaction to calcination is called recarbonation (also known as carbonation). Recarbonation of CaO takes places in the presence of CO_2 and in lower temperatures as calcination. Thus, recarbonation usually occurs after the kiln if kiln gases escape to the cooling zone. (Kumar *et al.* 2007; Stanmore & Gilot 2005) At temperatures over 500 °C recarbonation is fast. Below 500 °C recarbonation is slower but does still occur to a considerable extent. At first, recarbonation rate is high and high degree of conversion

is reached in seconds. After a while, a saturation degree of conversion is reached, and the saturation value depends on the temperature. (Manovic & Anthony 2010) $Ca(OH)_2$ may also react back to $CaCO_3$ with CO_2. H_2O is formed in the reaction which may further hydrate quicklime and cause a chain reaction. (Kumar *et al.* 2007)

Important characteristics of lime after calcination are proportion of calcium oxide and impurities and reactivity. The impurities in lime originate from limestone and fuel. In addition to impurities, calcination of limestone is almost always incomplete as mentioned in chapter 2.1. (Eriksson *et al.* 2014, p. 205; Kumar *et al.* 2007, p. 624; Stork *et al.* 2014) Lime reactivity describes how fast lime reacts with water. It is measured by timing the temperature rise from 20 °C to 60 °C when lime and water are mixed under standard conditions according to standard (SFS-EN 459-2 2011).The desired reactivity depends on the end-use of lime product. According to standard (SFS-EN 459-1 2015) high reactivity lime should reach the temperature of 60 °C in less than 10 minutes. Lime with high, medium, low or no reactivity are called soft burnt, medium burnt, hard burnt, and dead burnt respectively. Burning temperature and time, crystalline structure and impurities of limestone, kiln type and fuel affect the reactivity of lime. (Piringer 2017, p. 77; Stork *et al.* 2014, p. 14; Dowling *et al.* 2015, p. 16) High temperatures and long residence time in the kiln enhance sintering of the particles, which decreases the specific surface area of the lime particles and thus the reactivity of the lime product. CO_2 and H_2O in the kiln gases increase sintering rate. (Commandré *et al.* 2007)

2.3 Lime applications

Lime is a versatile natural chemical and it is widely used in various natural and industrial processes. (Valverde & Medina 2015; Stork *et al.* 2014) In this chapter, the most important lime applications are presented. Cement is discussed in separate chapter as it is one of the main applications of lime. Traditionally lime has been used in building and steel industries but to date lime market has expanded as new applications have been found (Dowling *et al.* 2015).

2.3.1 Main uses

In Figure 5 rough segmentation of lime uses and their shares are presented. This data is from Europe in 2012 and only includes lime that is sold on the market. Thus, the lime circulated in causticizing process in pulp production for example is not included and construction sector does not include cement. Main lime market areas in Europe are iron and steel manufacturing and environmental protection. (Stork *et al.* 2014, p. 7)

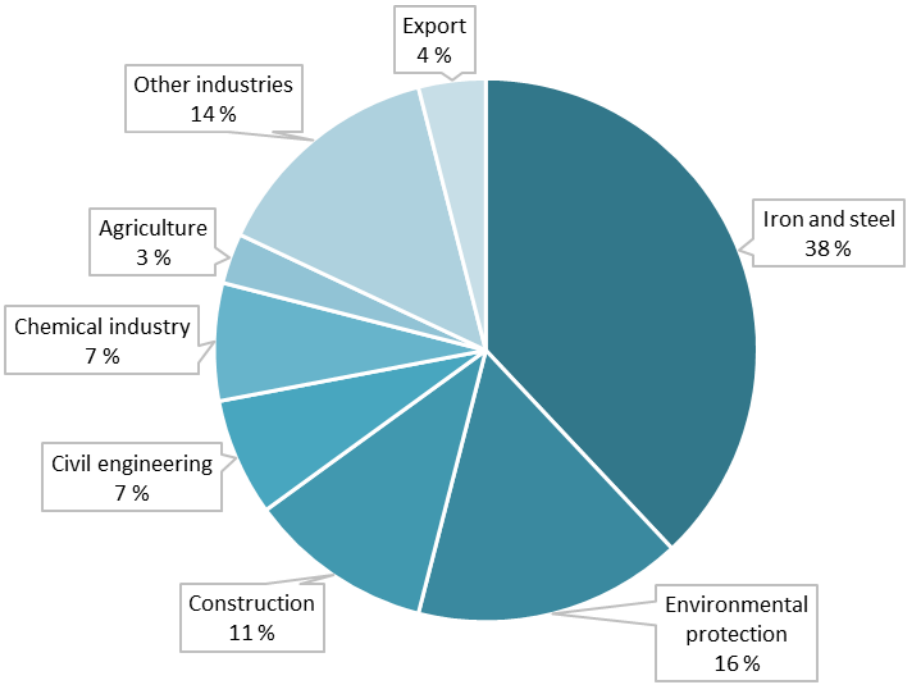

Figure 5. *Lime uses and their shares in Europe in 2012, adapted from (Stork et al. 2014, p. 7)*

In iron and steel manufacturing process, lime is added to blast furnace and converter to bind unwanted impurities, such as sulphur, aluminates, silicates, and phosphorous, from iron ore and other raw materials into slag. This process requires large quantities of quicklime. Lime is also used as purification agent in electric arc furnace where recycled scrap is processed, and also in production of non-ferrous metals. In these processes high content of CaO, low content of sulphur and specific chemical properties of lime are required. (EuLA 2020; Stork *et al.* 2014, p. 7)

Lime use in environmental protection covers waste water purification, drinking water preparation by adjusting the pH, water hardness and removing heavy metals, and desulphurization of flue gases. Other considerable uses for lime presented in Figure 5 are construction, civil engineering and chemical industry. Lime is used as filler and bonding agent in light weight construction materials or in construction materials that require high thermal insulation for example. In civil engineering lime is utilized in improving soil stability and durability and to dry wet soil. Hydrated lime can be added to asphalt to enhance its durability. In chemical industry lime is widely used for different purposes such as for production of welding gas, plastics, cosmetics, rubber and glass, and for food processing. (Stork *et al.* 2014, p. 7-9)

Lime is also utilized in pulp production process but as lime is only an intermediate product and the chemicals are circulated many times in the process it is not included in the data presented in Figure 5. In pulp production, the main application of lime is in causticizing

reaction in chemical recovery process. The aim of the chemical recovery is to regenerate the inorganic chemicals used in pulp cooking for reuse. In sulphate pulp mills (also known as kraft pulp mills), lime is mixed with water and green liquor which mainly contains sodium carbonate (Na_2CO_3) and sodium sulphide (Na_2S). Lime reacts with water and forms hydrated lime which then reacts onward with sodium carbonate. In the latter reaction (causticizing reaction), sodium hydroxide (NaOH) and calcium carbonate are generated. Chemical equation for causticizing reaction is following:

$$Ca(OH)_2 + Na_2CO_3 \rightarrow 2NaOH + CaCO_3. \quad (3)$$

Most large pulp mills have their own lime kilns for the recovery of lime. First, the waste calcium carbonate mud from the causticizing reaction is washed and dried. After drying, calcium carbonate is calcined in a rotary kiln. Recovery level is 90–98 %. Some makeup lime is required, and it is purchased from commercial lime kilns. (Bajpai 2015; Bajpai 2018) Other uses for lime in pulp and paper production are in preparation of bleach liquor for pulp bleaching, in treatment of the mill's liquid wastes and in making of precipitated calcium carbonate which is used as a filler in paper (Bajpai 2015, p. 38).

2.3.2 Cement

Cement is a key component in concrete and mortar in which it acts as a binder. The most of cement is used for concrete. Concrete is a mixture of cement, water, aggregates (such as gravel, crushed stone, sand and recycled concrete) and in some cases chemical admixtures. (CEMBUREAU 2018, p. 14-15) It is widely used due to its favorable properties like strength, durability and impermeability (Beyond Zero Emissions 2017, p. 10). Cement types are divided in 5 categories based on the main raw material. In total, there are 27 different types of cement. (CEMBUREAU 2018, p. 14-15) Portland cement is the most common cement type and it accounts for 98 % of world cement production (Beyond Zero Emissions 2017, p. 10).

In Figure 6, global cement production from 2010 to 2019 is presented. Cement production by country in year 2018 is presented in Figure 7. China is the biggest cement producer in the world with 54.5 % share of the global production. As the world population is growing and societies are developing and urbanizing, the role of building materials and thus cement in emerging countries becomes essential. (CEMBUREAU 2018, p. 6) This is already evident in India for example. During the last two decades cement production in China has more than tripled but to date the growth has stabilized which can be seen in Figure 5 as well. (CEMBUREAU 2020, p. 15)

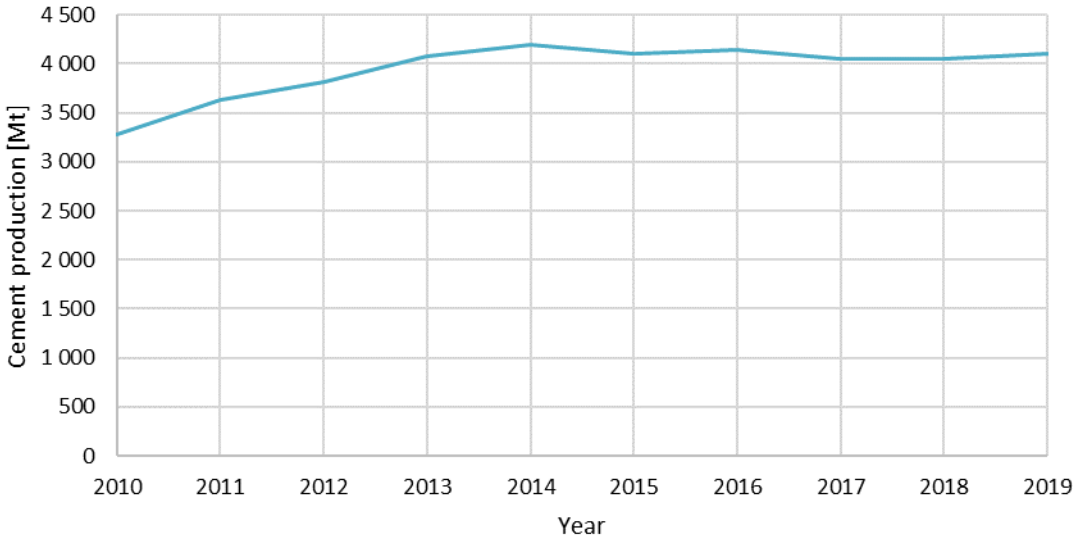

Figure 6. *Global cement production 2010-201: after 2014 the growth of cement production in China has stabilized which can be seen in the global cement production as well; adapted from (IEA 2020a)*

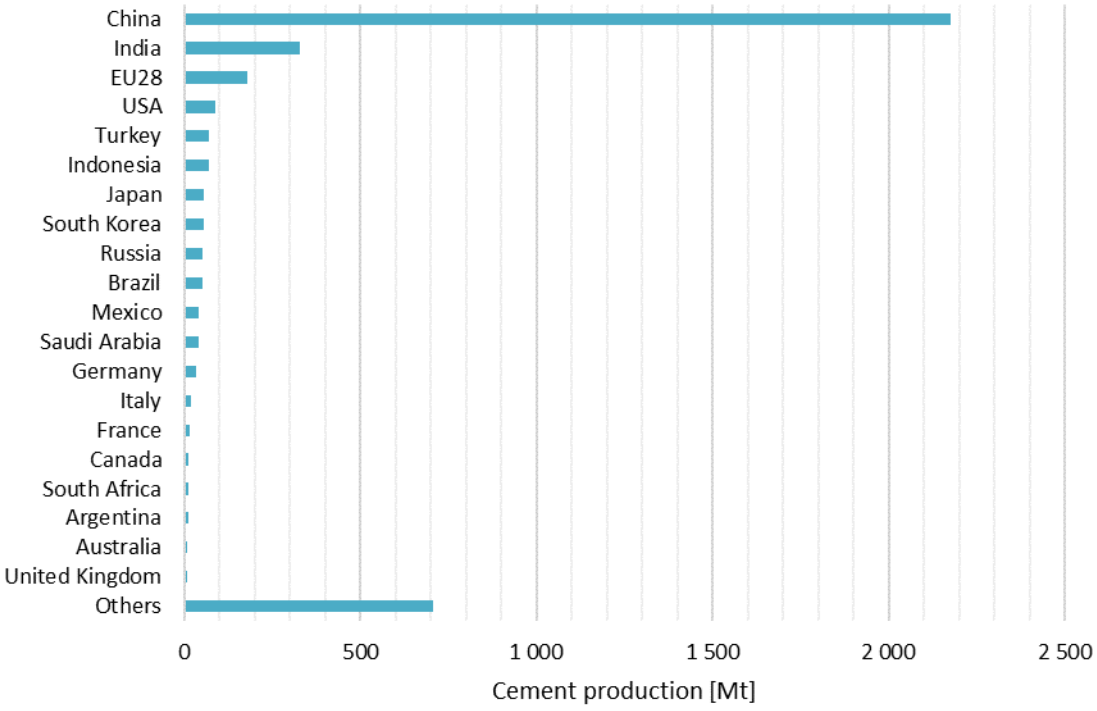

Figure 7. *Cement production by country in year 2018, adapted from (CEMBUREAU 2020, p. 15)*

2.4 Modern kiln types

Calcination takes place in lime kiln. Typical lime kilns can be grouped into two main categories according to kiln orientation: horizontal kilns and vertical kilns. Different types of modern lime kilns are listed in Table 2. (Stork *et al.* 2014; Piringer 2017) There are other types of kilns as well, such as fluidized bed type kiln (Boateng 2016). The kiln type significantly affects the properties of produced lime product (Stork *et al.* 2014).

Table 2. *Main lime kiln types grouped into horizontal and vertical kilns, adapted from* (Stork *et al.* 2014; Piringer 2017)

Horizontal kilns	**Vertical kilns**
Long rotary kiln (LRK)	Parallel flow regenerative kiln (PFRK)
Rotary kiln with pre-heater (PRK)	Annular shaft kiln (ASK)
	Mixed feed shaft kiln (MFSK)
	High performance shaft kiln (HPSK)

2.4.1 Horizontal kilns

Horizontal, rotary kilns are long, straight, cylindrical vessels. Most of them are lined with refractory materials to provide insulation and energy savings and to protect the outer shell from thermal damage. There may also be dams, lifters or tumblers inside the vessel to increase residence time and to enhance mixing, heat transfer and axial flow. Length of rotary kilns vary from 10 up to 150 meters depending on the application it is used for. (Boateng 2016) A simplified picture of rotary kiln with pre-heater is presented in Figure 8.

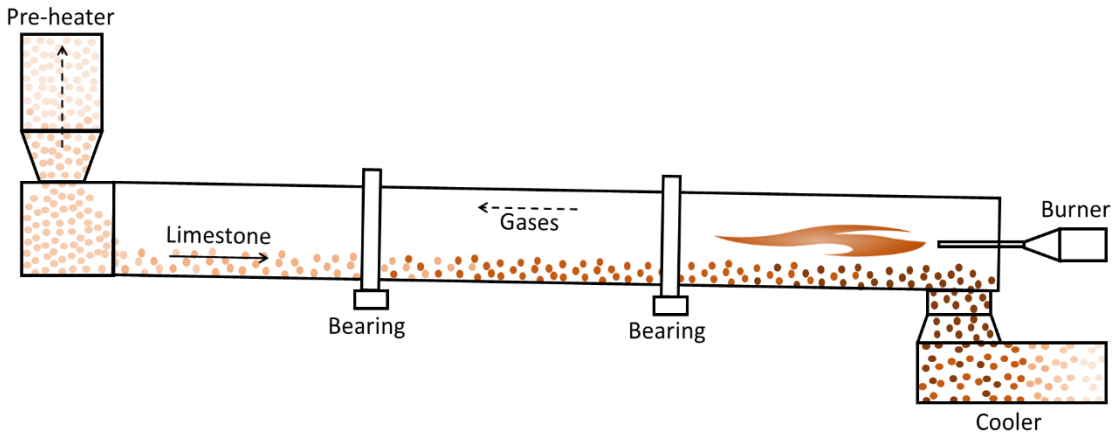

Figure 8. *Rotary kiln with pre-heater, adapted from* (Boateng 2016, p. 3; Shahin *et al.* 2016, p. 111)

In some kilns there is a separate pre-heater or pre-calciner before the kiln where countercurrent flue gas flow dries, pre-heats and in some cases (such as in cement raw meal processing) pre-calcines the limestone whereas in other rotary kilns drying and pre-

heating takes place in the first zone of the kiln vessel. Thus, rotary kilns without a pre-heater (LRK) are typically longer than kilns with a pre-heater (PRK). In a rotary kiln, limestone moves slowly towards the hot end of the kiln due to rotation and small axial inclination of the kiln. Combustion zone, i.e. burner and flame, is located in the end of the kiln. Heat transfer between limestone and hot flue gases occurs through radiation and convective modes. Combustion and process gases most commonly flow counter currently to opposite direction as limestone. In the end of the kiln behind the flame, the product is discharged into the cooler. The cooling air can be used as combustion air. (Shahin *et al.* 2016, p. 112; Boateng 2016)

Horizontal rotary kilns are less energy efficient than vertical kilns. However, production capacity of rotary kilns is typically higher than in vertical kilns and also calcination of smaller stone sizes is possible. In addition, calcination degree of limestone is usually higher and a wide range of reactivity can be produced with rotary kilns. (Stork *et al.* 2014; Piringer 2017; Boateng 2016) Rotation of horizontal kilns provides better mixing of the product and a uniform temperature profile. There are less process control challenges with rotary kilns than with vertical ones. (Boateng 2016)

2.4.2 Vertical kilns

Like horizontal rotary kilns, vertical kilns are divided into pre-heating, calcination and cooling zones as well. The main idea of most of the vertical kilns is the upward flowing combustion gases and counter currently downward flowing limestone particles. Pre-heating takes place at the top part of the kiln where limestone particles are fed to the kiln. Calcination starts in lower parts of the kiln when temperature rises high enough and is usually finished at the level of the burners. Cooling zone and output of lime are at the bottom of the kiln. Cooling air can be used as combustion air. (Sagastume Gutiérrez *et al.* 2013, p. 274; Piringer 2017) Vertical kilns are in general more energy efficient than horizontal kilns (Stork *et al.* 2014; Piringer 2017; Alcántara *et al.* 2018). However, the temperature profile is more difficult to control and hot and cold spots are formed more easily as there is no mixing of the particles in vertical kilns (Boateng 2016, p. 5).

Parallel flow regenerative kiln (PFRK) has been the leading kiln technology for lime calcination. It is cost-effective and the most energy efficient kiln technology, it is suitable for soft burnt lime and the lime produced is high quality. On the other hand, PFRK cannot be used to process small grain sizes (smaller than 10 mm). In Figure 9 the operational principle of PFRK is presented. PFRK is equipped with two shafts with a connective channel between them. Both shafts are filled with limestone. The operation of the kiln is cyclical. Fuel is burned only in one shaft at a time (called burning shaft). The combustion

gases from the burning shaft flow through the connective channel to the other shaft where they counter currently flow through the limestone and pre-heat it. The other shaft is called regenerative shaft. After calcination lime product is discharged from the bottom of the burning shaft and filled with limestone from the top. (Piringer 2017, pp. 83–84; Alcántara *et al.* 2018, pp. 395–396)

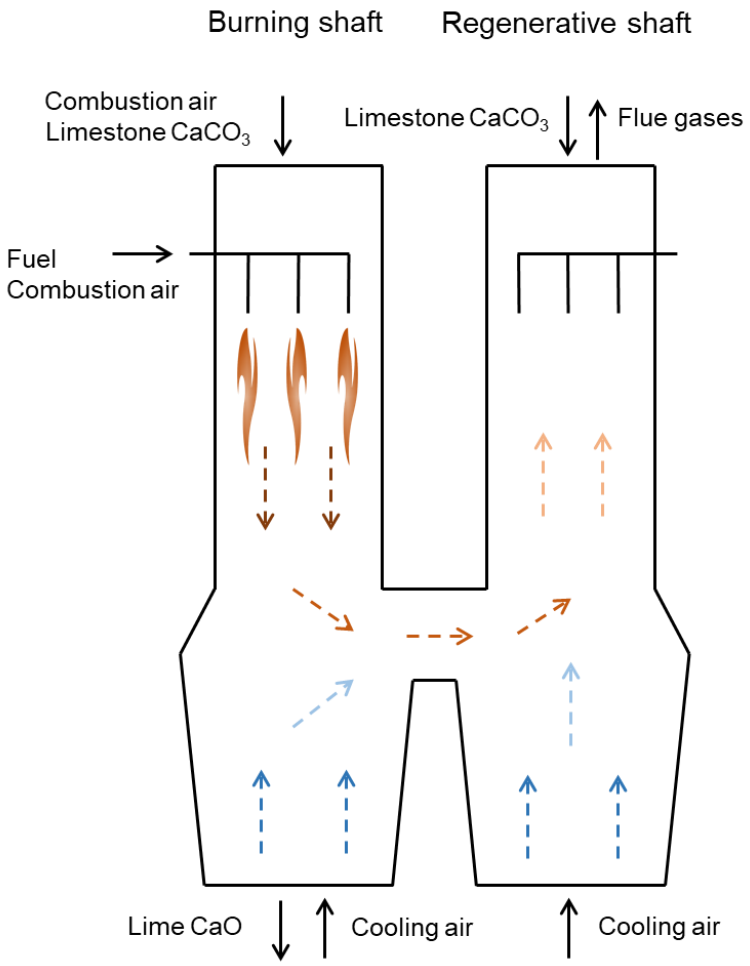

Figure 9. *Parallel flow regenerative kiln, adapted from (Piringer 2017, p. 83)*

Annular shaft kiln (ASK) is designed for soft burnt lime production as well. The shape of the kiln is annular and there are burners on two levels. (Senegačnik *et al.* 2008) In a more modern version of ASK the burners are located on same level opposite to each other. This type of kiln is called annular shaft kiln with opposite burners (OBASK). The aim of locating the burners opposite each other is to reduce construction costs which are relatively high for traditional ASK due to complex chamber structure. (Rong *et al.* 2017) Mixed feed shaft kiln (MFSK) is a traditional vertical kiln technology. Limestone and fuel (coke or anthracite) are both charged to the kiln from the top. MFSK is used for hard burnt lime production. The heat consumption of MFSK is low and CO_2 concentration of kiln-off gases is high which is requirement in some applications, but the fuels that can be

burned in MFSK are restricted to above mentioned coke and anthracite. (Piringer 2017) High performance shaft kiln (HPSK) is also used for production of hard burnt lime. The position of burners in the lower part of the calcination zone enables high temperatures and partial sintering of lime product to reduce reactivity. Otherwise, operational principle is similar to basic vertical kiln. (Piringer 2017, p. 86)

2.5 CO_2 emissions and emission reduction

Lime production is carbon and energy intensive. Emissions from lime production can be divided into process emissions and energy related emissions. Process related CO_2 emissions originate from the calcination reaction. CO_2 is released in decomposition of limestone as can be seen from equation 1. Theoretically, 0.785 tonnes of CO_2 is released per tonne of lime produced since the molar masses are 44 g/mol for CO_2 and 56 g/mol for CaO. However, calcination is usually not complete so the actual amount of CO_2 released is approximately 0.75 tonnes. These emission comprise over 60 % of the total CO_2 emissions from lime production. (Stork *et al.* 2014; Dowling *et al.* 2015; Jiang *et al.* 2019) Process emissions are dictated as fossil emissions which means that they need to be monitored and reported and emission allowances are required in EU Emissions Trading System (EU ETS) (European Commission 2015).

Energy related CO_2 emissions originate from fuel combustion in the kiln and they comprise 30-40 % of total CO_2 emissions. These emissions vary a lot depending on the kiln technology and fuel for example. (Stork *et al.* 2014; Dowling *et al.* 2015) Schorcht et al. (2013) state in their report that energy related emissions vary between 0.27-1.10 tonnes of CO_2 per tonne of lime for horizontal kilns and 0.20-0.71 tonnes of CO_2 per tonne of lime for vertical kilns. Approximately 2 % of total CO_2 emissions are caused during mining and limestone preparation and downstream processing and hydration (Stork *et al.* 2014; Dowling *et al.* 2015). Lime has one of the highest specific CO_2 emissions in comparison to other industries with high energy intensity such as energy generation and commercial aviation (Dowling *et al.* 2015, p. 15). In this thesis, focus is on CO_2 emissions but there are also some quantities of other emissions released in the production process such as sulphur oxides (SO_x), nitrogen oxides (NO_x), carbon monoxide (CO), volatile organic compounds (VOC), methane (CH_4), nitrous oxide (N_2O) and dust (Dowling *et al.* 2015, p. 16; Pacyna *et al.* 2019, p. 4).

According to IPCC Special Report (Rogelj *et al.* 2018) CO_2 emissions from industry should be reduced by 80 % in 2050 compared to 2010 levels to limit the global warming to 1.5 °C. In lime and cement production this implies that also process related emissions need to be reduced. IEA recognizes in their recent report (IEA 2020b) four key strategies

to meet the targets of their Sustainable Development Scenario. These strategies are electrification of transport, industry and building sectors, deployment of CCUS technologies, shift towards hydrogen and hydrogen-derived synthetic fuels, and use of more sustainable alternative fuels and feedstock. Three of these strategies are directly or indirectly covered in the kiln concept under development in Decarbonate project. It is important to consider how different reduction actions affect process emissions and energy related emissions. Most of the reduction actions only reduce energy-related emission and only few tackle process emissions. The main and at the moment only method for cutting process emissions is carbon capture and utilization or storage (CCUS). In case of cement for instance, alternative raw materials are also an option to reduce process emissions. (Stork *et al.* 2014) However, for many other lime applications alternative raw materials are not a feasible option. In next chapters the different actions, their potential reduction effect and limitations and challenges are discussed.

2.5.1 Electrification

IEA recognizes in their recent report (IEA 2020b) that electrification of the world economy is one of the core factors in the transition towards cleaner energy system and sustainable industry sector. The share of electricity in final energy use has been growing already for decades, and in industry sector electricity is already an important fuel. However, in heavy industries such as lime and cement production use of electricity lags behind. (IEA 2020b) IEA also recognizes that reliance on clean electricity sources such as wind and solar power could also lead to decreased electricity prices. Current prices of the DS futures of the Nordic power products indicate that electricity prices in the Nordic countries are expected to decrease in upcoming years (Nasdaq 2020).

Electrification can be divided into direct and indirect electrification. Direct electrification refers to the use of electricity as an input to the process. Such devices are electric heaters, heat pumps and electric vehicles for instance. (Ruhnau *et al.* 2019) In lime and cement production, direct electrification can be adopted by generating the heat with electric heating elements (also called resistors). The flowing current in the heating elements generates the heat by Joules effect (Lupi 2016). When it comes to indirect electrification, the system does not use electricity but synthetic fuels as an energy source. First, electrolysis is required for production of synthetic hydrogen which is then processed to synthetic fuels such as synthetic natural gas. This kind of processes are usually called power-to-gas or power-to-liquid processes. (Ruhnau *et al.* 2019) Synthetic fuels can be used in lime and cement production in the kiln as a source for the heat. Depending on the kiln type and fuel, no major technical modifications for the utilization

of synthetic fuels are required. In this thesis, focus is on direct electrification of lime and cement production.

2.5.2 CCUS

CCUS is expected to have an important contribution to the reduction of the carbon footprint of various industrial processes. In general, there are three different techniques for carbon capture from industrial processes: pre-, post- and oxy-combustion capture. Pre-combustion capture method is based on partial oxidation of the fuel through catalytic reforming or gasification for example. Post-combustion capture is an end-of-pipe solution: CO_2 is captured from the flue gases from the industrial process. Downside is that often the CO_2 concentration in the flue gases is low, and thus large amount of energy and major facilities are required for the capture. In oxy-combustion (also called oxy-fuel combustion) method oxygen or oxygen rich gas such as a mixture of oxygen and recycled flue gas (RFG) is utilized instead of air for combustion to avoid nitrogen contamination. The absence of nitrogen increases partial pressure of CO_2 in the flue gases and thus simplifies the capture process. Disadvantages are the investment and ancillary energy needed for cryogenic air separation for oxygen production. (Cormos *et al.* 2018, p. 883; Boot-Handford *et al.* 2014)

For lime and cement production CCUS is a viable option as the production process is highly CO_2 intensive and relatively simple with only one flue gas stream (Bui *et al.* 2018; Leeson *et al.* 2017). The CO_2 concentration in the flue gases from lime kiln varies from 22 % to 29 % (Nwaoha *et al.* 2018, p. 7102). In case of cement plant, the CO_2 concentration in flue gases from the kiln varies from 14 % to 33 % (Bosoaga *et al.* 2009, p. 134). Carbon neutral fuels and energy in combination with carbon capture open up opportunities for even “below zero emissions” operation (Eriksson *et al.* 2014). Pre-combustion technologies do not capture process emissions from lime or cement production which reduces CO_2 capture rate considerably. In addition, effects on the product quality need to be considered when developing CCUS technologies for lime and cement production. Suitable CO_2 capture technologies are solvent scrubbing, oxy-fuel combustion, calcium looping and direct capture. (Hills *et al.* 2016)

Solvent scrubbing is an end-of-pipe technology and thus does not have direct effects on the lime or cement manufacture process nor the product (Hills *et al.* 2016). Amine are one option for solvent used in the capture process. The amine sorbent is contacted with the flue gases in an absorption column where CO_2 is absorbed. The CO_2 rich solvent is then transferred to a separate column in which heat is required for CO_2 desorption and solvent regeneration. Downsides are that thermal energy demand of amine regeneration

is high and there are other environmental side effects from amines. (Cormos *et al.* 2018, p. 884) Thus, amine sorbents are not likely to be used on industrial scale CCUS technologies and more modern sorbents with lower heat requirement for regeneration are being developed (Leeson *et al.* 2017).

Oxy-fuel combustion has been acknowledged to be one of the most promising technologies for lime and cement production. Combustion in pure oxygen or increased oxygen concentration enhances the combustion process and increases flame temperature. Thus, RFG is usually added to moderate the temperatures. (Boot-Handford *et al.* 2014) Especially in case of lime high temperatures may be harmful and increase oxide melt phase (Eriksson *et al.* 2014). In cement production higher temperatures are required for clinker formation. Based on laboratory tests performed by the European Cement Research Academy (ECRA) oxy-fuel combustion has no considerable effects on the quality of clinker (Bui *et al.* 2018). Oxy-fuel combustion equipment affects the whole lime or cement production plant and requires large amount of R&D and will be expensive if implemented as retrofit. Thus, in case of retrofitting an existing plant a more feasible option seems to be partial oxy-fuel combustion approach. In partial oxy-fuel combustion only preheaters and pre-calciner depending on whether lime or cement plant is in question are oxy-fueled. (Hills *et al.* 2016)

In calcium looping (CaL), CO_2 is captured with CaO sorbent. Traditionally in power sector, CaL system consists of two parallel circulating fluidized beds in one of which capture of CO_2 through recarbonation takes place and in the other calcination to regenerate the $CaCO_3$ back to CaO. (Hills *et al.* 2016) CaL cycle could contribute to the thermal energy efficiency of the plant as it has high temperature heat recovery potential (Cormos *et al.* 2018).

Direct separation of CO_2 is not included in the three main CCUS technologies. However, in lime and cement production direct separation is a significant possibility. Direct separation in lime and cement production can be performed by indirect heating of limestone to prevent mixing of CO_2 from calcination process and diluting combustion gases. The gases from the indirectly heated kiln are virtually pure CO_2 and should be directly appropriate for compression, transport and utilization. Impurities in the lime or cement raw material may cause challenges for direct utilization. (Hills *et al.* 2016)

Direct separation technology is piloted in an ongoing project called Low Emissions Intensity Lime and Cement (LEILAC). LEILAC is funded by the consortium of eleven partner organizations and the European Union by the Horizon 2020 research and

innovation program. (LEILAC 2017) A schematic illustration of the pilot scale kiln used in experiments of LEILAC project is presented in Figure 10.

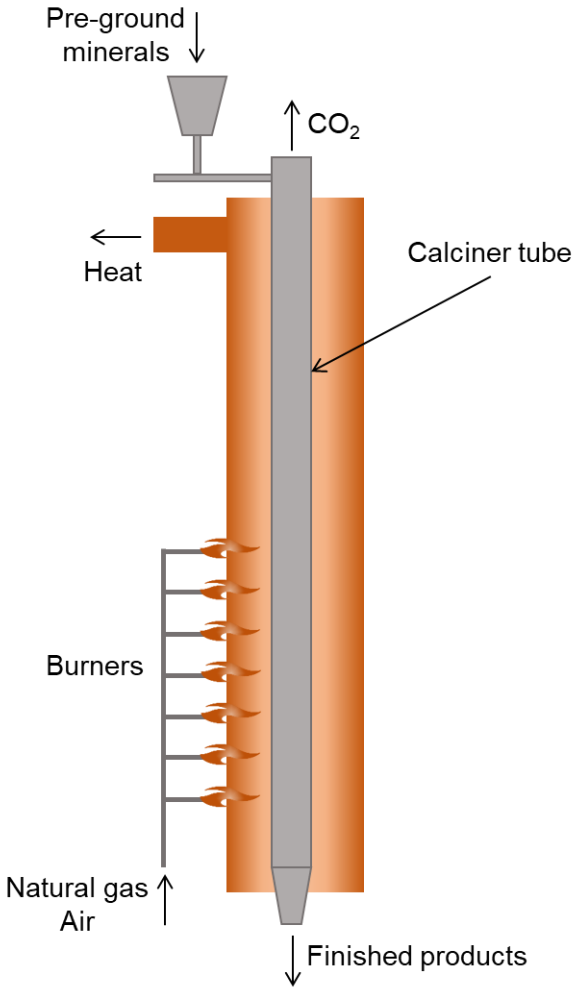

Figure 10. *The basic concept of the LEILAC project, adapted from* (LEILAC 2017)

Limestone is fed from top to the calciner tube which is indirectly heated by conductive and radiative heat transfer with flue gases from combustion of natural gas. CO_2 released in calcination flows upstream in the calciner tube and exit the tube from the top. As the flue gases from combustion are segregated the gases from the calciner tube should only consist of CO_2. The capacity of the pilot scale plant is around 240 t/d of cement raw meal or 190 t/d of limestone. In case of cement, this unit will only replace the pre-calciner. LEILAC project only captures the process emissions but does not reduce energy-related emission. However, direct separation could be combined with other carbon capture technologies. (LEILAC 2017; Hodgson *et al.* 2019) In consequence of the success of LEILAC project, LEILAC 2 project pilots indirect heating with multiple fuel sources, particularly electricity. Also, retrofitting of an existing cement plant with the new technology is demonstrated. A pilot plant will be built alongside an operational cement plant. (CORDIS 2020)

Most of the CCUS technologies in general are still on pilot scale or demonstration phase and unfortunately there has not been enough progress to achieve the international and national climate targets. Lack of proven models for commercialization of CCUS technologies, political attitude and public acceptance cause challenges for a wider deployment of CCUS. (Bui et al. 2018) General constrains for CCUS technologies are high transportation, energy and other additional costs compared to emitting the CO_2 and limited storage locations and their permanence (Rahman *et al.* 2017). In addition, development of CCUS technologies for industrial processes lags behind power sector. However, as many industrial processes do not have possible alternative raw materials or processes CCUS is important for mitigation of CO_2 emission. (Leeson et al. 2017)

Due to limitations on CO_2 storage, utilization seems a more tempting option. CO_2 with hydrogen (H_2) can be used to produce hydrocarbon fuels. In future, fuels produced of CO_2 emitted from power and industrial sector may serve as an option for finite fossil fuels. (Rahman *et al.* 2017) One objective of the project that this thesis is part of is to study production of synthetic fuels with two methods: Fischer-Tropsch synthesis and methanation of H_2 and CO_2 to synthetic natural gas (SNG). However, in this thesis processes for production of synthetic fuels are not discussed in more detail.

2.5.3 Other emission reduction methods

In addition to electrification and CCUS technologies, there are other methods and techniques to reduce CO_2 emissions from lime and cement production. These methods are discussed in this chapter. At present, the most common fuels used in lime production worldwide are coal, natural gas and oil. Fuel mix used by European lime producers is presented in Figure 11. In this data also hydrated lime and dolime products are taken into account in addition to quicklime. (Stork et al. 2014) One option for cutting energy related emissions is switching to fuels with low carbon intensity such as natural gas or biomass. Also, waste could be used as a fuel in lime kiln. (Stork et al. 2014, p. 37)

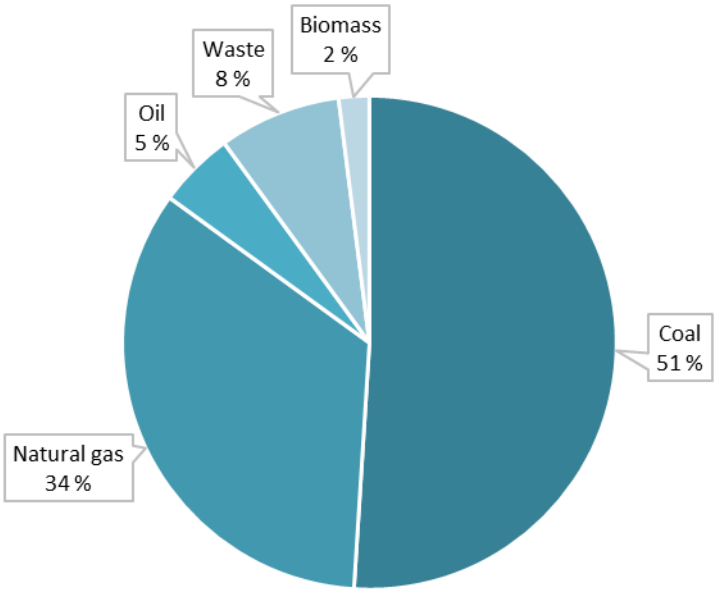

Figure 11. *Estimated fuel mix used by European lime producers, adapted from (Stork et al. 2014, p. 29)*

There are some limitations related to use of natural gas, biomass or waste as fuel in lime kilns. When it comes to natural gas, not all lime plants are connected to or located near natural gas grid. Investment costs required for connecting piping network could be significant. In addition, secure access to natural gas and supply in the future raise concerns. Price of natural gas is also relatively high. (Stork et al. 2014, p. 38)

Biomass may cause problems in the kiln by causing blockages which means that maintenance is needed more frequently. Biomass can also be converted to syngas. Sufficiency of biomass for all planned applications has been discussed lately and may evolve to a problem. (Stork et al. 2014) Also, the quality and purity of biomass and especially waste fuels need to be high and constant as the impurities in fuel contaminate the lime product (Stork et al. 2014; Piringer 2017). Kääntee et al. noticed in their study (2004) that changes in process conditions (such as amount of combustion air) in consequence of fuel switch had a considerable impact on the formation of clinker phases in the kiln. Thus, it is important to consider all the changes to the process conditions and their impact (Kääntee *et al.* 2004). Legislation impacts the use of biomass or waste as fuel. There are many waste types (pulverised, solid-lumps and liquid for instance) and not all kiln types are able to process all types of waste. (Stork et al. 2014, pp. 38–39)

Besides combustion of fuels and electricity, heat can be provided also with other heat sources, for example indirectly with solar energy or electricity, as mentioned in chapter 2.5.1. Indirect heating of limestone with solar energy has been experimented on laboratory scale by Abanades & André (2018). A cavity-type solar receiver was used to collect radiation and direct it to the rotary tube. The demonstration was successful and

complete calcination was reached. Argon was used as an input gas. (Abanades & André 2018) However, solar heating system requires specific climate and weather conditions which can be found only in limited areas. In Europe, appropriate locations can be found in southern parts of South-Europe. (Stork *et al.* 2014) Thus, solar energy is not a feasible option in most areas.

By increasing lime kilns energy efficiency, fuel consumption decreases which reduces flue gas emissions. As the calcination step of lime production is the most energy and emission intensive, concentrating on the efficiency of the kiln rather than other equipment has the biggest emission reduction potential. A certain amount of energy is necessary for calcination reaction to occur. (Stork et al. 2014) Based on the reaction enthalpy of calcination reaction, theoretical minimum energy consumption is 3.18 GJ per tonne of lime product.

There are still a lot of outdated lime kilns in use which do not meet the product and emission targets (Piringer 2017). By replacing old kilns with new highly efficient kilns, the biggest potential savings on fuel consumption could be achieved. In theory, this means replacing horizontal rotary kilns with vertical ones. There are challenges related to kiln type change as each kiln type has different capacity limits, specific applicability and the kiln type significantly affects the properties of lime. Switch from LRK to PRK also enhances energy efficiency by recovering energy from the flue gases. (Stork et al. 2014, pp. 33–35) In addition to switching kiln type, energy efficiency can be increased by using waste heat from the kiln, recovering energy from hydration step in case of hydrated lime or optimizing combustion and improving process control. Recovered heat can be used in milling of limestone, to dry limestone before the kiln, in other industrial processes in other sectors, as district heating for residential areas or to generate electricity. (Stork et al. 2014, pp. 35–36)

3. ELECTRIC HEATED ROTARY KILN CONCEPT

International and national strategies set ambitious goals for limiting climate change and global warming. Decarbonisation of industry sector is an important factor in the GHG emission reduction plans. For lime and cement industry ambitious goals mean that both process and energy-related emissions need to be reduced. In chapter 2.5, CO_2 emissions from lime and cement production process and emission reduction methods are discussed. The most promising reduction measures are electrification and CCUS. In Decarbonate project, electric heated rotary kiln equipped with CCUS is under development (Decarbonate 2020). The electric heated kiln concept under development is discussed in this chapter. First, the concept is presented. Advantages and downsides and challenges compared to traditional rotary kilns are examined. Next, heat transfer mechanisms and affecting factors are discussed.

3.1 Kiln concept

CCUS is one of the few emission mitigation methods that reduces process emissions from lime and cement production. With indirect heating direct separation of process gases is possible as the flue gases from combustion do not contaminate the CO_2 released from the calcination reaction. Thus, in lime and cement production carbon capture by direct separation is rather straightforward. For that reason, indirectly heated kiln was chosen to be the subject of review in Decarbonate project (Decarbonate 2020). Indirect heating is also under examination in LEILAC project. The pilot kiln in LEILAC project is vertical kiln whereas in Decarbonate project the studied kiln is horizontal rotary kiln. This technology was chosen because mixing of limestone is more efficient in horizontal rotary kiln compared to vertical one. In addition, horizontal rotary kiln technology is widely used in clinker production and in causticizing process in pulp mills. Similarly to LEILAC 2 project, the heat is generated by electricity in Decarbonate project. Energy-related CO_2 emissions are minimized if electricity is produced with renewable or low carbon energy sources instead of fossil fuels.

There are some advantages related to indirectly heated kiln compared to directly heated kiln technologies. The main advantages of indirect electric heating are the reduction of energy related emissions. On the other hand, content of CO_2 in the kiln off-gases is high which enables deployment of direct capture. Additionally, flame temperature and length are key factors when it comes to uniformity of the product quality and reactivity. However, combustion process is challenging to control precisely and there may occur hot and cold

spots in the kiln (Piringer 2017; Jiang *et al.* 2019). Temperature profile in an indirectly heated kilns is easier to control because there is no direct contact between flame and limestone. In addition, in electric heated kiln it is possible to have multiple temperature control zones to easily control and change the temperature profile. (Boateng 2016, p. 9) Furthermore, in indirectly heated kiln impurities in fuel and flue gases do not contaminate the product (Jiang *et al.* 2019).

However, there are also challenges and downsides related to indirectly heated kiln concept. Thermal efficiency of indirectly heated kilns is low in general. Heat losses through the shell have a major effect on the kiln efficiency. (Boateng 2016). However, in case of electric heating there are no flue gases from combustion which on the other hand reduces heat losses and enhances thermal efficiency. Additionally, if there is no gas supply to the kiln partial pressure of CO_2 in the kiln is supposed to be high. Thus, the required temperature for calcination is higher compared to traditional kiln in which especially nitrogen from combustion air lowers the partial pressure of CO_2. Higher temperature requirement increases energy consumption. On the other hand, it is possible to lower pressure in the kiln which lowers the partial pressure of CO_2. However, the energy consumption required for pumping the vacuum must be considered.

High partial pressure of CO_2 in the kiln gases may also cause recarbonation of CaO in cooler zones of the kiln. Abanades & André (2018) studied indirect heating with solar energy in their article, and most of their experiments were performed in argon atmosphere. However, they reported having recarbonation problems in an experiment run with CO_2 concentration of 50 % in the input gases. Calcination degree of only 56 % was reached in the experiment performed with CO_2 rich input gas. Calcination degree of over 90 % was reached in argon atmosphere when other test parameters apart from gas atmosphere were kept the same. (Abanades & André 2018) In addition to recarbonation, CO_2 in the kiln gases also enhances sintering which decreases the reactivity of the product (Commandré *et al.* 2007). In Table 3, the above mentioned advantages and downsides and challenges of electric heated rotary kiln compared to traditional rotary kiln are listed.

Table 3. *Advantages and downsides and challenges of electric heated rotary kiln technology compared to traditional rotary kiln technologies*

Advantages	**Downsides and challenges**
Reduction of energy related emission	Higher temperature required due to high CO_2 partial pressure in kiln gases
Enabling of the deployment of CCUS technologies (especially direct capture) due to high partial pressure of CO_2 in kiln off-gases	Greater heat losses through kiln shell
Temperature profile and process easier to control	Recarbonation in cooler zones of kiln due to high partial pressure of CO_2
No contamination of lime product from impurities in fuel and flue gases	Sintering enhanced due to high partial pressure of CO_2
Possibility for multiple temperature control zones	
Smaller heat losses due to absence of flue gases	

The operational principle of electric heated rotary kiln is similar to traditional horizontal rotary kiln technologies. After preparation, limestone is fed to the kiln where calcination takes place. Rotation and small inclination of the rotary tube move the limestone forward inside the tube. Rotary tube is heated with electric heating elements. The heating elements (also called resistors) are located outside the rotary tube. Around the kiln and heating elements are insulation layer and framework to minimize heat losses to environment. The outermost layer is a steel shell. A schematic illustration of the kiln concept is presented in Figure 12. In this thesis, specific structure of the kiln is not discussed in more detail. Partial pressure of CO_2 is expected to be high in kiln off-gases. Condensation of moisture from the kiln off-gases and purification might be required before utilization. Otherwise, gases are compressed and transported onward.

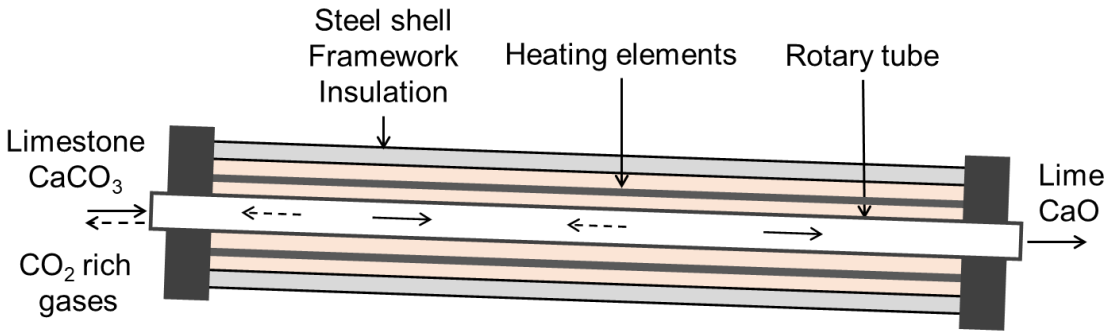

Figure 12. *Schematic illustration of the electric heated rotary kiln concept; solid particle flow in the kiln marked with solid arrows, gas flow marked with dashed arrows*

3.2 Heat transfer mechanisms in an electric heated rotary kiln

As thermal efficiency of indirectly heated kilns may be lower, heat transfer mechanisms need to be considered carefully. In general, heat is transferred mainly by thermal radiation but also by convection and conduction. Temperatures required for calcination are high and heat transfer is mainly due the radiation and convective heat transfer accounts for a minor fraction. In Figure 13, an illustration of the heat transfer mechanisms across the tube cross section is presented. From the electric heating elements to the outer surface of the rotary tube heat is transferred by radiation (Q_{HW} in Figure 13). The rotary tube should be able to absorb as much heat as possible which means that its emissivity should be high. Emissivity of a brand new cylinder is usually low. Thus, a preliminary oxidation of the surface is recommended to be performed before use. In addition to emissivity, temperature required for calcination is high so the material has to tolerate high thermal load without excessive heat expansion and deformation. Some of the heat generated by the heating elements is lost in form of conduction through the insulation layer (Q_L). (Kunii & Chisaki 2008, pp. 128–129; Lupi 2016)

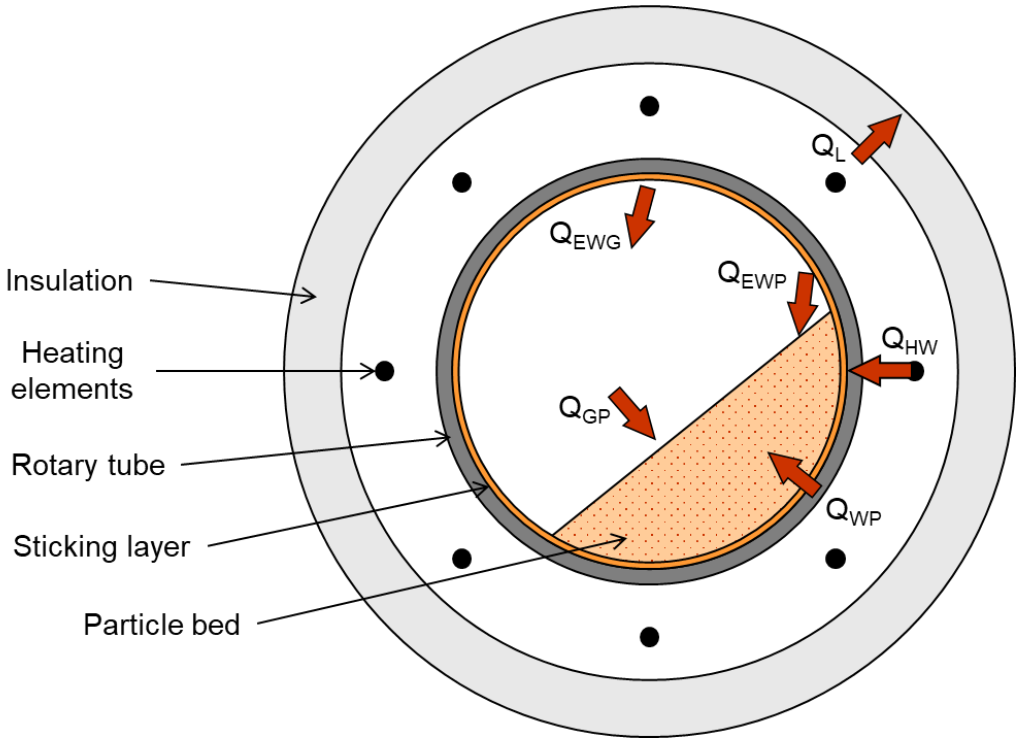

Figure 13. *Heat transfer mechanisms across the cross section of electric heated rotary kiln (Q=heat flow, L=heat loss, H=heating element, W=rotary tube wall, P=solid particles, EW=empty fraction of rotary tube wall, G=gases inside the rotary tube), adapted from (Kunii & Chisaki 2008)*

In a fraction of the rotary tube wall where solid particles are not in contact with the wall heat is transferred by radiation. Some fraction of the radiant heat from the empty fraction of rotary tube wall arrives at the surface of the particle bed (Q_{EWP}) and some fraction of radiation is absorbed by the gases inside the rotary tube (Q_{EWG}). The heat absorbed by the gases is emitted to the surface of particle bed (Q_{GP}). In continuous operation partial pressure of CO_2 in the kiln gases is expected to be high. Some heat from the empty fraction of the tube wall or the gases may be absorbed by cooler areas of the rotary tube wall. Heat is transferred by conduction in the fraction where particles are in contact with the rotary tube wall (Q_{WP}). (Kunii & Chisaki 2008; Shahin *et al.* 2016)

Heat losses from the rotary kiln reduce thermal efficiency. There are heat losses from both ends of the kiln and through the insulation layer. Heat is also lost by the hot lime product and gases exiting the kiln. Heat losses are impossible to avoid completely. (Kunii & Chisaki 2008; Lupi 2016) As mentioned in chapter 2, in traditional lime kilns heat is recovered from lime product by using combustion air as a cooling agent whereas hot flue gases are used to preheat the limestone. The latter is possible to utilize in case of indirectly heated lime kiln. However, combustion air is not needed in the new concept. Thus, new ways to exploit the waste heat from the product need to be developed.

Sticking of raw material to the tube walls hinders heat transfer from the tube wall. Sintering of the particles is enhanced by presence of CO_2 in the kiln gases (Stanmore & Gilot 2005, p. 1719). Impurities from the limestone may cause problems for heat transfer inside the rotary tube. Melting point of the impurities might be lower than the temperature in the kiln which enhances sticking of the solid particles to the inner surface of the cylinder. This significantly reduces heat transfer and thermal efficiency of the kiln. (Kunii & Chisaki 2008) The movement of the particle bed on the rotary tube wall also affects heat transfer. Slipping of the particle bed on the rotary tube wall should be prevented. If the bed slips instead of rolling, particles do not mix well and it causes temperature differences inside the bed. Through rolling motion, mixing of the bed is most effective. To minimize slipping motion in the rotary tube, the volumetric fraction of particle bed of the total cross sectional area of the rotary tube should be high enough. (Kunii & Chisaki 2008; Boateng 2016)

4. MATERIALS AND METHODS

Controlled experiments with a laboratory scale electric heated rotary kiln are performed in this thesis. The main objective of the experiments with the laboratory scale rotary kiln is to study calcination of calcium carbonate based materials in different gas atmospheres and under different CO_2 partial pressures. Calcination degree and reactivity of the samples treated under different process conditions and the CO_2 content in the kiln off-gases are examined. Following chapters describe first the laboratory scale rotary kiln used in experiments. Next the methods of analysis used for analyzing the samples are presented. In third subchapter, test matrix for the experiments is discussed, and finally the variables and boundaries related to the experiments are introduced.

4.1 Laboratory scale rotary kiln

Controlled experiments are performed with a laboratory scale electric heated rotary kiln. The kiln is manufactured by Nabertherm (RSRC 80/100/15 H2). A schematic illustration of the kiln is presented in Figure 14. The kiln is a batch type. However, it is possible to demonstrate continuous process to some extent. The feeder system consists of a 5 liter filling funnel and a screw conveyor. The filling funnel is equipped with electronic vibration generator to improve powder feed. The screw conveyor feeds the raw material to the rotary tube. Inclination of the kiln is adjusted manually. Raw material warms up as it passes the heated area and cools down in the insulated and cooled area. At the end of the rotary area the product falls into a collection bottle.

The kiln is equipped with gas supply system for several gases. Air and CO_2 were used in the experiments of this study. Gas input pipe is located in the collection bottle. Gas flows are controlled with manual rotameters. Gases flow upstream to material flow in the rotary tube. After the kiln gases are led to gas analyzer. The gas analyzer measures the concentration of oxygen (O_2), hydrogen (H_2), carbon monoxide (CO), carbon dioxide (CO_2) and methane (CH_4). The ranges for the concentrations are 0–25 %, 0–100 %, 0–50 %, 0–50 % and 0–30 %, respectively. Gas analyzer may show values outside these ranges if the concentration is higher but those results are not reliable. The most important results in these experiments are the concentration of CO_2 and O_2. These values indicate whether calcination occurs or not and to which extent. CO may also occur in the gases. However, H_2 and CH_4 are not expected to appear in kiln off-gases.

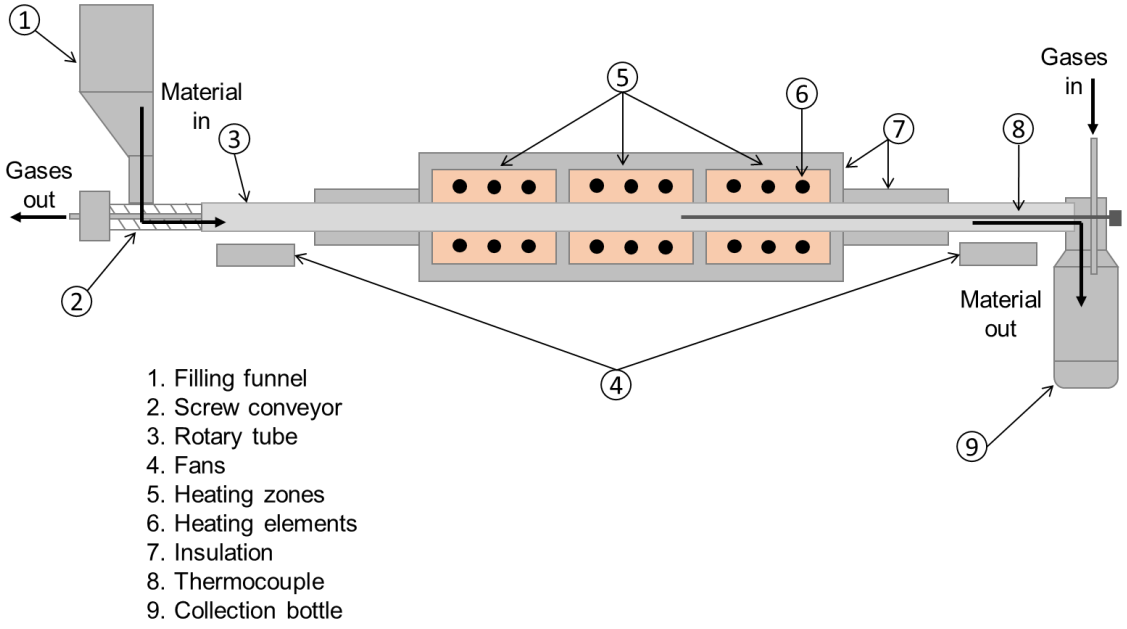

Figure 14. *Schematic illustration of the laboratory scale electric heated rotary kiln*

Tube material of the rotary tube is Kanthal APM. Rotary tube was pre-treated to oxidize the surface and to increase its emissivity and chemical resistance. At the end of the Kanthal APM tube before container bottle there is an additional tube part which rotates like the Kanthal APM tube but is made of different material. With temperatures above 500 °C the Kanthal APM tube must rotate to prevent deformation. Thus, during the cooling section of the experiment runs some unreacted raw material may reach the collection bottle.

The kiln is electric heated with silicon carbide heating elements. The heating elements are divided into three heating zones. Each of the zones is controlled separately which improves temperature uniformity inside the kiln. In each control area there are six heating elements. The heated area is insulated with fiber sheet insulation material. At the ends of the furnace tube there are fans for cooling. Thermocouple is used to measure the temperature inside the kiln. It is attached to the kiln from the end. Measurement point of the single-point C-type thermocouple is located approximately to the center of the heated area. In addition, a multipoint K-type thermocouple with 14 temperature measurement points is used for the longitudinal temperature distribution measurement. In Table 4, main characteristics of the laboratory scale rotary kiln are presented.

Table 4. *Characteristics of the laboratory scale rotary kiln*

Characteristic	Value
Lenght of Kanthal APM tube [m]	2.05
Inner diameter of Kanthal APM tube [mm]	66
Emissivity of fully oxidized Kanthal APM surface [-] (Kanthal 2018)	0.7
Total lenght of rotary tube [m]	2.3
Total lenght of heated area [m]	1.0
Maximum operating temperature of the kiln [°C]	1550
Maximum allowed temperature for Kanthal APM tube [°C] (Kanthal 2018)	1250

The kiln can be operated either with vacuum or slight positive pressure (+30 – +90 mbar) relative to atmospheric pressure. For vacuum operation, a diaphragm pump is added to the system. In this type of pump gases are not in contact with lubricant which prevents contamination of the gases. The level of vacuum was tested before actual experiments and a vacuum of 90 mbar in the kiln was reached. The pressure of the kiln is expressed by manual pressure gauges and with pressure and vacuum transmitters.

All experiment runs have a similar temperature program structure. In Figure 15, the basic program structure is illustrated. First, the kiln is heated to the set temperature (section 1). During the heating section, the furnace tube rotates and possible gas supply is on. Heating rate is fixed in these experiments to 300 °C/h. After the set temperature is reached screw conveyor is switched on and raw material is fed to the kiln (section 2). In third program section, the set temperature is maintained and furnace tube rotates but screw conveyor is switched off (section 3). The objective is that all the raw material fed to the kiln would reach the collection bottle. Last section is cooling (section 4). Cooling rate is 300 °C/h. When the kiln is operated with vacuum, a pumping section of 10 minutes is added before heating. In addition, after cooling a purging section is added: pump is switched off and nitrogen is fed to the kiln for purging.

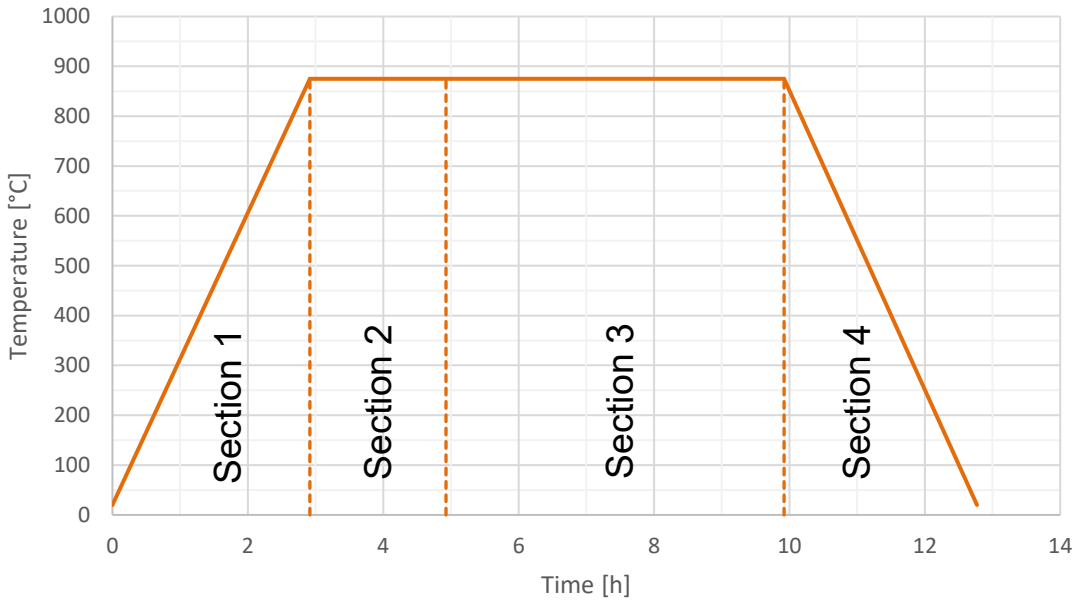

Figure 15. *Basic temperature program structure of the experiment runs*

4.2 Methods of analysis

Calcium carbonate based raw materials are calcined in the laboratory scale electric heated rotary kiln after which calcination degree of the samples is determined using thermal analysis techniques and X-ray diffraction (XRD). The used thermal analysis techniques are thermogravimetry (TG) and differential scanning calorimetry (DSC) preformed with a simultaneous TG-DSC analyzer. In addition, reactivity of some samples was measured according to standard (SFS-EN 459-2 2011). Particle size and dry matter content of the raw materials were measured as well. Analysis methods mentioned above are presented in next chapters.

4.2.1 TG-DSC

The main purpose of TG is to monitor change in sample mass with respect to temperature with a build-in balance. With DSC technique the difference in heat flow between a sample and inert reference substance can be observed. A reference holder is placed next to the sample holder. Thermocouples detect differences in temperature between the reference holder and sample holder. The temperature difference is then converted to thermal energy difference. These measurements are carried out under controlled temperature program. (Gaisford *et al.* 2019)

The TG-DSC apparatus used in the analysis is manufactured by Netzsch GmbH (STA 449 F1 Jupiter). The apparatus consists of furnace, heating elements, protective tube, radiation shields, thermocouples, sample carrier, balance system and gas supply

system. Proteus Analysis 6.0 software by Netzsch GmbH was used for the analysis of measurement data.

The heating program used in analyses consisted of linear heating section (10 °C/min), short constant segment at maximum temperature (10 min, either 1300 °C or 1100 °C) and cooling (40 °C/min). Analyses were performed in nitrogen atmosphere with gas flow of 60 ml/min. TG-DSC analysis was performed for raw materials as received and for all the samples treated in the laboratory scale rotary kiln experiment. To determine calcination degree of the sample treated in laboratory scale rotary kiln mass change of the sample is compared to the mass change of raw material as received. Additionally, enthalpy change due to calcination can be determined from DSC curves.

4.2.2 XRD

In this thesis, X-ray powder diffraction technique is used for confirmation of the calcination degrees determined with TG-DSC analysis. In general, XRD is used for determination of crystal structures and can also be used for identification of chemical composition of powders. In XRD measurement a beam of X-rays is directed to the sample. The crystals of the sample diffract the rays with a scattering angle of 2θ. The resulting data can be plotted showing intensity versus scattering angle. Peak positions, intensities, shapes and widths observed from the diffraction pattern are important parameters for analysis. Powder chemical composition is possible to identify by comparing diffraction pattern of the sample to diffraction patterns of known compounds. The intensities of the peaks indicate the amount of different components in the sample. A quantitative analysis can be done with respect to peak intensities and areas. (Girolami 2016, pp. 441–444)

In this thesis a qualitative analysis is performed for all the samples from laboratory scale rotary kilns. Quantitative analysis was not performed due to its complexity as the raw materials were not pure $CaCO_3$ but included other components and impurities. The equipment used for XRD analysis is manufactured by PANalytical (XRD X'Pert Powder). The diffraction patterns of the samples are compared to diffraction patterns of $CaCO_3$, CaO and $Ca(OH)_2$. To confirm the calcination degrees determined in TG-DSC analysis comparison is done also between diffraction patterns of the samples.

4.2.3 Reactivity measurements

Reactivity of the calcined samples is measured based on standard (SFS-EN 459-2 2011). Test arrangement had some differences compared to the standard. The blade shape differed from the blade stirrer presented in the standard and sample sizes were

smaller in some of the experiments due to small amount of output product from the laboratory scale rotary kiln. Either 50 g, 100 g or 150 g sample sizes were used. Despite the varying sample size, the mass ratio of sample and water was kept constant. Temperatures of the water and the samples varied from 21.5 °C to 23.2 °C based on ambient temperature.

Measured temperature values are plotted as a function of time, and the graph is called wet slaking curve. From the graphs can be seen the maximum observed temperature and time required to reach the temperature. Usually the time necessary to reach 60 °C is an interesting result but only in a few of the measurement 60 °C was reached. Thus, it is more reasonable to measure the time necessary to reach 50 °C.

4.2.4 Other methods

Before the actual experiments dry matter content and particle size of the raw materials were analyzed. Moisture analyzer used in analysis is manufactured by Precisa (335 XM 50). Moisture in the raw materials affects reactions in the laboratory scale rotary kiln and thus the results. When the raw material enters the laboratory scale rotary kiln it first dries out. Evaporated moisture in the kiln of gases lowers partial pressure of CO_2 to some extent depending on the moisture content. On the other hand, it also affects sintering of the product. After the kiln, moisture is condensed from the kiln off-gases before utilization of CO_2.

For particle size measurement an equipment manufactured by Malvern Panalytical (Mastersizer 3000) was used. Particle size has influence on the calcination rate for example. Thus, it is also an important factor to take into account when analyzing the results.

4.3 Test matrix

The main objective of the experiments is to test calcination in CO_2 atmosphere. In an indirectly heated kiln, partial pressure of CO_2 is high compared to traditional kilns were nitrogen from the combustion air and other flue gases lower the partial pressure of CO_2. In Table 5, a test matrix is presented. First case, air “normal” pressure (Air), is a reference case to which the other two cases are compared. In this case the supplied gas is air and calcination is tested in two temperatures, 875 °C and 925 °C. Pressure in case Air experiment runs is slight positive pressure (+30 – +90 mbar) relative to atmospheric pressure. In second case, CO_2 “normal” pressure (CO_2), CO_2 is fed to the kiln. The aim of this case is to test calcination in pure CO_2 atmosphere and in pressure close to atmospheric pressure (30–90 mbar positive). The pressure during the test run may vary

a little due to changes in the process (temperature, released CO_2). Due to higher partial pressure of CO_2 in the kiln, higher temperature is tested compared to case Air to achieve high enough calcination degrees. In third case calcination is tested in vacuum without gas supply. Partial pressure of CO_2 is lower in consequence of operation in vacuum which enables lower temperature compared to case CO_2. CO_2 concentration in kiln off gases is expected to be high which would enable more feasible CO_2 capture. In industrial applications calcination degree of the products is usually approximately 95 % as mentioned in chapter 2.1, and thus this is set as a target value.

Table 5. *Test matrix for the experiments*

Case acronym	Short case description	Temperature [°C]	Feed gas
Air	Air “normal” pressure	875	Air
		925	Air
CO_2	CO_2 "normal" pressure	875	CO_2
		925	CO_2
		975	CO_2
VAC	Vacuum	875	-
		925	-

Kiln experiments are performed for three different raw materials:

- cement raw meal,
- ground limestone, and
- lime mud from causticizing process.

Cement raw meal consists of limestone and other additional cement raw materials mentioned in chapter 2.1 required for clinker formation. The second raw material is pure limestone. According to the manufacturer, $CaCO_3$ content is 96.5 %. Third raw material is lime mud from pulp mill’s causticizing process and it includes some residues from the chemical recovery process. All above mentioned experiment cases are performed for each raw material.

4.4 Test parameters and variables

Before actual experiment runs, a reasonable rotation speed for the screw conveyor was determined. Rotation speed of 0.5 rpm was chosen based on the mass flows of raw materials. However, as blockages in the rotary tube turned out to be a problem rotation speed was reduced to 0.4 rpm. Dry matter content of the lime mud as received was 78.88 %. Due to its high moisture content, lime mud agglomerated to the screw

conveyor. Thus, it was dried at 105 °C. All experiments and analyses are performed for dried lime mud unless otherwise noted. Vibration of the filling funnel was adjusted for the raw materials. Residence time and thickness of powder bed in the rotary tube are dependent on input mass flow of raw material and rotation speed and inclination of the rotary tube. The chosen values for rotation speed and inclination of the rotary tube, and total throughput time are presented in Table 6. These values were used in all experiment runs. With higher rotation speeds bed thickness reduced too much and the bed was slipping instead of rolling.

Table 6. *Test parameters for the laboratory scale rotary kiln experiments*

Test parameter	**Value**
Rotation speed of the rotary tube [rpm]	1.0
Inclination of the rotary tube [°]	2.5
Total throughput time [h]	1

Duration of the program sections 2 and 3 was adjusted based on the desired output mass. Additionally, due to clogging of the rotary tube the duration of the sections was reduced especially in case of lime mud. Gas flow in cases Air and CO_2 was approximately 30 l/h in cases in which gas analyzer was not used. Gas analyzer requires higher gas flow, and thus in cases in which gas analyzer was used gas flow was approximately 50 l/h. Test variables for the laboratory scale rotary kiln experiments are presented in Table 7.

Table 7. *Test variables for the laboratory scale rotary kiln experiments*

Variable	Case acronym	T [°C]	Rotation speed of screw conveyor [rpm]	Gas input flow [l/h]	Section 2 duration [h]	Section 3 duration [h]	Raw material input [g/h]	Actual product output [g]
Cement raw meal	Air	875	0.5	30	2	5	825	939
		925	0.4	50	2	5	648	658
	CO_2	875	0.5	30	2	5	825	130
		925	0.5	30	2	5	825	56
		975	0.4	30	1	3	648	291
	VAC	875	0.5	0	2	5	825	356
		925	0.4	0	1	3	648	30
Ground limestone	Air	875	0.5	30	2	5	945	577
		925	0.4	50	2	5	756	864
	CO_2	875	0.5	30	2	5	945	1017
		925	0.5	50	2	5	945	1525
		975	0.4	50	1	3	756	128
	VAC	875	0.5	0	2	5	945	1253
		925	0.4	0	1	3	756	208
Lime mud	Air	875	0.5	50	3	5	480	25
		925	0.4	50	2	5	384	307
	CO_2	875	0.4	50	1	3	384	177
		925	0.4	50	1	3	384	155
		975	0.4	50	1	3	384	169
	VAC	875	0.4	0	1	3	384	72
		925	0.4	0	1	3	384	65

Dry matter contents of the raw materials are presented in Table 8. Additionally, densities of the raw materials were measured and the results are presented also in Table 8. Densities of the raw materials differ considerably and thus mass flows from the screw conveyor to the rotary tube differ as well.

Table 8. *Dry matter content and density of the raw materials*

Variable	Cement raw meal	Ground limestone	Lime mud
Dry matter content [%]	99.83	99.88	99.93
Density [kg/m^3]	1 219	1 756	719

In Figure 16, cumulative particle size distributions of the raw materials on logarithmic scale are presented.

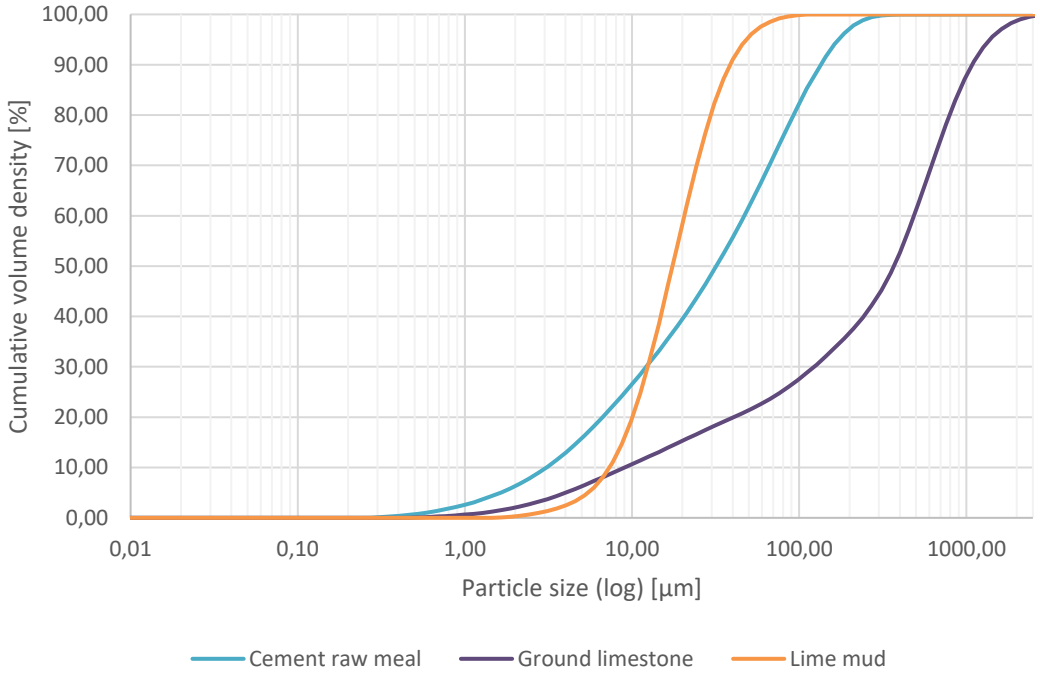

Figure 16. *Particle size distributions of the raw materials used in the experiments*

From the Figure 16 can be seen, that the particle size of ground limestone is considerably larger compared to cement raw meal and lime mud. Lime mud has smallest particle size. Particle size of the raw materials is taken into account when analyzing the results.

5. RESULTS AND DISCUSSION

In this chapter the results from experiments with laboratory scale rotary kiln are compiled. The measured and studied properties are presented. The research questions concerning calcination degree and reactivity of the lime product and amount of released CO_2 are answered. First, calcination degrees of the samples after experiments are presented. In second subchapter results from reactivity measurements are presented. The amount of released CO_2 and CO_2 concentration in kiln off gases are discussed in chapter 5.3. Final section of this chapter consists of overall discussion, other important measured properties and results and important aspects about the operation of indirectly heated laboratory scale rotary kiln.

5.1 Calcination degree

The effect of indirect heating and differing process conditions compared to traditional rotary kiln technologies to calcination degree of the lime product is one of the main focus area of this thesis. The theoretical maximum loss of mass during calcination is 44.0 % in case of complete calcination and pure $CaCO_3$. However, the raw materials in the experiments contain other components and impurities. The maximum mass loss due to calcination at 700–800 °C for the raw materials was analyzed with TG. Based on this mass change the $CaCO_3$ content of the raw material is determined. The results are presented in Table 9. Cement raw meal shows the lowest mass change and ground limestone highest. Cement raw meal contains also other components that are required for clinker formation and thus the amount of $CaCO_3$ is lower. In TG curve of ground limestone as received is a sharp mass reduction at 400–500 °C which is due to cracking of the powder. This was confirmed with an experiment performed by heating the ground limestone in a plate in chamber furnace to 500 °C. For ground limestone the mass change due to calcination is in line with the reported amount of $CaCO_3$ of 96.5 %. Based on the TG-DSC and XRD analysis of lime mud there are some unreacted $Ca(OH)_2$ residues from causticizing process. $Ca(OH)_2$ decomposes at around 400–500 °C (Zelić *et al.* 2002). The amount of $Ca(OH)_2$ in lime mud is approximately 5.1 % based on the mass change showed in TG curve. The effect of decomposition of $Ca(OH)_2$ and also the mass reduction due to crackling of ground limestone are eliminated from the mass change related to calcination.

Table 9. *Calcination related mass change and calculated $CaCO_3$ content of the raw materials as received determined by TG*

	Cement raw meal	**Ground limestone**	**Lime mud**
Mass change due to calcination	33.4 %	42.6 %	41.3 %
$CaCO_3$ content	75.9 %	96.8 %	93.9 %

In Figure 17, data from TG-DSC analysis of cement raw meal case CO_2 is presented. TG-DSC graphs for other cases and raw materials are presented in appendix A. There are four measurements included into the graph presented in Figure 17. “As received” refers to the cement raw meal as received, and “875 °C”, “925 °C” and “975 °C” to the samples treated in the laboratory scale rotary kiln at 875 °C, 925 °C and 975 °C respectively. A mass change at around 400 °C can be observed in TG curve of sample treated in the laboratory scale rotary kiln at 925 °C. Similar mass change was observed also from TG curves of same other samples presented in appendix A. This is most likely due to decomposition of $Ca(OH)_2$. After the experiment runs with laboratory scale rotary kiln, samples were stored in airtight plastic bags. However, before TG-DSC measurements the samples that were about to be measured were in contact with ambient air, and CaO in the samples may have reacted with moisture in the air and formed $Ca(OH)_2$. From the TG curves in Figure 17 can be seen that the sample treated at 875 °C shows a considerable mass change at 700–800 °C compared to samples treated at 925 °C and 975 °C. This indicates that the calcination degree of the sample treated at 875 °C is significantly lower.

Enthalpy of change caused by a chemical or physical change in the sample can be observed from DSC curve. In Figure 17, the hatched area indicates enthalpy of change due to calcination at 600–800 °C and due to decomposition of $Ca(OH)_2$ at 300–400 °C. Enthalpy of change of a sample with high calcination degree is lower than of a sample with low calcination degree.

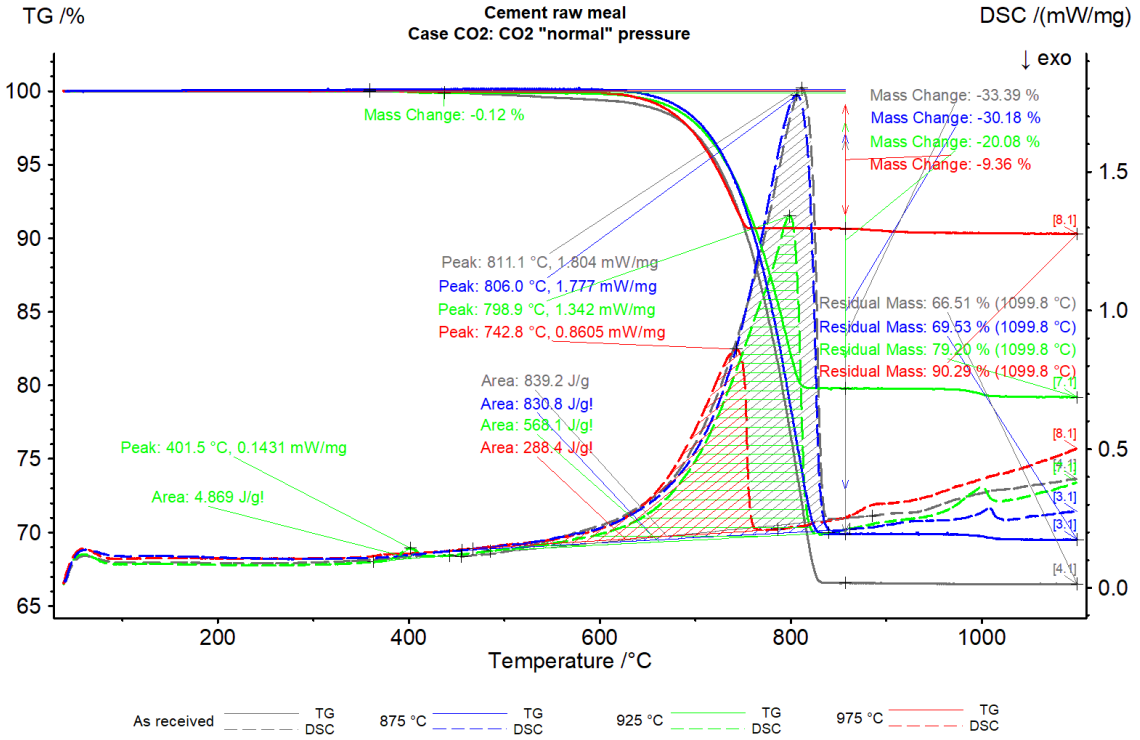

Figure 17. *TG-DSC curves of cement raw meal case CO_2: "CO_2 "normal" pressure" samples compared to cement raw meal as received*

Table 10 shows the calculated calcination degrees of all the samples treated with the laboratory scale rotary kiln. Calcination degree is calculated by comparing the mass change determined from TG curves as presented in Figure 17 to raw materials as received mass changes presented in Table 9. Target value for calcination degree is 95 %.

Table 10. *Calcination degree of the samples from laboratory scale rotary kiln determined by TG*

Cases			Calcination degree		
Case acronym	**Short case description**	**T [°C]**	**Cement raw meal**	**Ground limestone**	**Lime mud**
Air	Air "normal" pressure	875	47.8 %	29.3 %	96.5 %
		925	98.8 %	94.6 %	99.0 %
CO_2	CO_2 "normal" pressure	875	9.7 %	3.7 %	0.0 %
		925	39.8 %	17.8 %	61.3 %
		975	72.2 %	54.8 %	56.1 %
VAC	Vacuum	875	59.2 %	72.7 %	82.1 %
		925	81.2 %	80.9 %	68.8 %

Case Air acts as a reference case for the other two cases. Target calcination degree in case Air was achieved at 875 °C for lime mud and at 925 °C for cement raw meal. Taking into account measurement accuracy and other aspects related to the measurements and

analysis calcination degree of ground limestone at 925 °C is in line with the target value. Target value for calcination degree was not achieved in cases CO_2 and VAC. The highest achieved calcination degree in case CO_2 is 72.2 % for cement raw meal at 975 °C and in case VAC 82.1 % for lime mud at 875 °C.

In case Air the increase in temperature clearly increased the calcination degree. However, in case CO_2 calcination degree of lime mud is lower at 975 °C compared to 925 °C. Same pattern can be noted in case VAC. Taking this into account, increasing temperature in cases CO_2 and VAC will probably not increase the calcination degree of the lime product at least in case of lime mud. This result indicates that recarbonation occurred at the end of the kiln in cases CO_2 and VAC. In case Air air flow to the kiln purged the CO_2 away from the calcined product, and thus prevented recarbonation.

Highest calcination degrees are achieved in case Air while in case CO_2 calcination degrees are lowest despite the highest temperature. However, at 875 °C calcination degrees are higher in case VAC compared to case Air apart from lime mud. Thus, it would be justified to assume that calcination degrees in case VAC at 925 °C would be higher compared to calcination degrees in case Air at same temperature but the results are reversed. This also indicates that recarbonation probably occurred in case VAC at the end of the kiln. Partial pressure of CO_2 was highest in case CO_2 experiments which affects the calcination rate and thus is one reason for lowest calcination degrees. Highest calcination degrees are achieved with lime mud of the three raw materials whereas ground limestone has lowest calcination degrees. A parameter that affects calcination rate is particle size. Ground limestone was coarsest and lime mud finest of the three raw materials when it comes to particle size which explains the differing calcination degrees.

Enthalpies of change in the sample caused by calcination reaction are presented in Table 11. As mentioned in chapter 2, reaction enthalpy of calcination is 178.3 kJ/mol and molar mass of $CaCO_3$ is 100 g/mol. Calculated from these values, the minimum theoretical energy consumption for calcination is 1781.4 kJ/kg of $CaCO_3$. However, reaction enthalpy depends on the temperature and the above mentioned reaction enthalpy is related to temperature of 25 °C. This is one reason for considerably smaller enthalpies of change of the raw materials as received. The enthalpy of change for samples calcined in the laboratory scale rotary kiln is smaller compared to raw materials as received because the content of $CaCO_3$ is smaller. Also, cement raw meal contains considerably less $CaCO_3$ than ground limestone or lime mud. This data is relevant when developing the electric heated kiln concept. Especially, in indirectly heated kilns efficiency of heat transfer is central. To optimize the heat transfer in electric heated kiln the actual values of enthalpies of change are valuable.

Table 11. *Ethalpy of change of the samples in consequence of calcination determined by DSC*

Cases			Enthalpy of change [J/g]		
Case acronym	**Short case description**	**T [°C]**	**Cement raw meal**	**Ground limestone**	**Lime mud**
	As received		839.2	1 222.8	1 388.7
Air	Air “normal” pressure	875	432.7	869.9	41.9
		925	5.5	55.3	0
CO_2	CO_2 “normal” pressure	875	830.8	1 253.0	1 428.0
		925	411.8	996.8	514.6
		975	288.4	669.8	585.2
VAC	Vacuum	875	397.6	349.7	246.1
		925	189.4	273.0	453.8

In Figure 18, diffractograms of case CO_2 samples of cement raw meal from XRD analysis are presented. Uppermost is cement raw meal as received, then the samples treated at 875 °C, 925 °C and 975 °C in the laboratory scale rotary kiln, and on the bottom is a sample which is fully calcined with TG-DSC. In the TG-DSC measurement the cement raw meal sample was heated to 1300 °C to fully calcine it. Similar measurement with TG-DSC was performed for ground limestone and lime mud as received for a fully calcined reference. After the TG-DSC measurement samples were in contact with ambient air and reacted moisture in the air. $Ca(OH)_2$ was formed which is evident in the diffractograms of the samples. The phases of $CaCO_3$, CaO and $Ca(OH)_2$ are marked on the peak list on bottom of the Figure 18. Additionally, the main peak of the $CaCO_3$, CaO and $Ca(OH)_2$ phases are illustrated with blue, orange and green squares respectively. Diffractograms of other cases and raw materials are presented in appendix B.

From the Figure 18 can be seen that pattern of as received cement raw meal does not match with the peaks of CaO phase but matches with the peaks of $CaCO_3$ phase, and on the other hand pattern of fully calcined cement raw meal does not match with the peaks of $CaCO_3$ phase but matches with the peaks of CaO phase. In fully calcined sample some of the clinker phases have already formed which can be noted from the diffractogram as there are some peaks that do not match with the patterns of other samples nor the patterns of $CaCO_3$, CaO or $Ca(OH)_2$ phases.

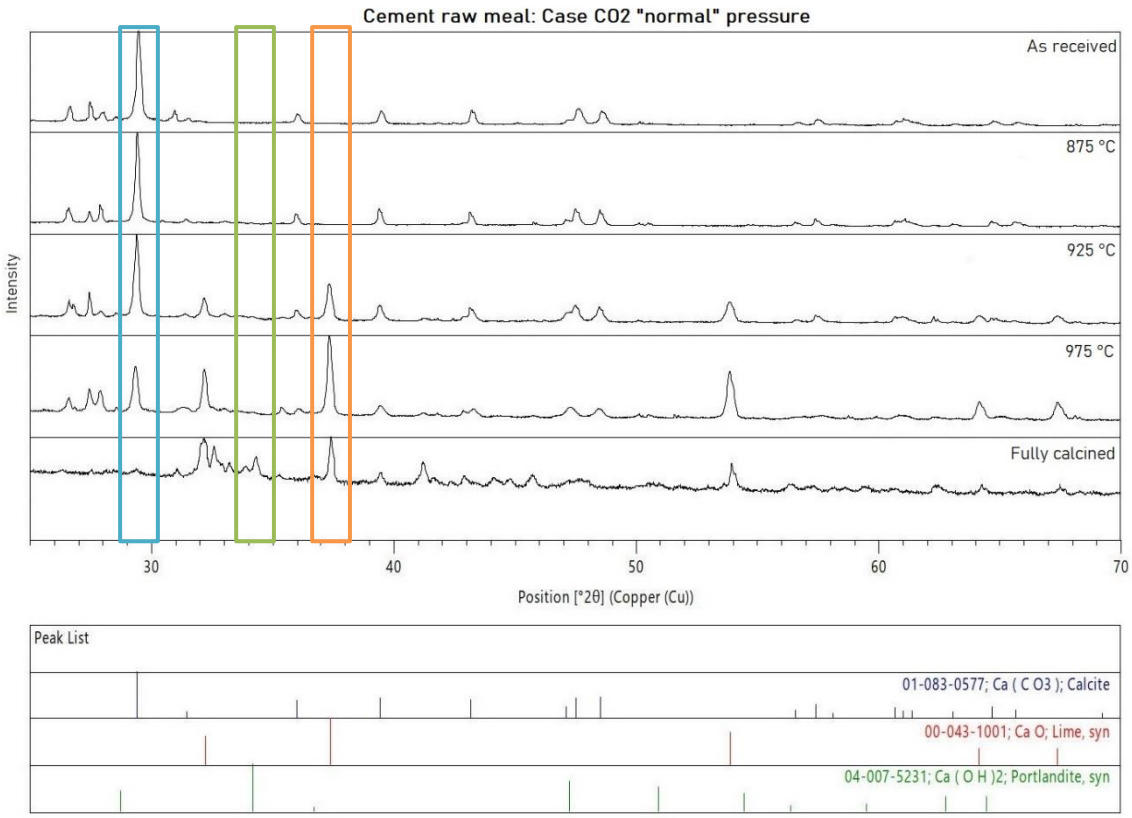

Figure 18. *Diffractograms of cement raw meal case CO_2 samples after the laboratory scale rotary kiln calcined at 875 °C, 925 °C and 975 °C compared to as received and fully calcined cement raw meal, main peaks of $CaCO_3$, CaO and $Ca(OH)_2$ phases marked with blue, orange and green squares respectively*

The pattern of sample treated at 875 °C matches with the pattern of cement raw meal as received. There are no peaks that match with the peaks of CaO phase. From these observations can be concluded that calcination of $CaCO_3$ has not occurred. In the pattern of the sample treated at 925 °C there are some peaks that match with the peaks of CaO phase. However, there are still higher peaks that match with the peaks of $CaCO_3$ phase. In pattern of sample treated at 975 °C the peaks that match with CaO phase are higher and peaks that match with $CaCO_3$ are lower compared to the pattern of sample treated at 925 °C. Based on this a conclusion can be made that calcination degree of the sample treated at 975 °C is higher compared to the sample treated at 925 °C. XRD analyses of cement raw meal case CO_2 samples are in accordance with the calcination degrees presented in Table 10. A similar qualitative analysis is conducted for all other cases as well, and results of calcination degree based on TG-DSC analysis are in accordance with the qualitative analysis based on XRD patterns presented in appendix B.

5.2 Reactivity

Reactivity was not measured for all the cases and temperatures. Some samples from the laboratory scale rotary kiln were too small, and it is not reasonable to measure reactivity of the sample which does not contain or contains only small fraction of CaO. However, at least one sample per case and raw material are involved. The decision of which samples to measure was done based on the calcination degree and the amount of product after the rotary kiln experiment. In Figures19, 20 and 21 wet slaking curves for cement raw meal, ground limestone and lime mud respectively are presented.

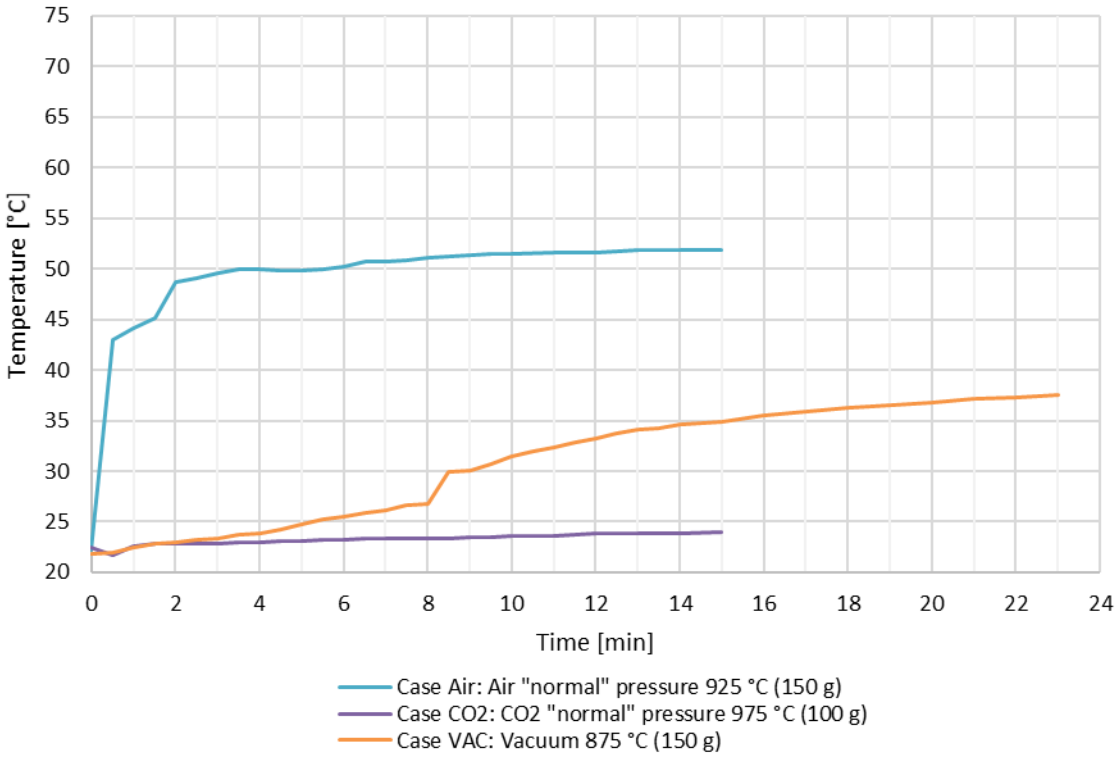

Figure 19. *Wet slaking curves, cement raw meal*

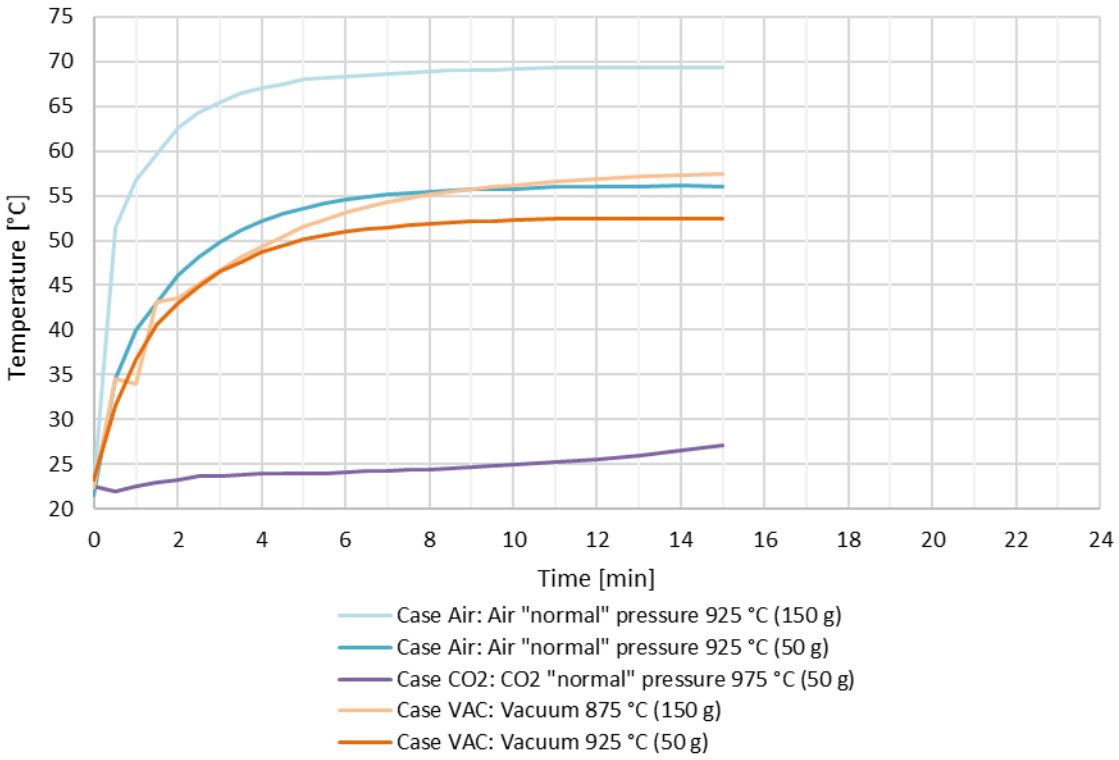

Figure 20. *Wet slaking curves, ground limestone*

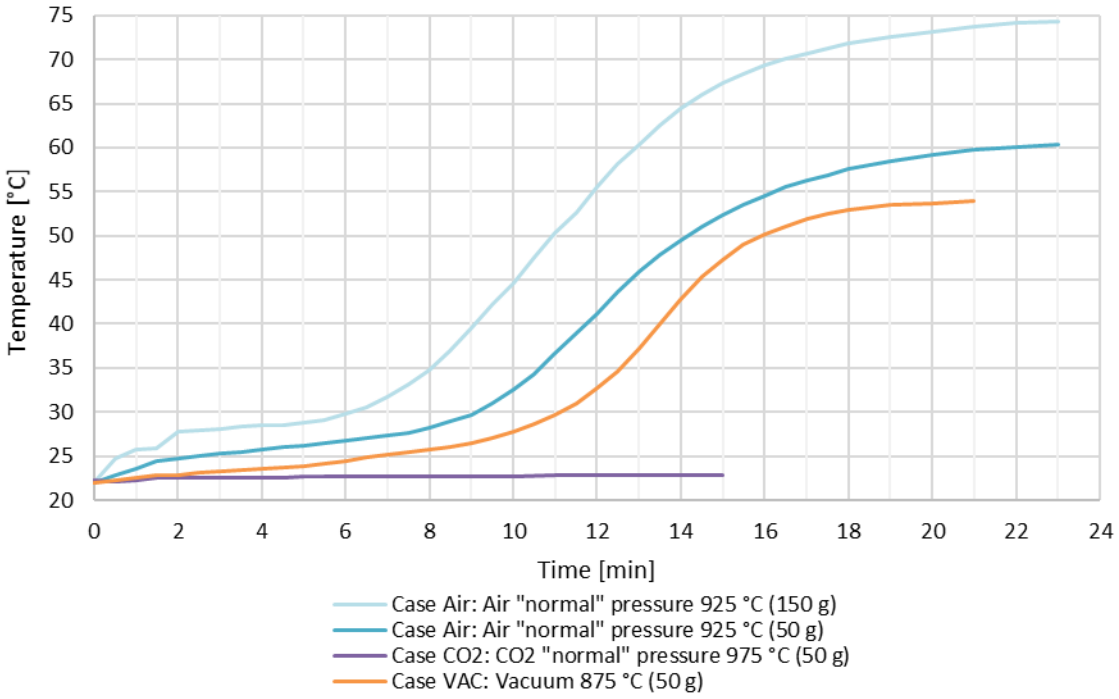

Figure 21. *Wet slaking curves, lime mud; reactivity rate low in the beginning due to sintered particles*

The effect of sample size has to be considered when analyzing the reactivity results. Two measurements were done for ground limestone and lime mud case Air samples calcined at 925 °C to compare hydration reaction between sample sizes 150 g and 50 g. For both

raw materials the maximum observed temperature for the 50 g sample size was 80 % of the maximum observed temperature for the 150 g sample size. Apart from the maximum temperature, reaction rate was higher for 150 g sample size. The results are rational as there is more of CaO to react, and thus more energy is released to heat the system.

Hydration reaction was fastest for samples of case Air. In addition to reaction rate, the maximum observed temperatures were highest for case Air. Reactivity of case VAC samples is also high and close to case Air. Case CO_2 showed lowest reactivity rates and maximum temperatures. However, samples of case CO_2 did not mix as well as other samples which affected the measurement and results. This was with high certainty not related to differences between samples of different cases but only an unfortunate contingency. A blade shape in accordance with the standard (SFS-EN 459-2 2011) would improve mixing. However, in case CO_2 the amount of CO_2 in the kiln gases in the laboratory scale rotary kiln was highest. CO_2 enhances sintering of the particles and thus reduces reactivity. The effect of CO_2 in the kiln gases in electric heated rotary on the reactivity of the product requires more studying. Also, CaO content affects the reactivity of the sample. The higher the calcination degree is, the more there is CaO to react and thus more energy is released.

The reaction is clearly faster for ground limestone compared to lime mud. However, the maximum temperatures reached in the reactivity measurements are higher in case of lime mud. The reactivity is not particularly important characteristic for cement raw meal as lime is only an intermediate product in clinker production. However, measurements were performed for cement raw meal for comparison. Particle size is one possible explanation for the slow reaction rate of lime mud samples. Reactivity of particles decreases and the particle starts to sinter if they are heated unnecessarily after complete calcination as discussed in chapter 2. In the experiments with laboratory scale rotary kiln, total throughput time was same for all experiment runs. Thus, because the lime mud particles calcine faster than coarser ground limestone particles, the calcined lime mud particles have started to sinter. Also, in cases VAC the low pressure in the kiln increases calcination rate and sintering of the particles may occur in greater extent than in case Air experiment runs with laboratory scale rotary kiln. In further experiments, the throughput time should be adjusted for each raw material to achieve soft burnt particles and high reactivity.

According to standard (SFS-EN 459-1 2015) high reactivity lime should reach temperature of 60 °C in less than 10 minutes. In the experiments of this thesis, only ground limestone case Air sample fulfils the condition by reaching 60 °C in approximately 1.5 minutes. Lime mud Case Air sample (150 g) also reaches 60 °C but in 13 minutes.

None of the case CO_2 or case VAC samples reach 60 °C. Reasons for low reactivity might be too high temperature in the laboratory scale rotary kiln, too long throughput time or the high partial pressure of CO_2 in the kiln gases. All of these factors enhance sintering and must be considered when planning further experiments.

5.3 Amount and concentration of released CO_2

Mass balances of calcination in the laboratory scale rotary kiln for each raw material are presented in Figures 22, 23 and 24. In mass balance calculations, calcination degree is assumed to be 100 % and calculations are based on 1 kg/h input mass flow. $CaCO_3$ contents presented in Table 9 are used and also moisture contents presented in Table 8 and $Ca(OH)_2$ residue in lime mud are taken into account. Impurities and other components in raw materials are assumed to exit the kiln in solid form with CaO because there is no data about their composition and how they would react in the kiln. Thus, the gases exiting the kiln are assumed to contain only CO_2 and H_2O. For density of CO_2 a value of 1.842 kg/m^3 at normal temperature and pressure (20 °C, 1 atm) is used in the calculations.

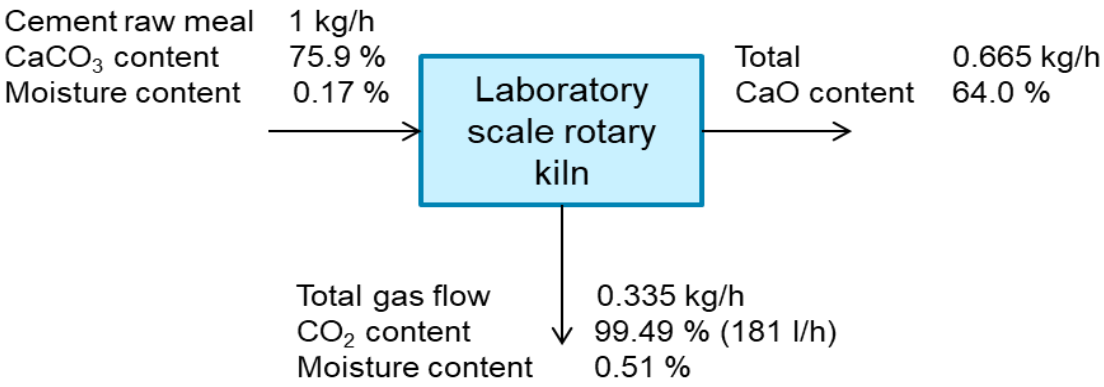

Figure 22. *Mass balance of the laboratory scale rotary kiln for cement raw meal*

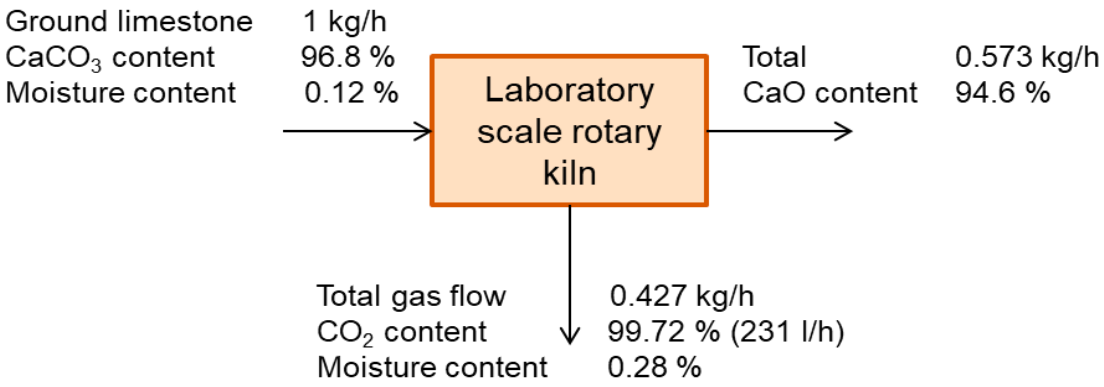

Figure 23. *Mass balance of the laboratory scale rotary kiln for ground limestone*

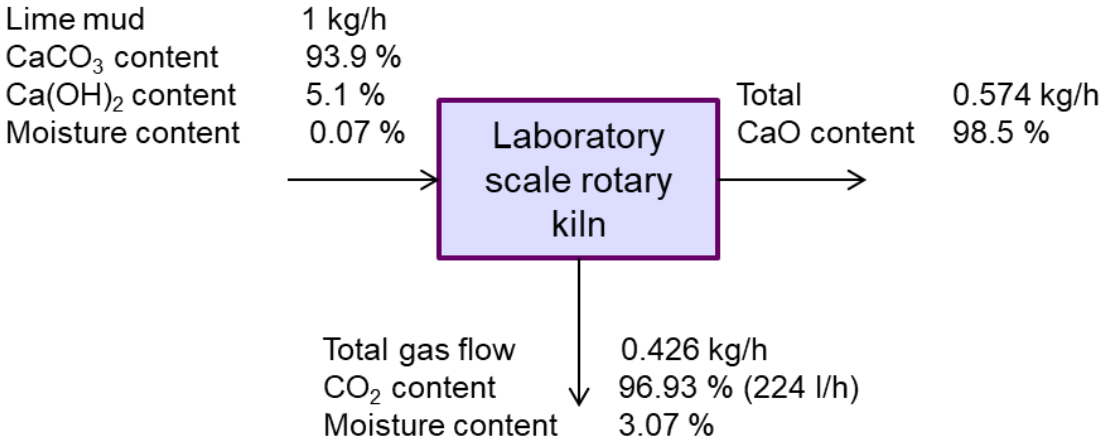

Figure 24. *Mass balance of the laboratory scale rotary kiln for lime mud*

CO_2 flow is highest in case of ground limestone. However, CaO content in solid output is higher for lime mud even though $CaCO_3$ content is higher in ground limestone. This is due to the $Ca(OH)_2$ which decomposes to CaO and H_2O in the kiln. For that reason also the moisture content in output gases is higher in case of lime mud. In case of cement raw meal output solid flow is higher and output gas flow lower compared to other two raw materials in consequence of higher content of other components in the raw material.

The actual input raw material flow and thus the output CO_2 flow depend on the rotation speed of the screw conveyor and density of raw material. Rotation speed of the screw conveyor in the experiments was either 0.4 rpm or 0.5 rpm and the chosen rotation speeds for each experiment run are presented in Table 7. In Table 12 the theoretical maximum CO_2 flows are presented for both rotation speed values.

Table 12. *Theoretical maximum CO_2 flow from the laboratory scale rotary kiln in case of rotation speed of the screw conveyor 0.4 rpm and 0.5 rpm*

		Cement raw meal	Ground limestone	Lime mud
Screw conveyor: 0.4 rpm	**Input mass flow [g/h]**	648	756	384
	CO_2 flow [l/h]	117	175	86
Screw conveyor: 0.5 rpm	**Input mass flow [g/h]**	825	945	480
	CO_2 flow [l/h]	149	218	108

Additionally, calcination rate and blockages in the kiln for instance affect the CO_2 flow from the kiln. Actual gas flows from the laboratory scale rotary kiln were not measured. However, from the gas analyzer data some information of the gas flow can be observed. In Figure 25 O_2, CO_2 and CO contents in the kiln off-gases in an experiment run with laboratory scale rotary kiln are presented. The case under consideration in Figure 25 is case Vacuum at 925 °C and ground limestone. Temperature profile of the heated area during the experiment run is also illustrated. Temperature is measured with the multipoint thermocouple. As presented in Table 7, section 2 or the rotation of screw conveyor lasted for an hour and section 3 lasted for three hours. Rotation speed of the screw conveyor was 0.4 rpm. Similar graphs for other cases in which gas analyzer was used are presented in appendix C.

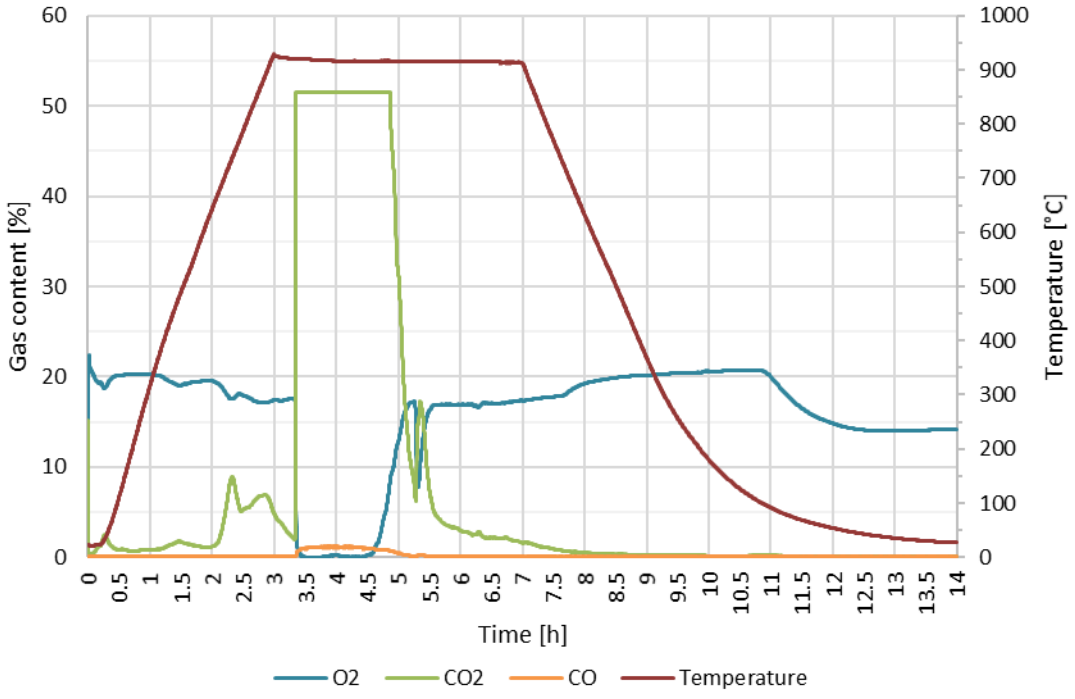

Figure 25. *O_2, CO_2 and CO contents in an experiment run with ground limestone, case Vacuum 925 °C; the measurement range of CO_2 content limited to 50 %*

From the graph can be seen that CO_2 content increased sharply 25 minutes after the beginning of section 2 (see Figure 15), that is approximately at the moment when the raw material reached the heated area and calcination started when taking into account the delay between the time when the CO_2 is released in the kiln and when it entered the gas analyzer. CO_2 content remained at high level, approximately at 51.5 %, for an hour and a half. During this time, CO was also formed in the kiln. Maximum CO content was 1.2 %. O_2 content on the other hand fell close to zero. Thus, there was almost pure CO_2 atmosphere in the rotary tube. For cement raw meal gas content graph of case VAC at 925 °C looks very similar. The only major difference is CO content which is higher in case of cement raw meal with a maximum value of 11.5 %. Actually, this was the highest content of CO in all of the cases. Compared to other two raw materials, in case VAC experiment runs with lime mud lower CO_2 contents were reached but otherwise the graphs are similar. However, mass flow to the kiln was lowest for lime mud and thus the CO_2 flow is also lowest.

In case Air experiment runs in general CO_2 content increases quickly after the raw material reaches the heated area similarly to the vacuum case presented above. There are one or two peaks in CO_2 content, and O_2 content falls to a minimum at the same time as CO_2 content reached its maximum value. Case CO_2 experiments are not as interesting as the other two due to the CO_2 supply to the kiln during the program and the differences in the CO_2 amount do not show in the graphs. However, in case CO_2 graphs of ground limestone the CO_2 content rapidly falls an hour after the screw conveyor started rotating and stayed at low level for several hours. No explicit reason was found for the phenomenon.

As mentioned in Chapter 2.5.1, the concentration of CO_2 in the flue gases is 22–-29 % and 14–33 % for traditional by combustion heated lime and cement plants respectively. The concentration of CO_2 in cases Air is similar but in cases CO_2 and cases VAC much higher compared to above mentioned ranges. The measurement ranges of the gas analyzer limit the examination of the deployment of CCUS technologies and especially the direct capture. However, the results seem promising. In case VAC for cement raw meal and ground limestone, the CO_2 concentration exceeded 50 %. In cases CO_2, 50 % concentration is also exceeded, but the supply of CO_2 to the kiln must be considered. To confirm the actual value for the CO_2 concentration a more comprehensive gas analysis is needed. In any case, the concentration in cases VAC are considerably higher compared to traditional kilns which facilitates the deployment of CCUS technologies.

5.4 Overall discussion

Experiments with laboratory scale rotary kiln showed good results when it comes to calcination in an electric heated rotary kiln. However, some major challenges, such as recarbonation and blockages emerged during the experiment that affected the results substantially. Recarbonation occurs in the kiln in temperatures below the required temperature for calcination and its effect to the calcination degrees of the samples is discussed in chapter 5.1. A longitudinal temperature profile measured with the multipoint thermocouple is presented in Figure 26. The temperature profile is of case Air at 925 °C of lime mud. The end of the heated are is illustrated in the graph with the orange dashed line.

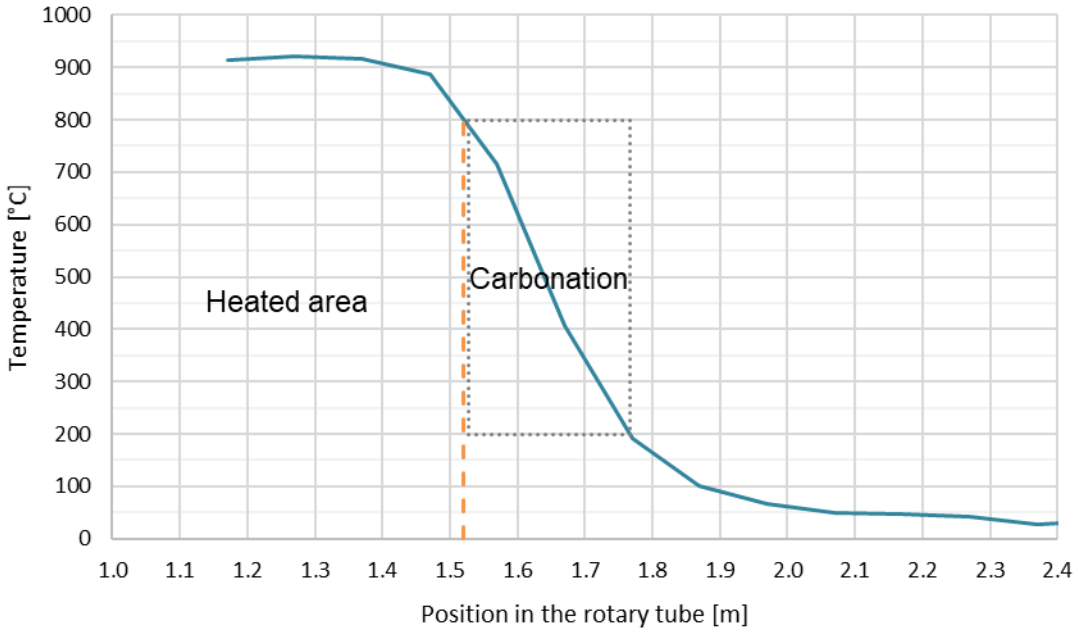

Figure 26. *Longitudinal temperature profile in the laboratory scale rotary tube from the experiment run of case Air at 925 °C for lime mud*

Temperature profile in the end of the kiln is optimal for recarbonation. Recarbonation is fast in temperature range of 500–800 °C but occurs considerably also in lower temperatures. It takes approximately 7 minutes for the product to cool from 800 °C to 200 °C. This area is marked to the Figure 26 with grey box. Recarbonation rate is fastest at the beginning of reaction, and thus 7 minutes is a long enough period for recarbonation to occur. Additionally, gas is fed to the end of the kiln to collection bottle and therefore in case CO_2 in the area where recarbonation occurs CO_2 is abundantly present. In case VAC on the other hand, CO_2 is not fed to the kiln but the CO_2 released from the calcination reaction is not purged away from the calcined product as in case Air. Measures to prevent recarbonation in the laboratory scale rotary kiln used in the

experiments are limited. In general, faster cooling and change of gas atmosphere after calcination are two possible solutions to prevent recarbonation. However, technical solutions require more studying and experimenting.

Blockages in the rotary tube were formed either in the beginning or in the end of the heated area. In cases Air and CO_2, the blockage formed mainly in the beginning of the heated area whereas in case VAC if there was blockage it was in the end of the heated area. At both ends of the heated area, temperature changes quickly which may be the reason for formation of blockages. Blockages in the rotary tube affect the raw material bed flow inside the rotary tube which on the other hand has an influence on the calcination degree and reactivity of the product and also the amount of released CO_2. Inner diameter of the rotary tube was very small compared to industrial scale lime and cement kilns. Even a small blockage clogs the tube quickly whereas in an industrial scale kiln small blockages do not have as large effect on the operation. Thus, as the upcoming experiments are planned to be performed with a larger pilot scale rotary kiln in which the effect of blockages may be lower. Notwithstanding, a technical solution may be required to prevent blockages. Calcination degree and reactivity of the product are more uniform if the blockages can be prevented.

There were also smaller factors that may have affected the results. The laboratory scale rotary kiln is gas-tight but some unavoidable gas leaks may occur due to operation and components. The leaks may affect the results especially in case VAC. In cases Air and CO_2 the pressure in the kiln is slightly positive compared to ambient pressure, and thus the direction of the leaks is from the kiln to ambient. Additionally, ambient temperature and air humidity may have influenced the results. In the line from rotary kiln to gas analyzer, plastic pipes were used. Gases, especially oxygen, may diffuse through plastic materials. The direction of diffusion depends on the oxygen content in the kiln off-gases. Either way, the diffusion of oxygen may have distorted the data received from gas analyzer. However, these factors only have minor effects on the results.

There are also some other aspects to consider when estimating the results. Lime mud was dried before the experiments in consequence of agglomeration in the feeder. Agglomeration may not be a problem in larger scale kilns but it requires confirmation with pilot scale experiments. Moisture content of the lime mud as received is high and it must be considered when planning further experiments and developing the electric heated kiln concept. Inside the kiln, moisture is first evaporated from the raw material. Steam in the kiln gasses reduces CO_2 partial pressure which may lower the temperature required for calcination but on the other hand steam enhances sintering of the particles and causes unnecessary heat losses. After the kiln, steam is condensed from the kiln off-gases. The

technical solution is straightforward, however when it comes to energy economics the issue is more complicated.

In case of cement, temperatures of the experiments are not high enough to form clinker phases. In the experiments of this thesis higher temperatures were not tested due to possible sintering and melting of the powder which would render the rotary tube unusable. However, this is not a problem when the kiln is purposed only to produce clinker. In this thesis the effect of electric heating on the formation of clinker phases was not studied but only the calcination of $CaCO_3$.

Based on the results of this thesis, experiments with pilot scale rotary kiln will be planned. High partial pressure of CO_2 in the kiln enables the deployment of direct capture after the kiln but also causes challenges. The main challenge based on the literature review and the experiments is recarbonation. Parameters for the pilot scale experiments are evaluated based on the results of this thesis. In addition to planning further experiments, the results are significant when developing electric heated rotary kiln technologies for lime and cement production.

6. CONCLUSIONS

In this thesis, calcination of calcium carbonate based materials in electric heated rotary kiln is studied. The objective is to recognize the advantages and challenges related to the electric heated kiln technology to improve the kiln concept and design and recognize the further experiment needs. International and national climate targets put pressure on decarbonization of industry sector in which cement industry is one of the main CO_2 emitters. Emissions from lime and cement production can be divided into process and energy related emissions. There are many measures to reduce energy related emissions whereas only CCUS technologies tackle process emissions. Alternative raw materials may also reduce process emission but in most cases they are not a feasible option. The most effective way to reduce process emissions is direct capture. By indirect heating, the CO_2 released in calcination reaction can be segregated from the flue gases originating from the combustion of fuel, and thus can be directly captured after the kiln. Condensation of the moisture in the gases and purification may be required before utilization of CO_2. Additionally, with electric heating energy related emissions are minimized compared to traditional kilns in which heat is generated by combustion. Electric heating is seen as a potential technology to reduce energy related CO_2 emissions from lime and cement production and to transform the unavoidable process emissions to usable products.

There is a scarcity of studies related to indirectly and especially electric heated lime kilns. LEILAC is an ongoing project that focuses on demonstrating indirectly heated vertical kiln technology. However, heat is generated by combustion of natural gas instead of electricity. A new project, LEILAC 2, is already established to demonstrate electricity as heat source. Results are not yet released of the experiments of LEILAC project. However, the results are said to be promising, and the establishment of LEILAC 2 speaks on behalf of it. Additionally, indirect heating with solar power is demonstrated in few studies.

The main difference of electric heated kiln compared to traditional kiln is the differing gas atmosphere in the kiln when it comes to factors that affect calcination reaction. In electric heated kiln, the partial pressure of CO_2 is high in the kiln gases if no gas is supplied to the kiln. Consequently, the required temperature may be higher and recarbonation may occur in the kiln. There are also some differences in heat transfer and efficiency between electric heated and traditional kiln types. In electric heated kiln, there are greater losses through the kiln shell, but on the other hand there are no heat losses caused by flue

gases. In addition, advantages of electric heating are reduced energy related emissions, easier process and temperature control compared to control of combustion, possibility for multiple temperature control zones, avoidance of contamination of the product due to impurities in fuel, and enabling the deployment of CCUS technologies and especially direct capture.

The controlled experiments of the thesis are performed with laboratory scale electric heated rotary kiln for three calcium carbonate based raw materials. The experiments involved three cases. Case Air was a demonstration case with air supply to the kiln. The objective of the other two cases was to demonstrate calcination in CO_2 atmosphere because it was the main difference in the process conditions between electric heated and traditional kiln types. CO_2 was supplied to the kiln in case CO_2. Case VAC was performed in vacuum without gas supply to the kiln.

The experiments showed promising results of calcination in electric heated rotary kiln. However, there were some major challenges that require more research. The main challenge was recarbonation of CaO in the kiln. Calcination degrees of case CO_2 and VAC samples compared to case Air samples are considerably lower, though higher temperature was tested in case CO_2 and in case VAC lower total pressure in the kiln is expected to increase calcination rate. To confirm that complete calcination is possible in CO_2 atmosphere, TG-DSC analysis with CO_2 purging instead of nitrogen are recommended. Within the limits of this thesis, TG-DSC analyses with CO_2 supply were not performed. In theory, recarbonation can be prevented by rapidly cooling the product and changing the gas atmosphere. However, feasible technical solutions need to be studied and tested. Experiments with a pilot scale electric heated rotary kiln are being planned, and recarbonation is one of the main issues that require consideration.

Other major challenge was blockages in the rotary tube. Blockages limited the demonstration of continuous operation with the laboratory scale rotary kiln. Further research is needed to investigate whether blockages form and cause problems in larger scale kiln. Continuity of the process can be demonstrated in the pilot scale experiments. The measurement range of the gas analyzer is limited to 50 %, and thus the analysis of the concentration of CO_2 is inadequate. Mass spectrometry analyses are suggested alongside a TG-DSC analysis, and a more comprehensive analysis of the kiln off-gas composition and concentrations of the components is recommended. However, 50 % CO_2 concentration in the kiln off-gases was exceeded in case VAC experiments which is considerably higher compared to CO_2 concentration in the kiln off-gases of traditional kiln types. Additionally, reactivity of the samples was affected by sintering. High temperature in the kiln, long throughput time of the material and presence of CO_2 in the

kiln gases cause sintering. Kiln temperature and throughput time need to be adjusted for the pilot scale experiments.

In addition, calcination in hydrogen rich atmosphere is of interest. If H_2 is supplied to the kiln, kiln off-gases are expected to be a mixture of H_2 and CO_2, and suitable as they are for further processing to synthetic fuels. Experiments with the laboratory scale rotary kiln in H_2 rich gas atmosphere were not performed within the limits of this thesis. Suitable ratio of H_2 and CO_2 must be considered and also possible reactions between the gas components in the kiln. Methanation of the kiln off-gases is about to be tested as well.

Economic feasibility of the electric heated rotary kiln is recommended to be studied as well. Price of electricity has a great impact on the operational costs. Consequently, a more feasible option may be a hybrid kiln with a possibility for use of multiple fuels. During times of low electricity prices electricity could be used to generate the heat, and at other times combustion is used for heat generation. To minimize energy-related emissions from combustion, low-carbon fuels such as biofuels could be used. Synthetic fuels could be used as well. Thus, a full electrification could be achieved with partly direct and partly indirect electrification. However, this requires extensive research on the effects of the changes between heat sources on the product quality and operation of the kiln.

REFERENCES

Abanades, S. & André, L. (2018). Design and demonstration of a high temperature solar-heated rotary tube reactor for continuous particles calcination. Applied Energy. Vol.212, pp. 1310–1320.

Alcántara, V., Cadavid, Y., Sánchez, M., Uribe, C., Echeverri-Uribe, C., Morales, J., Obando, J. & Amell, A. (2018). A study case of energy efficiency, energy profile, and technological gap of combustion systems in the Colombian lime industry. Applied Thermal Engineering. Vol.128, pp. 393–401.

Apodaca, L.E. (2020). Lime. In: Mineral commodity summaries 2020. U.S. Geological Survey. pp. 96–97.

Ar, İ & Doğu, G. (2001). Calcination kinetics of high purity limestones. Chemical Engineering Journal. Vol.83(2), pp. 131–137.

Bajpai, P. (2018). Kraft Spent Liquor Recovery. In: Biermann's Handbook of Pulp and Paper - Raw Material and Pulp Making. 3rd ed. Elsevier. pp. 425–451.

Bajpai, P. (2015). Pulp and paper industry: chemicals. Elsevier. Amsterdam, Netherlands.

Baker, E.H. (1962). 87. The calcium oxide–carbon dioxide system in the pressure range 1—300 atmospheres. Journal of the Chemical Society (Resumed). , pp. 464–470.

Barin, I. (1989). Thermochemical data of pure substances. VCH.

Barin, I. & Knacke, O. (1973). Thermochemical properties of inorganic substances. Springer. Berlin.

Beyond Zero Emissions (2017). Zero Carbon Industry Plan: Rethinking Cement. Beyond Zero Emissions. 95 p.

Boateng, A.A. (2016). Basic Description of Rotary Kiln Operation. In: Rotary Kilns. 2nd ed. Butterworth-Heinemann. Boston. pp. 13–26.

Boot-Handford, M., Abanades, J.C., Anthony, E.J., Blunt, M.J., Brandani, S., Mac Dowell, N., Fernández, J.,R., Ferrari, M., Gross, R., Hallett, J.P., Haszeldine, R.S., Heptonstall, P., Lyngfelt, A., Makuch, Z., Mangano, E., Porter, R.T.J., Pourkashanian, M., Rochelle, G.T., Shah, N., Yao, J.G. & Fennell, P.S. (2014). Carbon capture and storage update. Energy & environmental science. Vol.7(1), pp. 130–189.

Bosoaga, A., Masek, O. & Oakey, J.E. (2009). CO_2 Capture Technologies for Cement Industry. Energy Procedia. Vol.1(1), pp. 133–140.

Britannica Academic (2020). Standard atmosphere. Britannica Academic, Encyclopædia Britannica. Available (cited on 15.5.2020): https://academic-eb-com.libproxy.tuni.fi/ levels/collegiate/article/ standard-atmosphere/10118.

Bui, M., Adjiman, C.S., Bardow, A., Anthony, E.J., Boston, A., Brown, S., Fennell, P.S., Fuss, S., Galindo, A., Hackett, L.A., Hallett, J.P., Herzog, H.J., Jackson, G., Kemper, J., Krevor, S., Maitland, G.C., Matuszewski, M., Metcalfe, I.S., Petit, C., Puxty, G., Reimer, J., Reiner, D.M., Rubin, E.S., Scott, S.A., Shah, N., Smit, B., Trusler, J.P.M., Webley, P., Wilcox, J. & Mac Dowell, N. (2018). Carbon capture and storage (CCS): the way forward. Energy & environmental science. Vol.11(5), pp. 1062–1176.

CEMBUREAU (2020). 2019 Activity Report. The European Cement Association CEMBUREAU. 39 p.

CEMBUREAU (2018). The role of cement in the 2050 low carbon economy. The European Cement Association CEMBUREAU. pp. 64. Available (cited on 21.4.2020): https://lowcarboneconomy.cembureau.eu/wp-content/uploads/2018/09/cembureau-full-report.pdf.

Commandré, J., Salvador, S. & Nzihou, A. (2007). Reactivity of Laboratory and Industrial Limes. Chemical engineering research & design. Vol.85(4), pp. 473–480.

CORDIS (2020). LOW EMISSIONS INTENSITY LIME AND CEMENT 2: DEMONSTRATION SCALE. The Community Research and Development Information Service (CORDIS). Available (cited on 11.10.2020): https://cordis.europa.eu/project/id/884170.

Cormos, A., Dinca, C., Petrescu, L., Andreea Chisalita, D., Szima, S. & Cormos, C. (2018). Carbon capture and utilisation technologies applied to energy conversion systems and other energy-intensive industrial applications. Fuel. Vol.211, pp. 883–890.

Decarbonate (2020). Available (cited on 28.9.2020): https://www.decarbonate.fi/.

Dennis, J.S. & Hayhurst, A.N. (1987). The effect of CO_2 on the kinetics and extent of calcination of limestone and dolomite particles in fluidised beds. Chemical engineering science. Vol.42(10), pp. 2361–2372.

Dowling, A., O'Dwyer, J. & Adley, C.C. (2015). Lime in the limelight. Journal of Cleaner Production. Vol.92, pp. 13–22.

Eriksson, M., Hökfors, B. & Backman, R. (2014). Oxyfuel combustion in rotary kiln lime production. Energy Science & Engineering. Vol.2(4), pp. 204–215.

EuLA (2020). Iron & Steel. European Lime Association EuLA. Available (cited on 27.5.2020): https://www.eula.eu/lime-applications/iron-steel/.

European Commission (2019). COMMUNICATION FROM THE COMMISSION TO THE EUROPEAN PARLIAMENT, THE EUROPEAN COUNCIL, THE COUNCIL, THE EUROPEAN ECONOMIC AND SOCIAL COMMITTEE AND THE COMMITTEE OF THE REGIONS: The European Green Deal. European Commission. 24 p.

European Commission (2015). EU ETS Handbook. European Commission. 138 p.

Finnsementti (2012). Suomalainen sementti. Finnsementti. 27 p.

Gaisford, S., Kett, V. & Haines, P. (2019). Principles of Thermal Analysis and Calorimetry. 2nd ed. Royal Society of Chemistry.

Gao, T., Shen, L., Shen, M., Liu, L. & Chen, F. (2016). Analysis of material flow and consumption in cement production process. Journal of Cleaner Production. Vol.112, pp. 553–565.

García-Labiano, F., Abad, A., de Diego, L.F., Gayán, P. & Adánez, J. (2002). Calcination of calcium-based sorbents at pressure in a broad range of CO_2 concentrations. Chemical Engineering Science. Vol.57(13), pp. 2381–2393.

Girolami, G.S. (2016). X-Ray Crystallography. University Science Books.

Haimei, Z. (2011). Cement. In: Building Materials in Civil Engineering. Woodhead Publishing. pp. 46–80.

Hills, T., Leeson, D., Florin, N. & Fennell, P. (2016). Carbon Capture in the Cement Industry: Technologies, Progress, and Retrofitting. Environmental science & technology. Vol.50(1), pp. 368–377.

Hodgson, P., Sceats, M., Vincent, A., Rennie, D., Fennell, P. & Hills, T. 2019, "Direct Separation Calcination Technology for Carbon Capture: Demonstrating a Low Cost Solution for the Lime and Cement Industries in the LEILAC Project", *14th International Conference on Greenhouse Gas Control Technologies*. 14 p.

IEA (2020a). Cement. International Energy Agency IEA. Available (cited on 18.8.2020): https://www.iea.org/reports/cement.

IEA (2020b). Energy Technology Perspectives 2020. International Energy Agency IEA. 398 p.

Jiang, B., Xia, D., Yu, B., Xiong, R., Ao, W., Zhang, P.K. & Cong, L. (2019). An environment-friendly process for limestone calcination with CO_2 looping and recovery. Journal of Cleaner Production. Vol.240, 11 p.

Kanthal (2018). Kanthal® APM. Available (cited on 15.9.2020): https://www.kanthal.com/en/products/material-datasheets/tube/kanthal-apm/.

Kumar, G.S., Ramakrishnan, A. & Hung, Y. (2007). Lime Calcination. In: Advanced physicochemical treatment technologies. Humana Press. Totowa. pp. 611–633.

Kunii, D. & Chisaki, T. (2008). Rotary reactor engineering. 1st ed. Elsevier. Amsterdam.

Kääntee, U., Zevenhoven, R., Backman, R. & Hupa, M. (2004). Cement manufacturing using alternative fuels and the advantages of process modelling. Fuel Processing Technology. Vol.85(4), pp. 293–301.

Leeson, D., Mac Dowell, N., Shah, N., Petit, C. & Fennell, P.S. (2017). A Techno-economic analysis and systematic review of carbon capture and storage (CCS) applied to the iron and steel, cement, oil refining and pulp and paper industries, as well as other high purity sources. International journal of greenhouse gas control. Vol.61, pp. 71–84.

Lehne, J. & Preston, F. (2018). Making Concrete Change: Innovation in Low-carbon Cement and Concrete. Catham House. pp. 138. Available (cited on 21.4.2020): https://reader.chathamhouse.org/making-concrete-change-innovation-low-carbon-cement-and-concrete#.

LEILAC (2017). Public LEILAC FEED Summary Report. LEILAC. 28 p. Available (cited on 22.4.2020): https://www.project-leilac.eu/publications.

Lupi, S. (2016). Fundamentals of Electroheat: Electrical Technologies for Process Heating. Springer International Publishing AG.

Manovic, V. & Anthony, E.J. (2010). Carbonation of CaO-Based Sorbents Enhanced by Steam Addition. Industrial & Engineering Chemistry Research; Ind.Eng.Chem.Res. Vol.49(19), pp. 9105–9110.

Nasdaq (2020). Market Prices. Available (cited on 11.10.2020): http://www.nasdaqomx.com/commodities/market-prices.

Nwaoha, C., Tontiwachwuthikul, P. & Benamor, A. (2018). CO_2 capture from lime kiln using AMP-DA2MP amine solvent blend: A pilot plant study. Journal of Environmental Chemical Engineering. Vol.6(6), pp. 7102–7110.

Oates, J.A.H. (1998). Lime and limestone: chemistry and technology, production and uses. John Wiley & Sons. Weinheim.

Pacyna, J.M., Rentz, O., Oertel, D., Trozzi, C., Pulles, T. & Appelman, W. (2019). Lime production 2019. In: EMEP/EEA air pollutant emission inventory guidebook 2019. European Environment Agency. 17 p.

Pales, A.F., Levi, P. & Vass, T. (2019). Tracking Industry. International Energy Agency IEA. Available (cited on 20.4.2020): https://www.iea.org/reports/tracking-industry#.

Piringer, H. (2017). Lime Shaft Kilns. Energy Procedia. Vol.120, pp. 75–95.

Rahman, F.A., Aziz, M.M.A., Saidur, R., Bakar, Wan Azelee Wan Abu, Hainin, M.R., Putrajaya, R. & Hassan, N.A. (2017). Pollution to solution: Capture and sequestration of carbon dioxide (CO_2) and its utilization as a renewable energy source for a sustainable future. Renewable and Sustainable Energy Reviews. Vol.71, pp. 112–126.

Rogelj, J., Shindell, D., Jiang, K., Fifita, S., Forster, P., Ginzburg, V., Handa, C., Kheshgi, H., Kobayashi, S., Kriegler, E., Mundaca, L., Séférian, R. & Vilariño, M.V. (2018). Mitigation Pathways Compatible with 1.5°C in the Context of Sustainable Development. In: Global Warming of 1.5°C. Eds. V. Mason-Delmotte, P. Zhai, H.-. Pörtner, D. Roberts, J. Skea, P.R. Shukla, A. Pirani, W. Moufouma-Okia, C. Péan, R. Pidcock, S. Connors, J.B.R. Matthews, Y. Chen, X. Zhou, M.I. Gomis, E. Lonnoy, T. Maycock, M. Tignor & T. Waterfield. The Intergovernmental Panel on Climate Change IPCC. pp. 93–174.

Rong, W., Li, B., Qi, F. & Cheung, S.C.P. (2017). Energy and exergy analysis of an annular shaft kiln with opposite burners. Applied Thermal Engineering. Vol.119, pp. 629–638.

Ruhnau, O., Bannik, S., Otten, S., Praktiknjo, A. & Robinius, M. (2019). Direct or indirect electrification? A review of heat generation and road transport decarbonisation scenarios for Germany 2050. Energy (Oxford). Vol.166, pp. 989–999.

Sagastume Gutiérrez, A., Cogollos Martínez, J.B. & Vandecasteele, C. (2013). Energy and exergy assessments of a lime shaft kiln. Applied Thermal Engineering. Vol.51(1-2), pp. 273–280.

Schorcht, F., Kourti, I., Scalet, B.M., Roudier, S. & Sancho, L.D. (2013). Best Available Techniques (BAT) Reference Document for the Production of Cement, Lime and Magnesium Oxide: Industrial Emissions Directive 2010/75/EU Integrated Pollution Prevention and control. Joint Research Centre of the European Commission.

Senegačnik, A., Oman, J. & Širok, B. (2008). Annular shaft kiln for lime burning with kiln gas recirculation. Applied Thermal Engineering. Vol.28(7), pp. 785–792.

SFS-EN 459-1 (2015). SFS-EN 459-1: "Building lime. Part 1: Definitions, specifications and conformity criteria". Suomen Standardisoimisliitto SFS. 51 p.

SFS-EN 459-2 (2011). SFS-EN 459-2: "Building lime. Part 2: Test methods". Suomen Standardisoimisliitto SFS. 66 p.

Shahin, H., Hassanpour, S. & Saboonchi, A. (2016). Thermal energy analysis of a lime production process: Rotary kiln, preheater and cooler. Energy Conversion and Management. Vol.114, pp. 110–121.

Silcox, G.D., Kramlich, J.C. & Pershing, D.W. (1989). A Mathematical Model for the Flash Calcination of Dispersed $CaCO_3$ and $Ca(OH)_2$ Particles. Industrial and Engineering Chemistry Research. Vol.28(2), pp. 155–160.

Stanmore, B.R. & Gilot, P. (2005). Review—calcination and carbonation of limestone during thermal cycling for CO_2 sequestration. Fuel Processing Technology. Vol.86(16), pp. 1707–1743.

Stork, M., Meinderstma, W., Overgaag, M. & Neelis, M. (2014). A Competitive and Efficient Lime Industry, Cornerstone for a Sustainable Europe (Lime Roadmap). European Lime Association. 72 p.

UNFCCC (2020). Paris Agreement - Status of Ratification. The United Nations Framework Convention on Climate Change UNFCCC. Available (cited on 6.10.2020): https://unfccc.int/process/the-paris-agreement/status-of-ratification.

United Nations (2015). Paris Agreement. United Nations. 25 p.

Valtioneuvosto (2019). Pääministeri Sanna Marinin hallituksen ohjelma 10.12.2019: OSALLISTAVA JA OSAAVA SUOMI – sosiaalisesti, taloudellisesti ja ekologisesti kestävä yhteiskunta, Valtioneuvosto, Helsinki.

Valverde, J.M. & Medina, S. (2015). Crystallographic transformation of limestone during calcination under CO_2. Physical Chemistry Chemical Physics. Vol.17(34), pp. 21912–21926.

Zelić, J., Rušić, D. & Krstulović, R. (2002). Kinetic Analysis of Thermal Decomposition of $Ca(OH)_2$ Formed During Hydration of Commercial Portland Cement by DSC. Journal of Thermal Analysis and Calorimetry. Vol.67(3), pp. 613–622.

APPENDIX A: TG-DSC GRAPHS

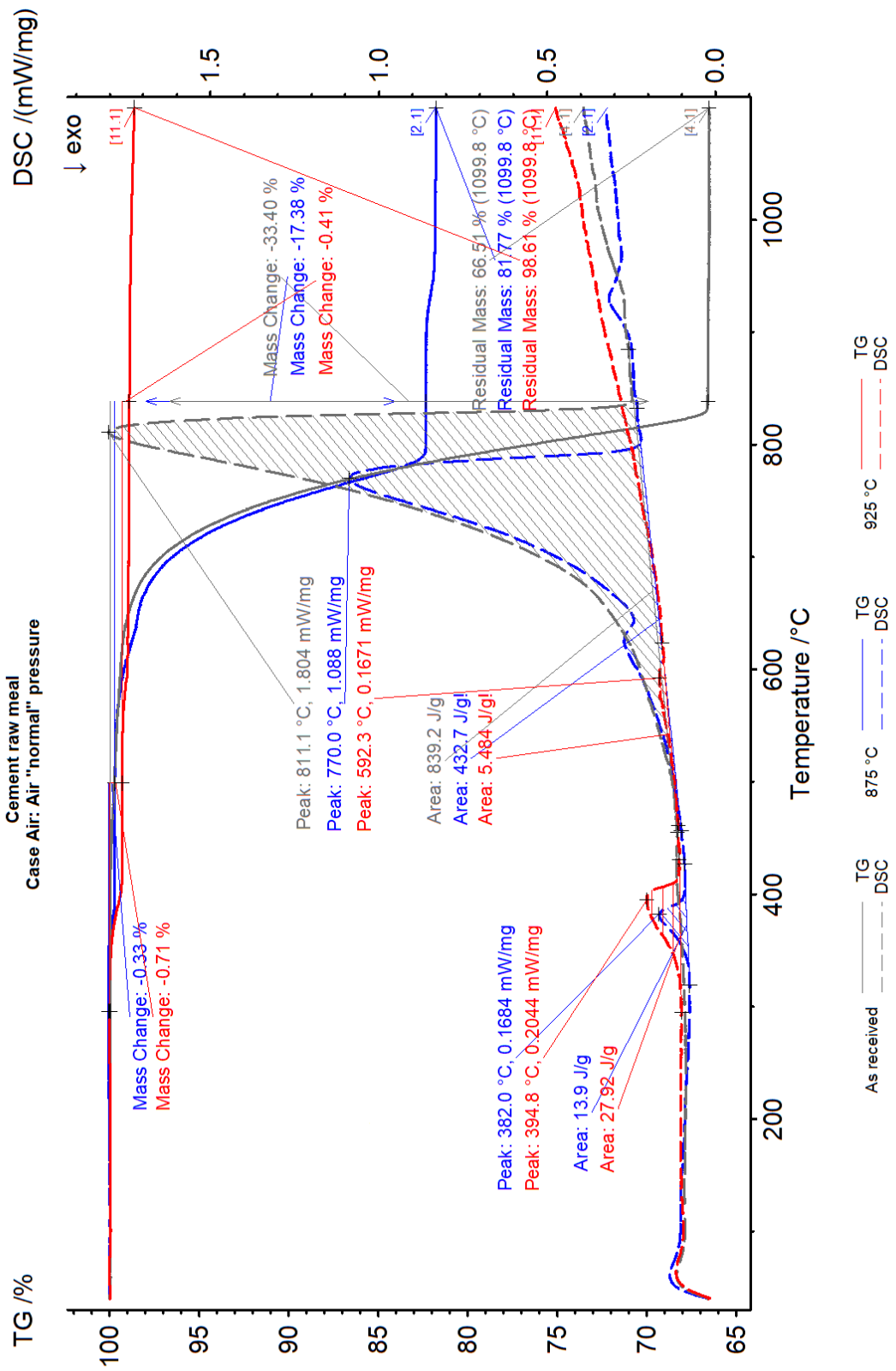

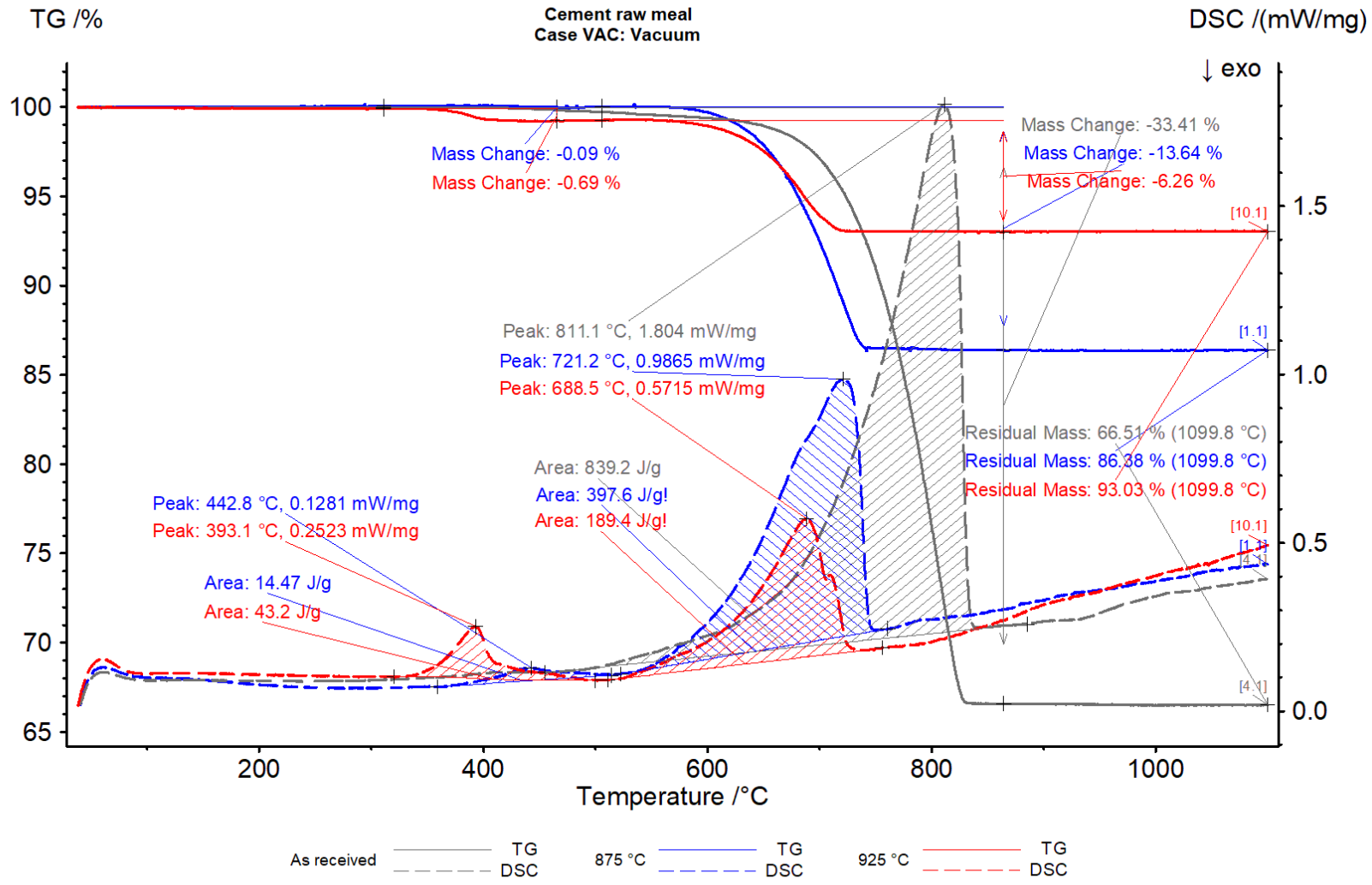
Cement raw meal
Case VAC: Vacuum
TG /%
DSC /(mW/mg)
↓ exo
100
95
90
85
80
75
70
65
1.5
1.0
0.5
0.0
200
400
600
800
1000
Temperature /°C
Mass Change: -0.09 %
Mass Change: -0.69 %
Mass Change: -33.41 %
Mass Change: -13.64 %
Mass Change: -6.26 %
[10.1]
[1.1]
[4.1]
Peak: 811.1 °C, 1.804 mW/mg
Peak: 721.2 °C, 0.9865 mW/mg
Peak: 688.5 °C, 0.5715 mW/mg
Residual Mass: 66.51 % (1099.8 °C)
Residual Mass: 86.38 % (1099.8 °C)
Residual Mass: 93.03 % (1099.8 °C)
Area: 839.2 J/g
Area: 397.6 J/g!
Area: 189.4 J/g!
Peak: 442.8 °C, 0.1281 mW/mg
Peak: 393.1 °C, 0.2523 mW/mg
Area: 14.47 J/g
Area: 43.2 J/g
As received
TG
DSC
875 °C
TG
DSC
925 °C
TG
DSC

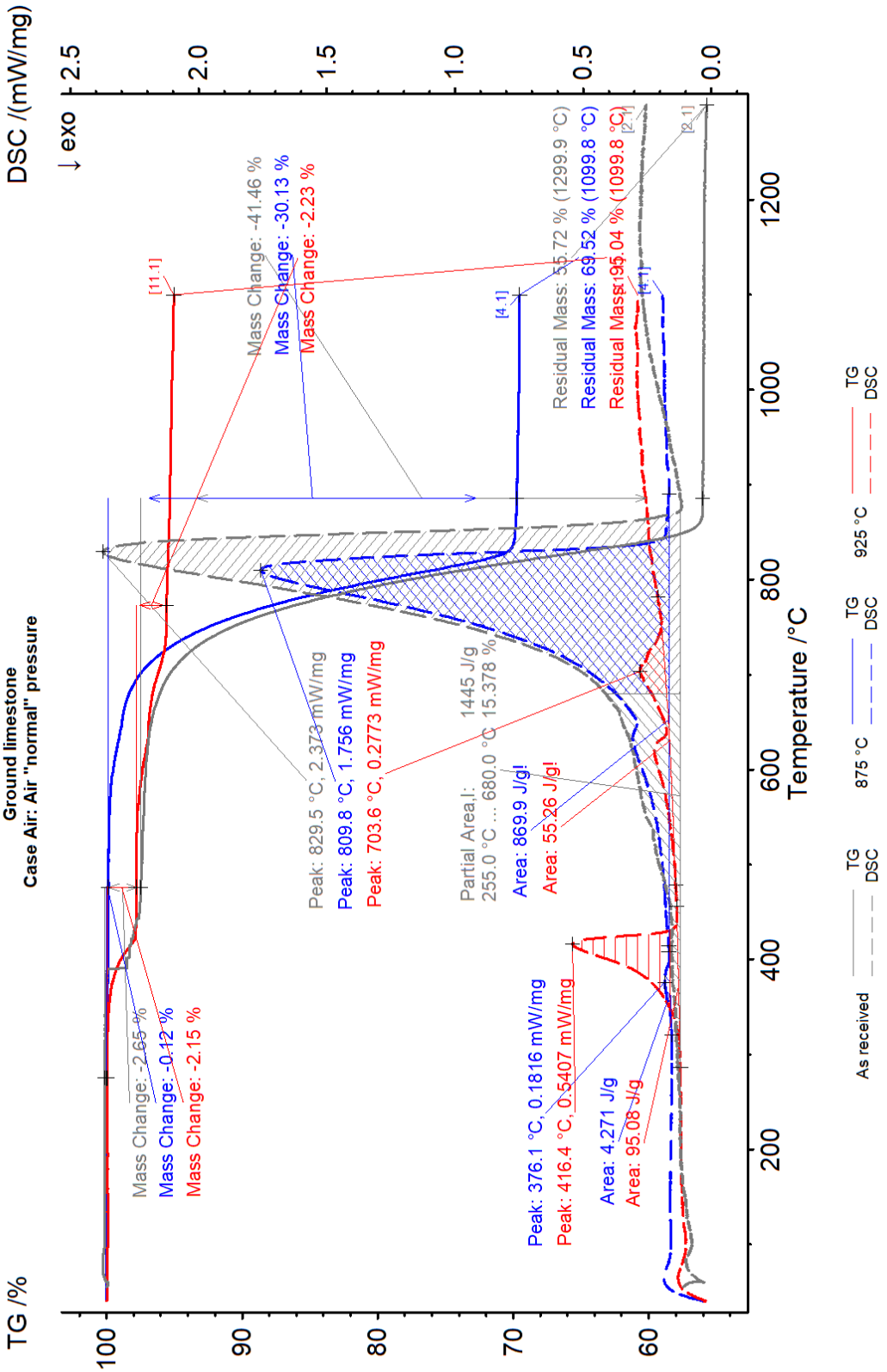
Ground limestone
Case Air: Air "normal" pressure
TG /%
DSC /(mW/mg)
↓ exo
Temperature /°C
Mass Change: -2.65 %
Mass Change: -0.12 %
Mass Change: -2.15 %
Mass Change: -41.46 %
Mass Change: -30.13 %
Mass Change: -2.23 %
Residual Mass: 55.72 % (1299.9 °C)
Residual Mass: 69.52 % (1099.8 °C)
Residual Mass: 95.04 % (1099.8 °C)
Peak: 829.5 °C, 2.373 mW/mg
Peak: 809.8 °C, 1.756 mW/mg
Peak: 703.6 °C, 0.2773 mW/mg
Partial Area,I:
255.0 °C ... 680.0 °C 15.378 %
1445 J/g
Area: 869.9 J/g
Area: 55.26 J/g
Peak: 376.1 °C, 0.1816 mW/mg
Peak: 416.4 °C, 0.5407 mW/mg
Area: 4.271 J/g
Area: 95.08 J/g
[11,1]
[4,1]
[4,1]
[2,1]
[2,1]
As received
TG
DSC
875 °C
TG
DSC
925 °C
TG
DSC

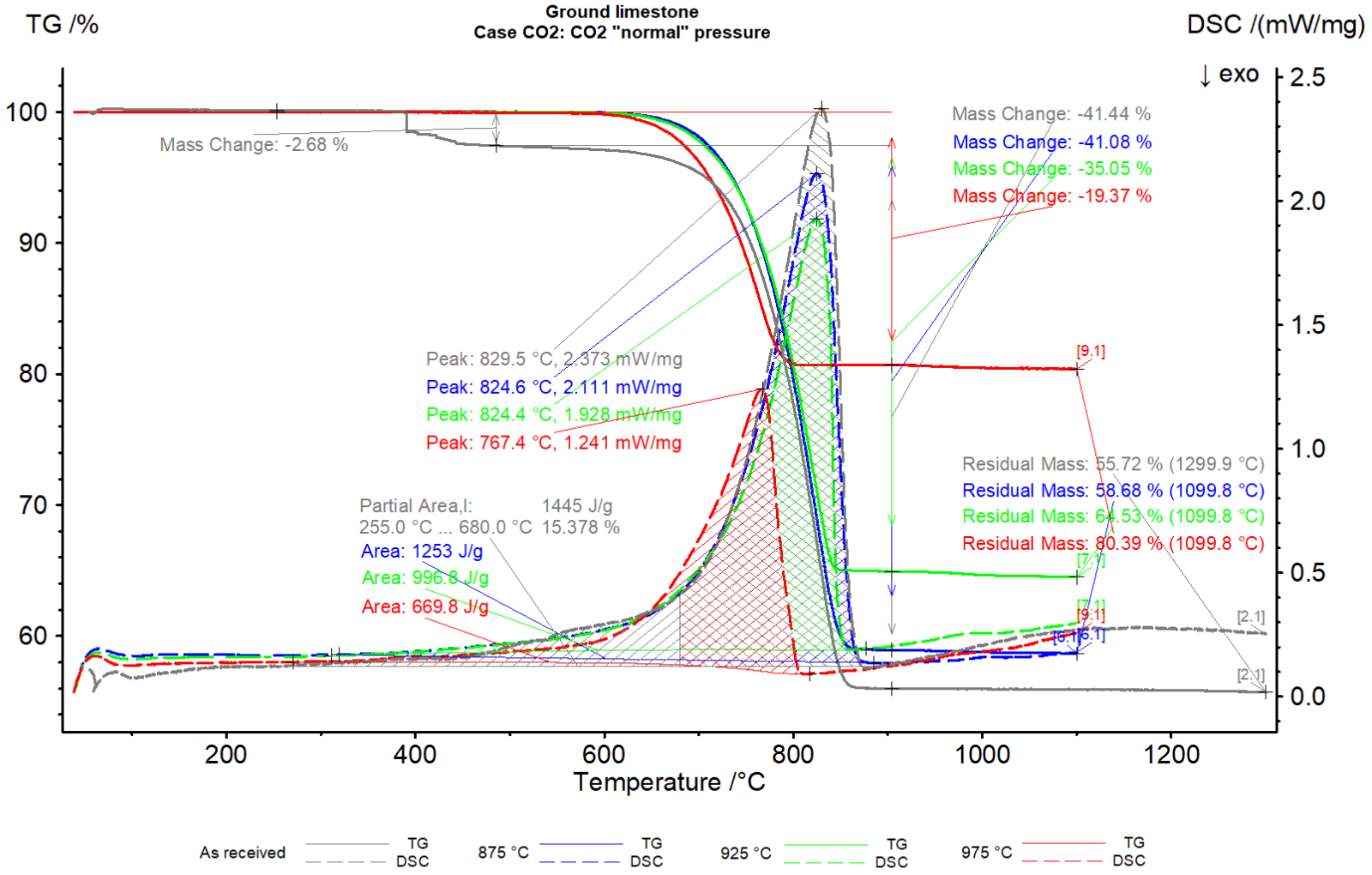
Ground limestone
Case CO2: CO2 "normal" pressure
TG /%
DSC /(mW/mg)
↓ exo
Mass Change: -2.68 %
Mass Change: -41.44 %
Mass Change: -41.08 %
Mass Change: -35.05 %
Mass Change: -19.37 %
Peak: 829.5 °C, 2.373 mW/mg
Peak: 824.6 °C, 2.111 mW/mg
Peak: 824.4 °C, 1.928 mW/mg
Peak: 767.4 °C, 1.241 mW/mg
Partial Area,I: 1445 J/g
255.0 °C ... 680.0 °C 15.378 %
Area: 1253 J/g
Area: 996.8 J/g
Area: 669.8 J/g
Residual Mass: 55.72 % (1299.9 °C)
Residual Mass: 58.68 % (1099.8 °C)
Residual Mass: 64.53 % (1099.8 °C)
Residual Mass: 80.39 % (1099.8 °C)
[9,1]
[7,1]
[9,1]
[8,1]
[6,1]
[2,1]
[2,1]
100
90
80
70
60
2.5
2.0
1.5
1.0
0.5
0.0
200
400
600
800
1000
1200
Temperature /°C
As received TG DSC
875 °C TG DSC
925 °C TG DSC
975 °C TG DSC

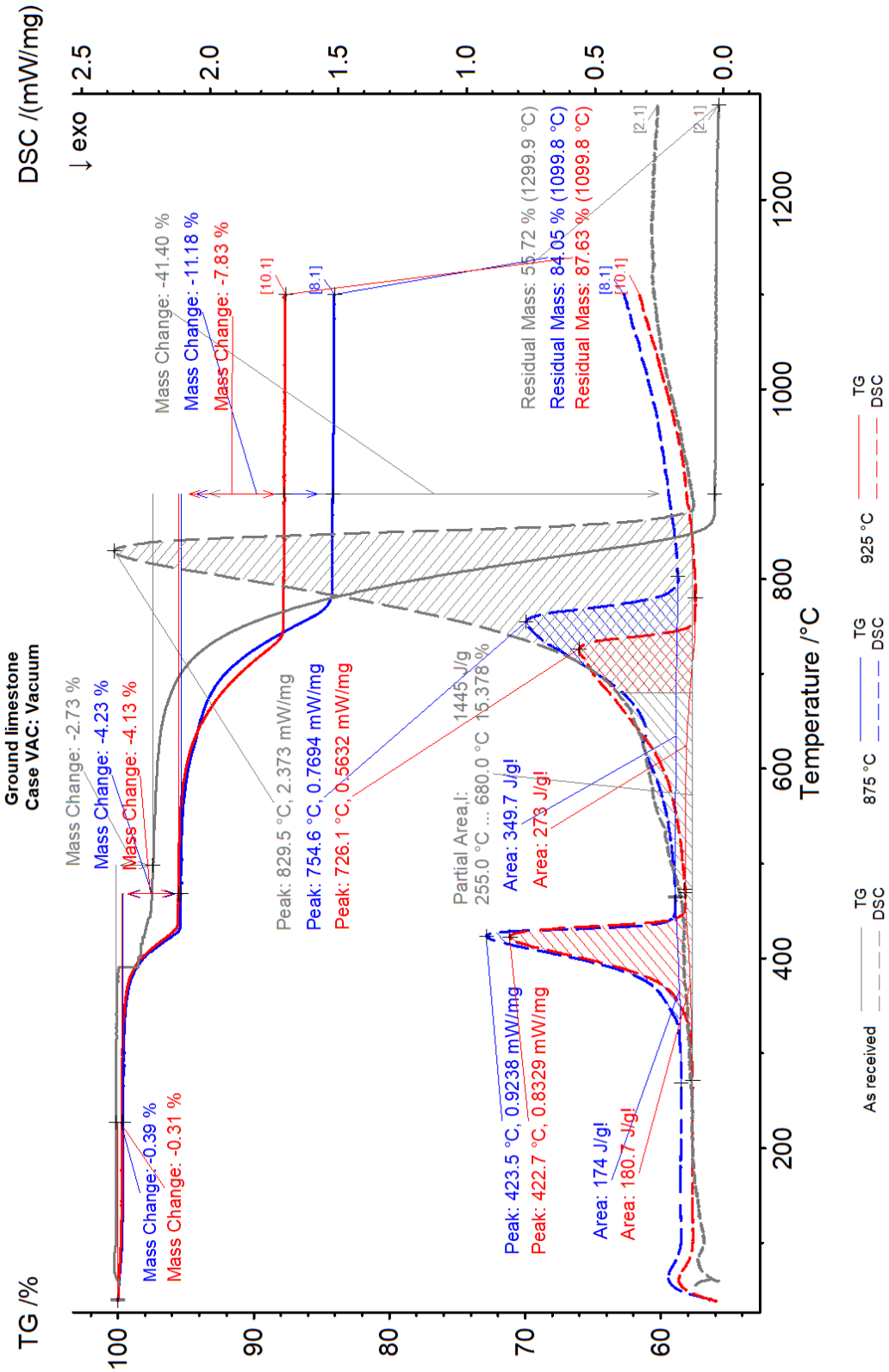
Ground limestone
Case VAC: Vacuum
TG /%
DSC /(mW/mg)
↓ exo
Temperature /°C
Mass Change: -2.73 %
Mass Change: -4.23 %
Mass Change: -4.13 %
Mass Change: -0.39 %
Mass Change: -0.31 %
Mass Change: -41.40 %
Mass Change: -11.18 %
Mass Change: -7.83 %
Residual Mass: 55.72 % (1299.9 °C)
Residual Mass: 84.05 % (1099.8 °C)
Residual Mass: 87.63 % (1099.8 °C)
Peak: 829.5 °C, 2.373 mW/mg
Peak: 754.6 °C, 0.7694 mW/mg
Peak: 726.1 °C, 0.5632 mW/mg
Partial Area.I:
255.0 °C ... 680.0 °C
1445 J/g
15.378 %
Area: 349.7 J/g!
Area: 273 J/g!
Peak: 423.5 °C, 0.9238 mW/mg
Peak: 422.7 °C, 0.8329 mW/mg
Area: 174 J/g!
Area: 180.7 J/g!
[10.1]
[8.1]
[2.1]
As received
TG
DSC
875 °C
925 °C

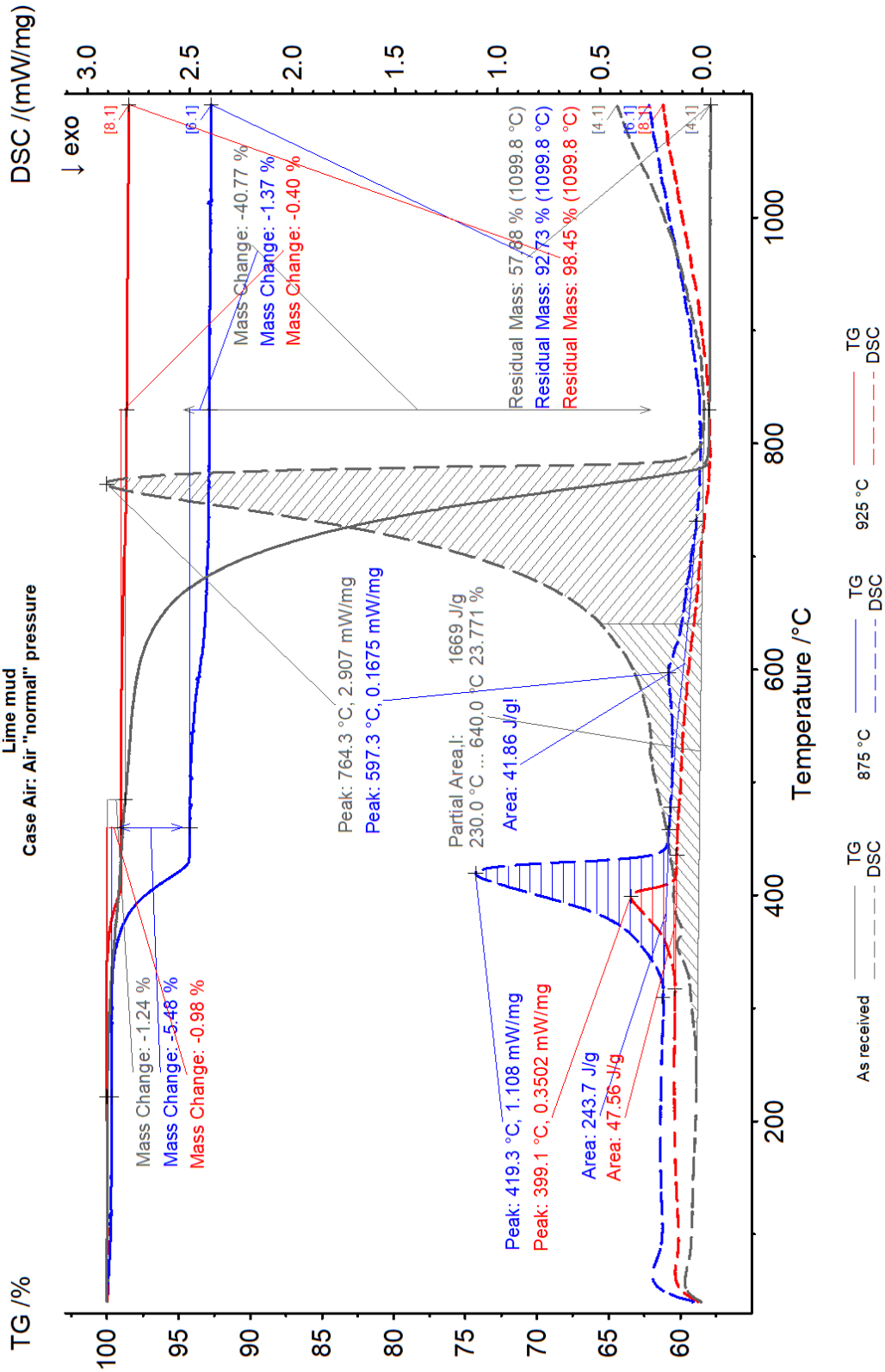
Lime mud
Case Air: Air "normal" pressure
TG /%
DSC /(mW/mg)
↓ exo
Temperature /°C
Mass Change: -1.24 %
Mass Change: -5.48 %
Mass Change: -0.98 %
Mass Change: -40.77 %
Mass Change: -1.37 %
Mass Change: -0.40 %
Residual Mass: 57.88 % (1099.8 °C)
Residual Mass: 92.73 % (1099.8 °C)
Residual Mass: 98.45 % (1099.8 °C)
Peak: 764.3 °C, 2.907 mW/mg
Peak: 597.3 °C, 0.1675 mW/mg
Partial Area.I:
230.0 °C ... 640.0 °C
1669 J/g
23.771 %
Area: 41.86 J/g!
Peak: 419.3 °C, 1.108 mW/mg
Peak: 399.1 °C, 0.3502 mW/mg
Area: 243.7 J/g
Area: 47.56 J/g
As received
TG
DSC
875 °C
925 °C

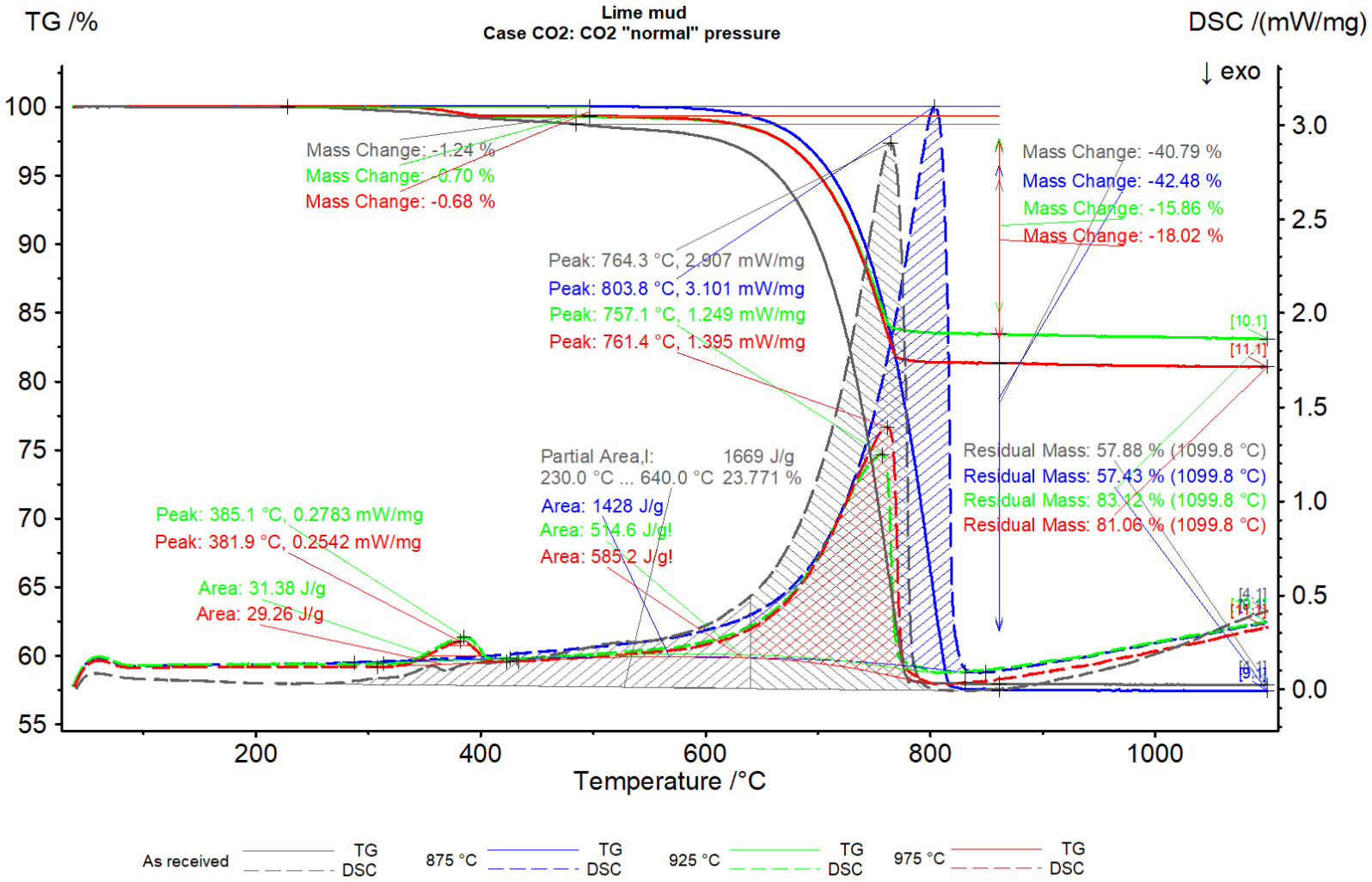
Lime mud
Case CO2: CO2 "normal" pressure
TG /%
DSC /(mW/mg)
↓ exo
Mass Change: -1.24 %
Mass Change: -0.70 %
Mass Change: -0.68 %
Mass Change: -40.79 %
Mass Change: -42.48 %
Mass Change: -15.86 %
Mass Change: -18.02 %
Peak: 764.3 °C, 2.907 mW/mg
Peak: 803.8 °C, 3.101 mW/mg
Peak: 757.1 °C, 1.249 mW/mg
Peak: 761.4 °C, 1.395 mW/mg
[10.1]
[11.1]
Partial Area,I: 1669 J/g
230.0 °C ... 640.0 °C 23.771 %
Area: 1428 J/g
Area: 514.6 J/g!
Area: 585.2 J/g!
Residual Mass: 57.88 % (1099.8 °C)
Residual Mass: 57.43 % (1099.8 °C)
Residual Mass: 83.12 % (1099.8 °C)
Residual Mass: 81.06 % (1099.8 °C)
Peak: 385.1 °C, 0.2783 mW/mg
Peak: 381.9 °C, 0.2542 mW/mg
Area: 31.38 J/g
Area: 29.26 J/g
[4.1]
[9.1]
100
95
90
85
80
75
70
65
60
55
3.0
2.5
2.0
1.5
1.0
0.5
0.0
200
400
600
800
1000
Temperature /°C
As received TG DSC
875 °C TG DSC
925 °C TG DSC
975 °C TG DSC

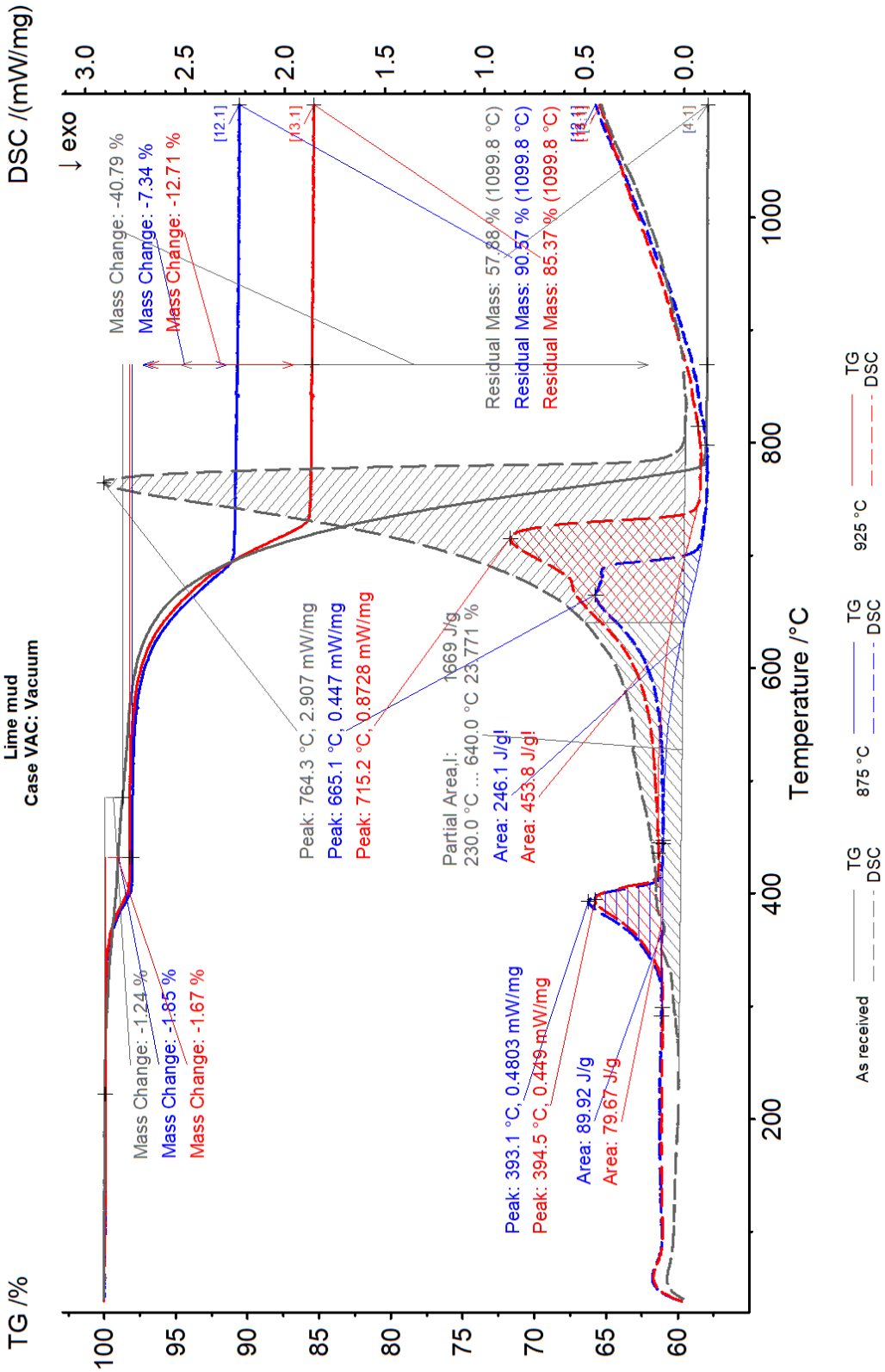
Lime mud
Case VAC: Vacuum
TG /%
DSC /(mW/mg)
↓ exo
Temperature /°C
Mass Change: -1.24 %
Mass Change: -1.85 %
Mass Change: -1.67 %
Mass Change: -40.79 %
Mass Change: -7.34 %
Mass Change: -12.71 %
Residual Mass: 57.88 % (1099.8 °C)
Residual Mass: 90.57 % (1099.8 °C)
Residual Mass: 85.37 % (1099.8 °C)
Peak: 764.3 °C, 2.907 mW/mg
Peak: 665.1 °C, 0.447 mW/mg
Peak: 715.2 °C, 0.8728 mW/mg
Partial Area.I:
230.0 °C ... 640.0 °C 23.771 %
1669 J/g
Area: 246.1 J/g
Area: 453.8 J/g
Peak: 393.1 °C, 0.4803 mW/mg
Peak: 394.5 °C, 0.449 mW/mg
Area: 89.92 J/g
Area: 79.67 J/g
[12.1]
[13.1]
[4.1]
As received
TG
DSC
875 °C
925 °C

APPENDIX B: XRD PATTERNS

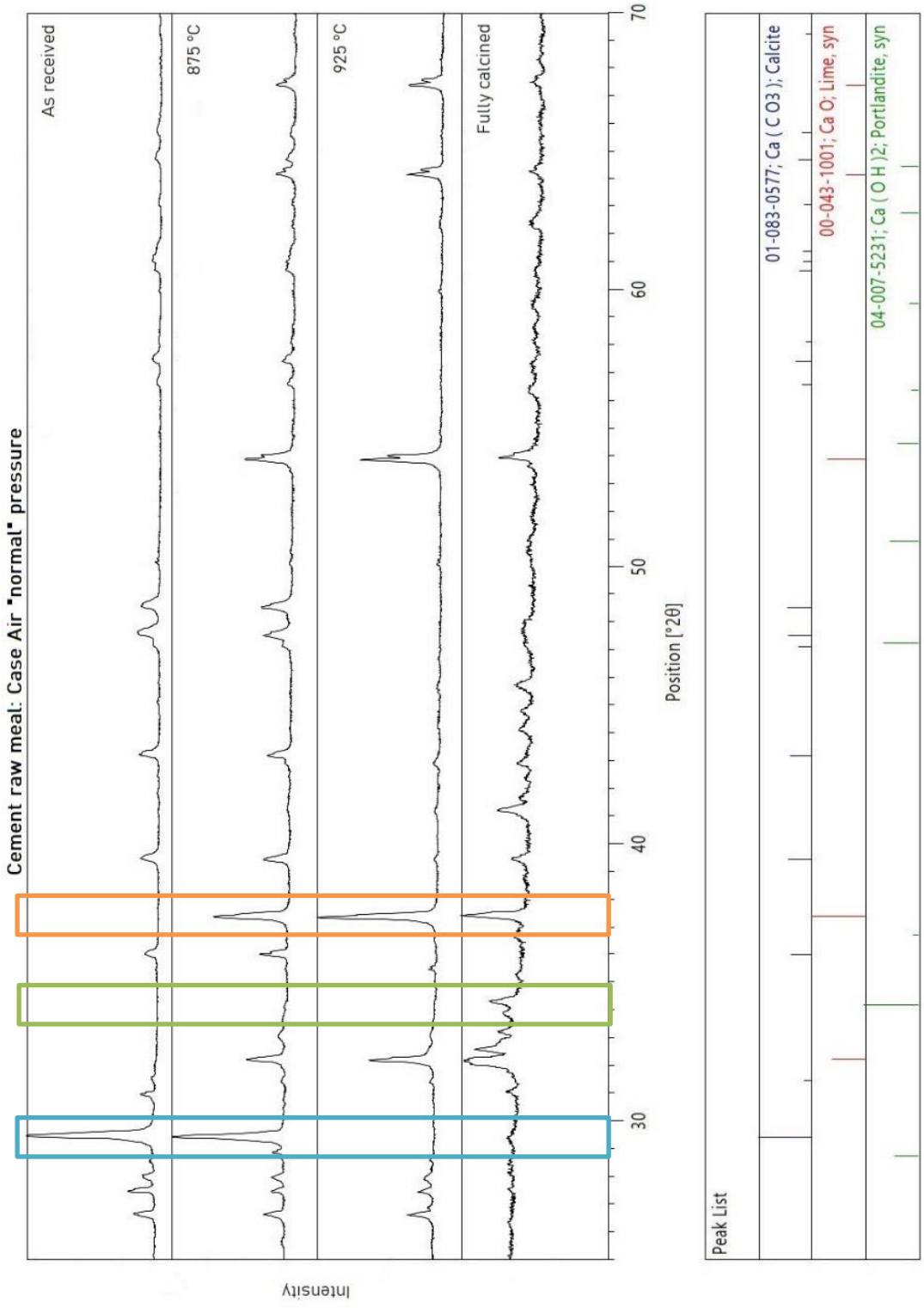

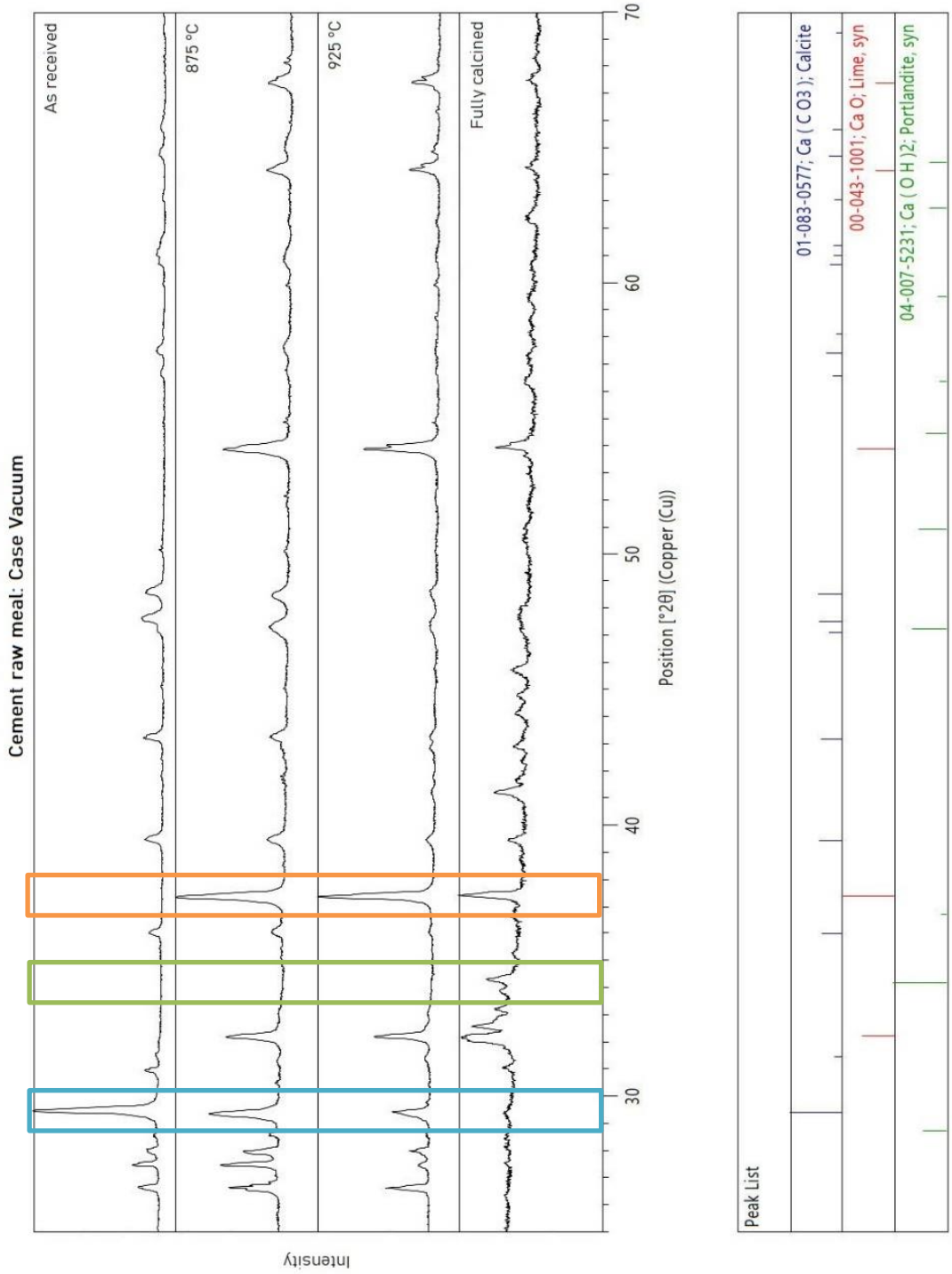
Cement raw meal: Case Vacuum
As received
875 °C
925 °C
Fully calcined
Intensity
Position [°2θ] (Copper (Cu))
30
40
50
60
70
Peak List
01-083-0577; Ca (C O3); Calcite
00-043-1001; Ca O; Lime, syn
04-007-5231; Ca (O H)2; Portlandite, syn

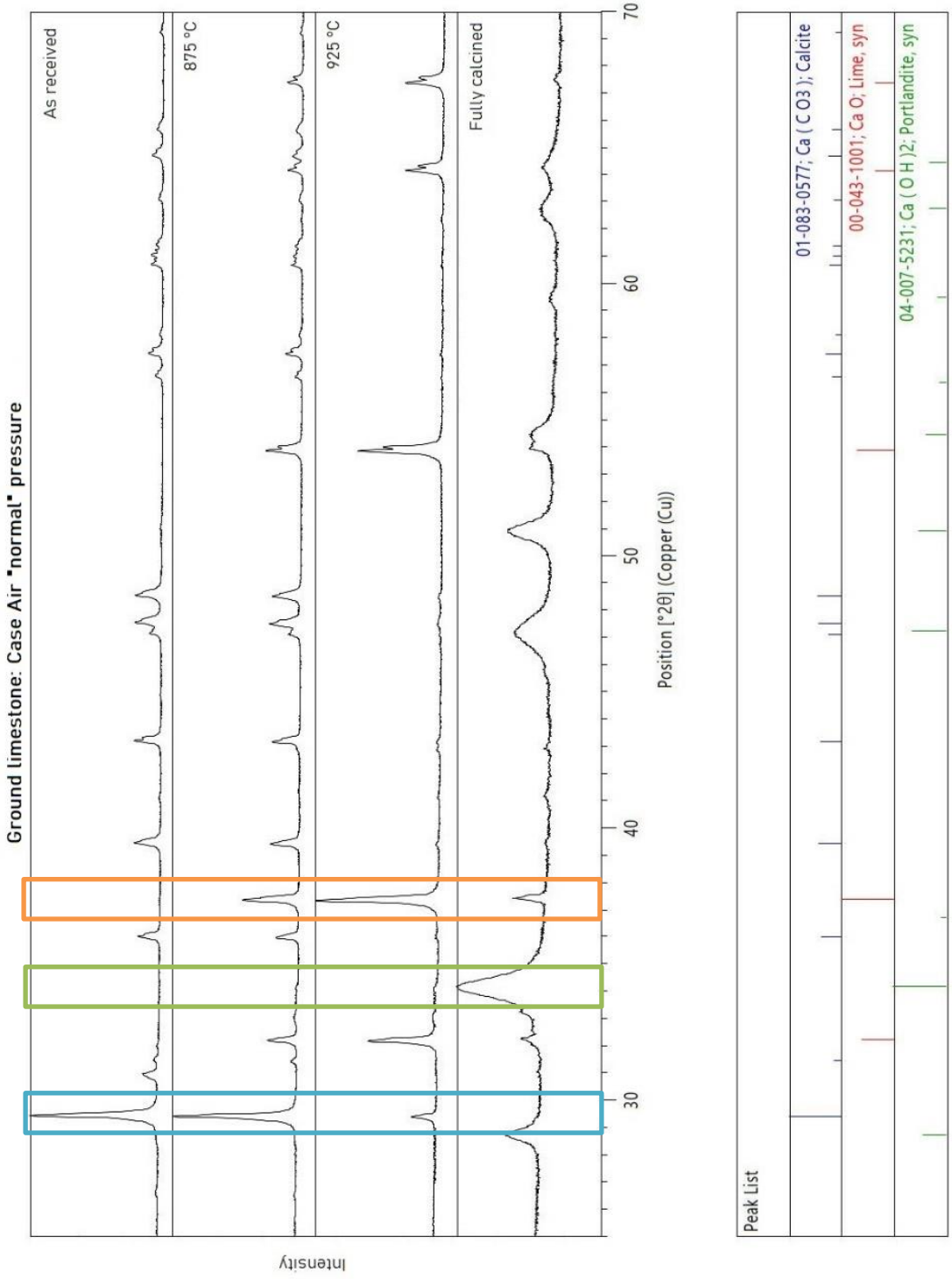
Ground limestone: Case Air "normal" pressure
As received
875 °C
925 °C
Fully calcined
Intensity
30
40
50
60
70
Position [°2θ] (Copper (Cu))
Peak List
01-083-0577; Ca (C O3); Calcite
00-043-1001; Ca O; Lime, syn
04-007-5231; Ca (O H)2; Portlandite, syn

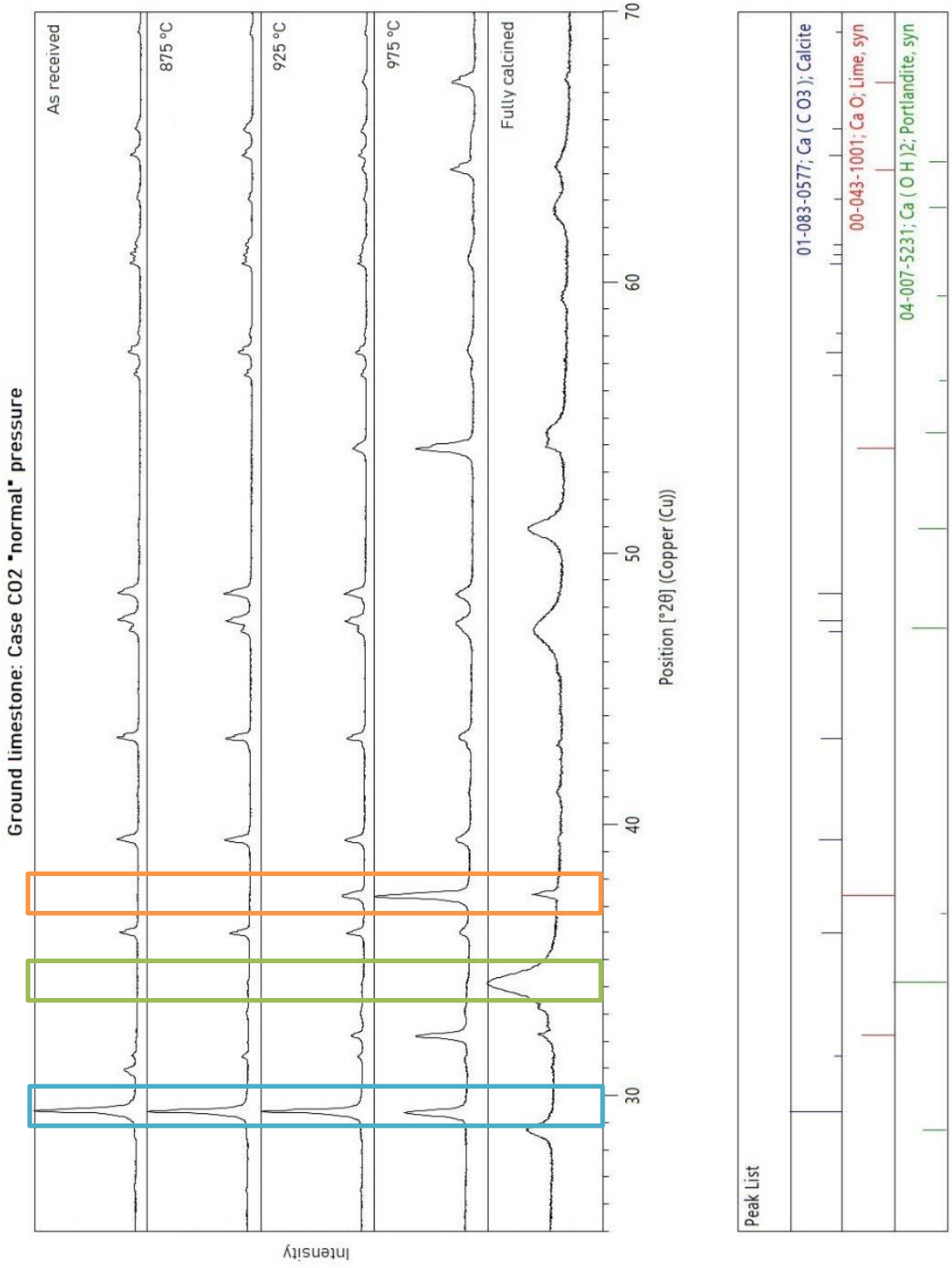
Ground limestone: Case CO2 "normal" pressure
As received
875 °C
925 °C
975 °C
Fully calcined
Intensity
30
40
50
60
70
Position [°2θ] (Copper (Cu))
Peak List
01-083-0577; Ca (C O3); Calcite
00-043-1001; Ca O; Lime, syn
04-007-5231; Ca (O H)2; Portlandite, syn

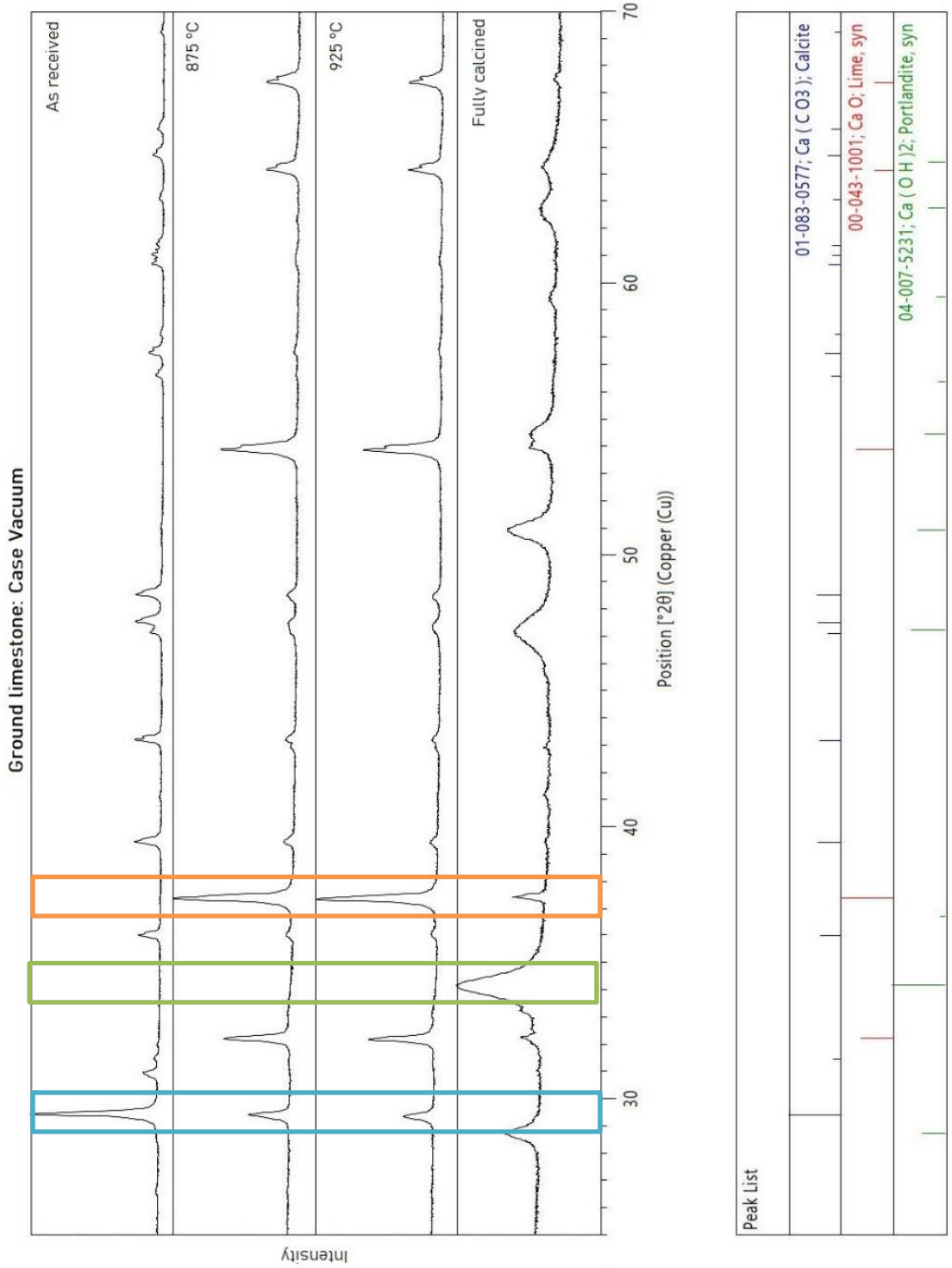
Ground limestone: Case Vacuum
As received
875 °C
925 °C
Fully calcined
Intensity
30
40
50
60
70
Position [°2θ] (Copper (Cu))
Peak List
01-083-0577; Ca (C O3); Calcite
00-043-1001; Ca O; Lime, syn
04-007-5231; Ca (O H)2; Portlandite, syn

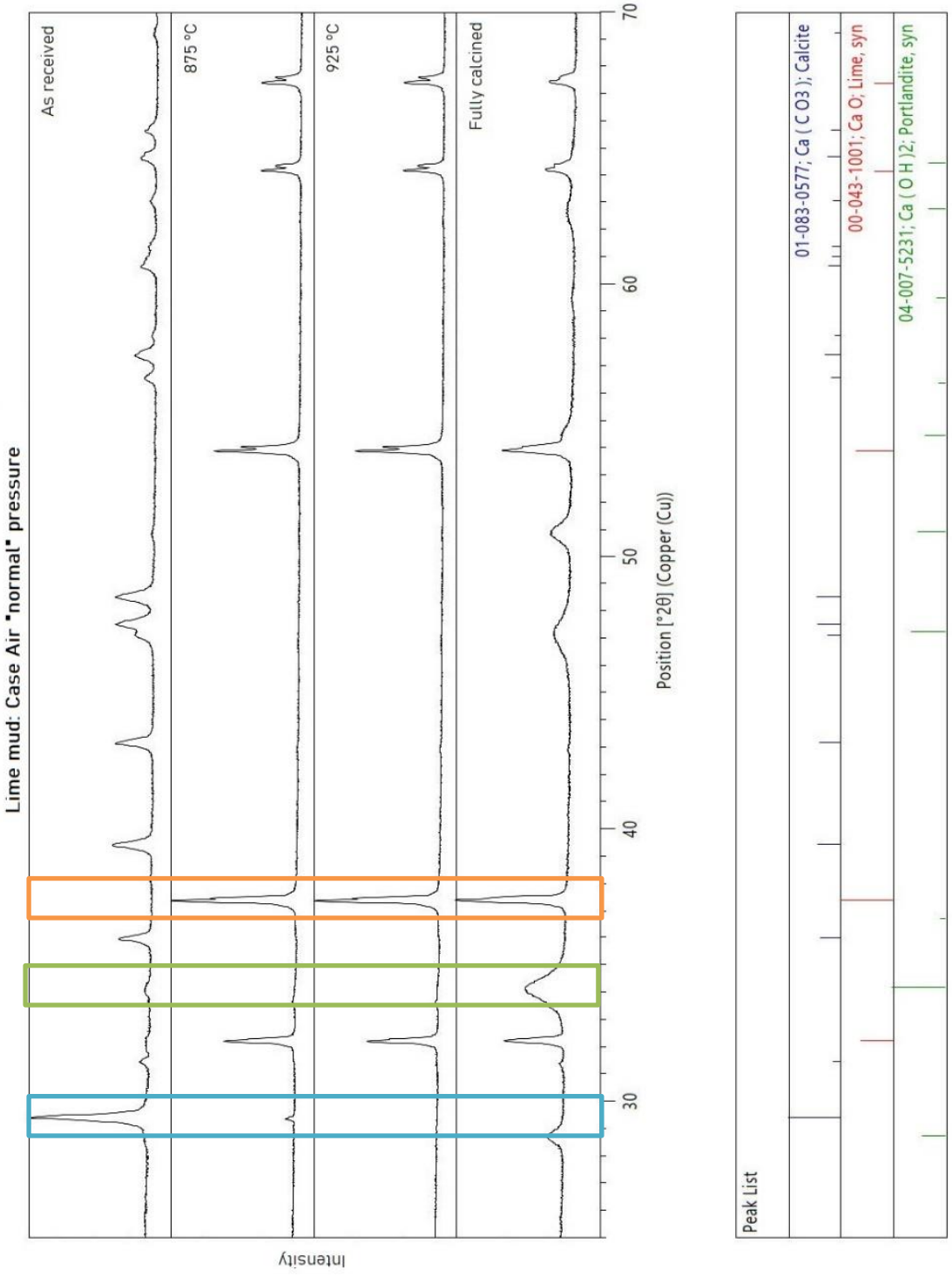
Lime mud: Case Air "normal" pressure
As received
875 °C
925 °C
Fully calcined
Intensity
30
40
50
60
70
Position [°2θ] (Copper (Cu))
Peak List
01-083-0577; Ca (C O3); Calcite
00-043-1001; Ca O; Lime, syn
04-007-5231; Ca (O H)2; Portlandite, syn

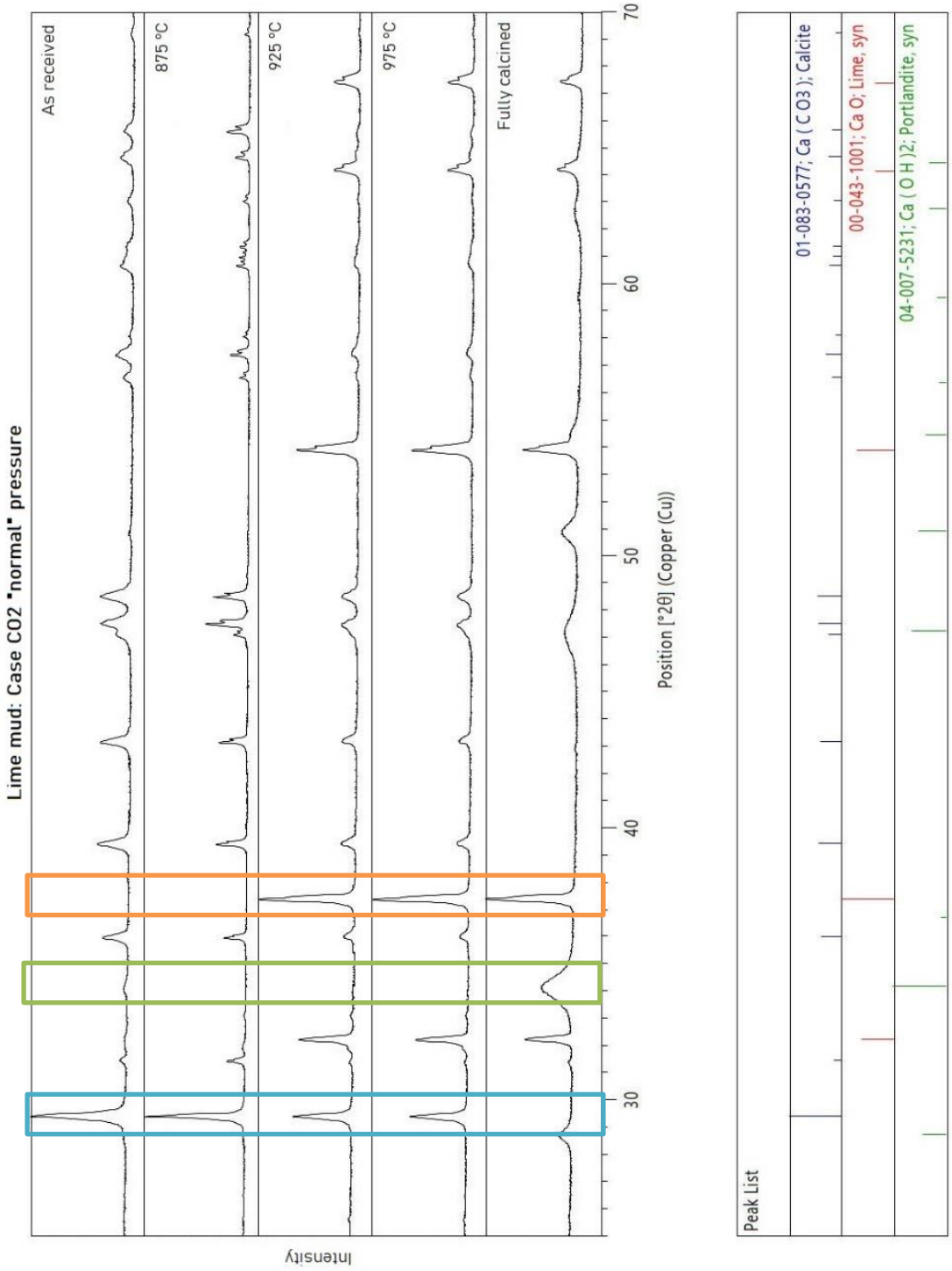
Lime mud: Case CO2 "normal" pressure
As received
875 °C
925 °C
975 °C
Fully calcined
Intensity
30
40
50
60
70
Position [°2θ] (Copper (Cu))
Peak List
01-083-0577; Ca (C O3); Calcite
00-043-1001; Ca O; Lime, syn
04-007-5231; Ca (O H)2; Portlandite, syn

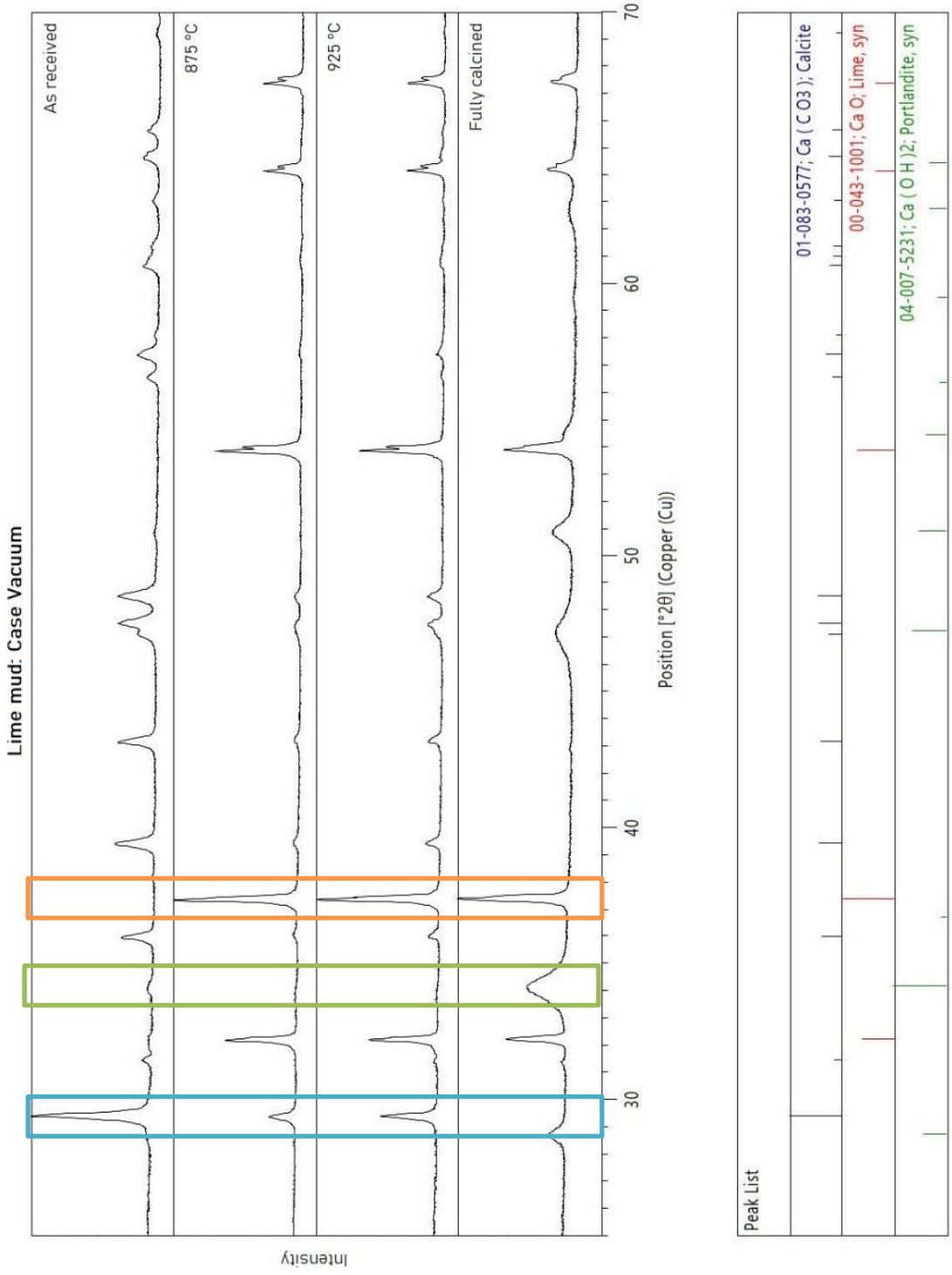
Lime mud: Case Vacuum
As received
875 °C
925 °C
Fully calcined
Intensity
30
40
50
60
70
Position [°2θ] (Copper (Cu))
Peak List
01-083-0577; Ca (C O3); Calcite
00-043-1001; Ca O; Lime, syn
04-007-5231; Ca (O H)2; Portlandite, syn

APPENDIX C: KILN OFF-GAS COMPOSITION GRAPHS

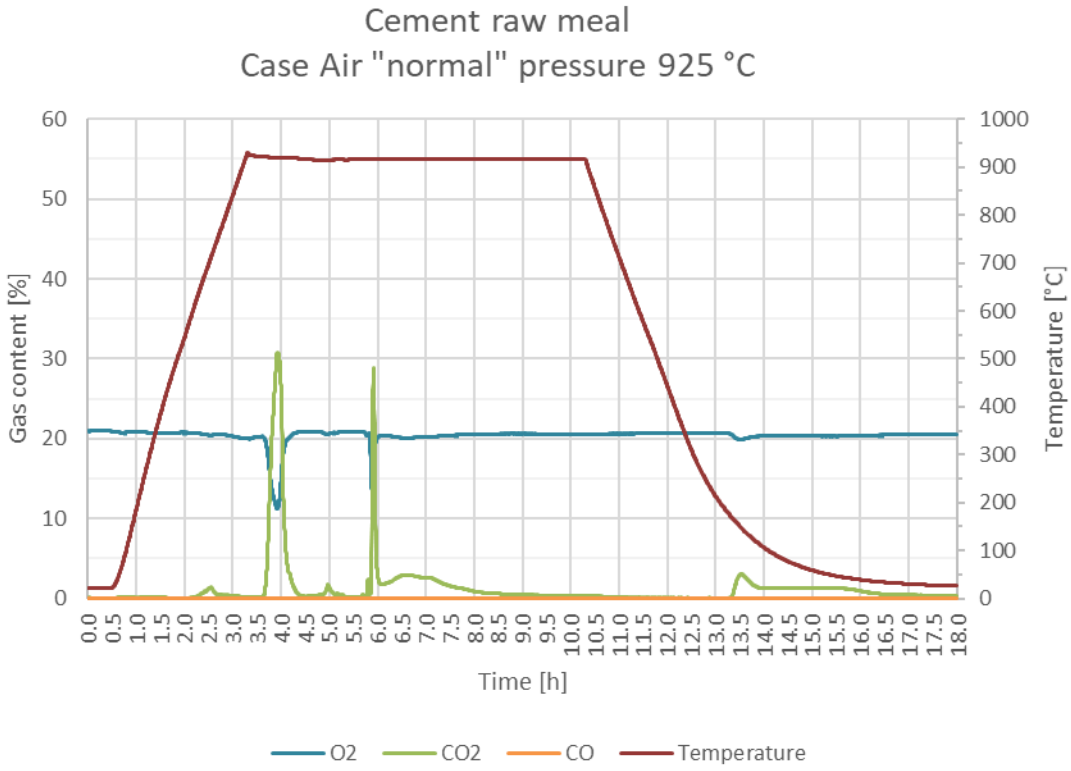

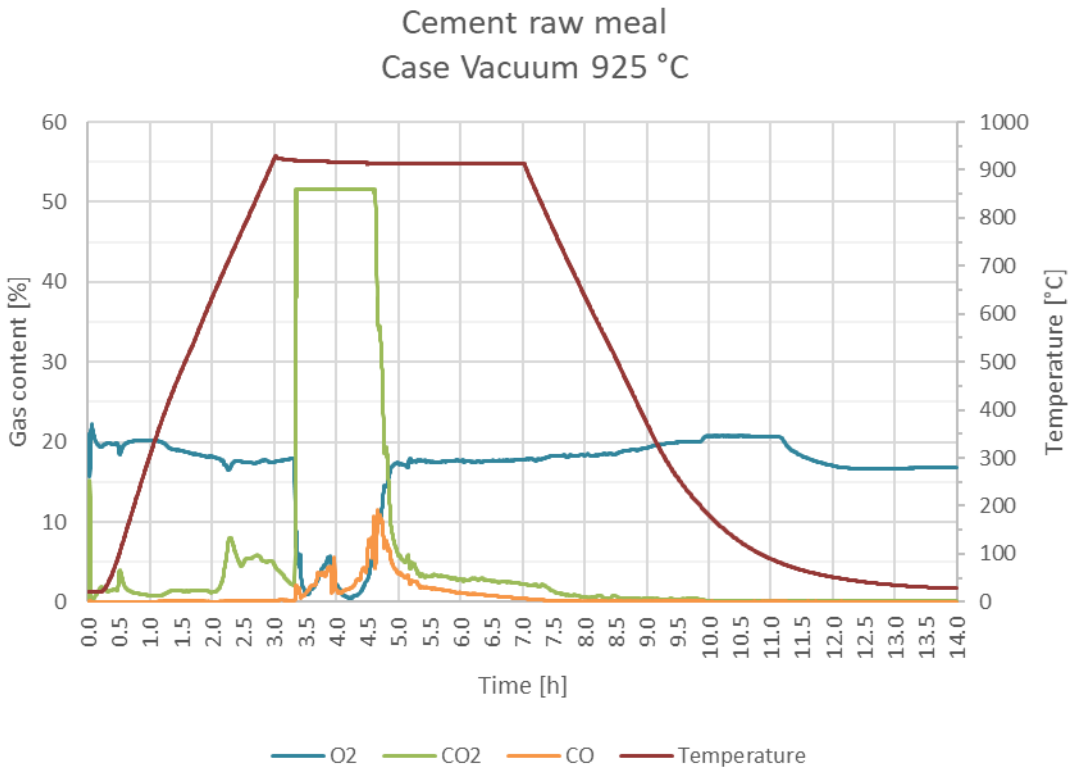

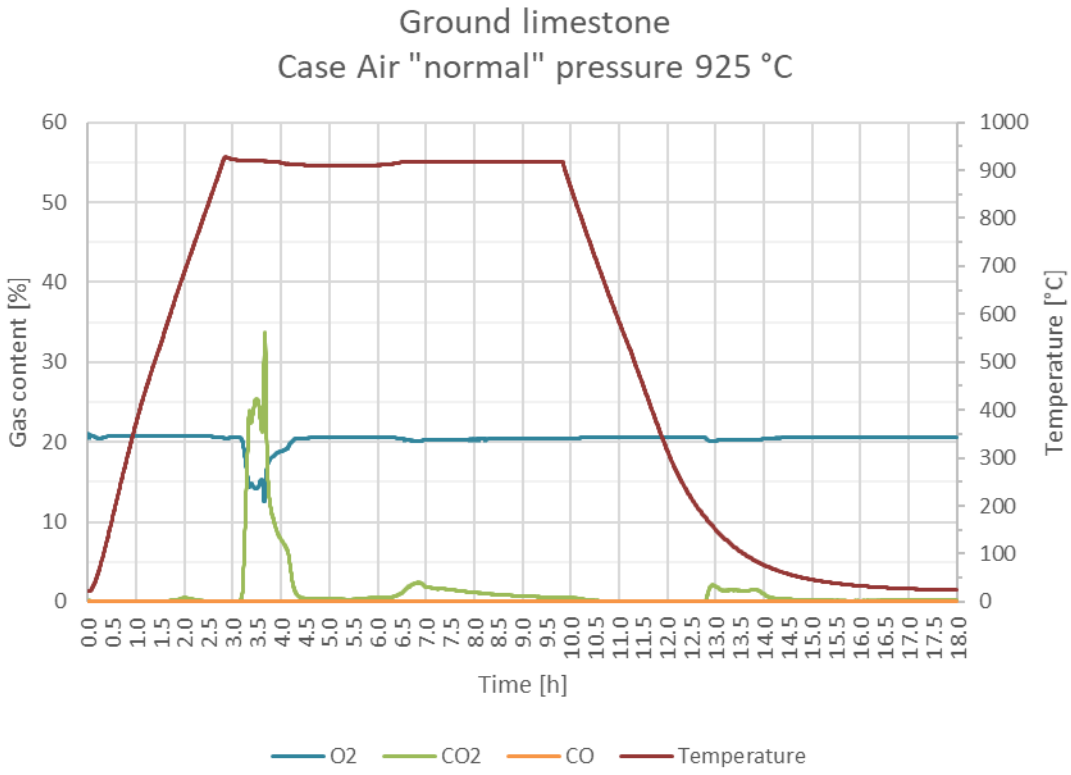

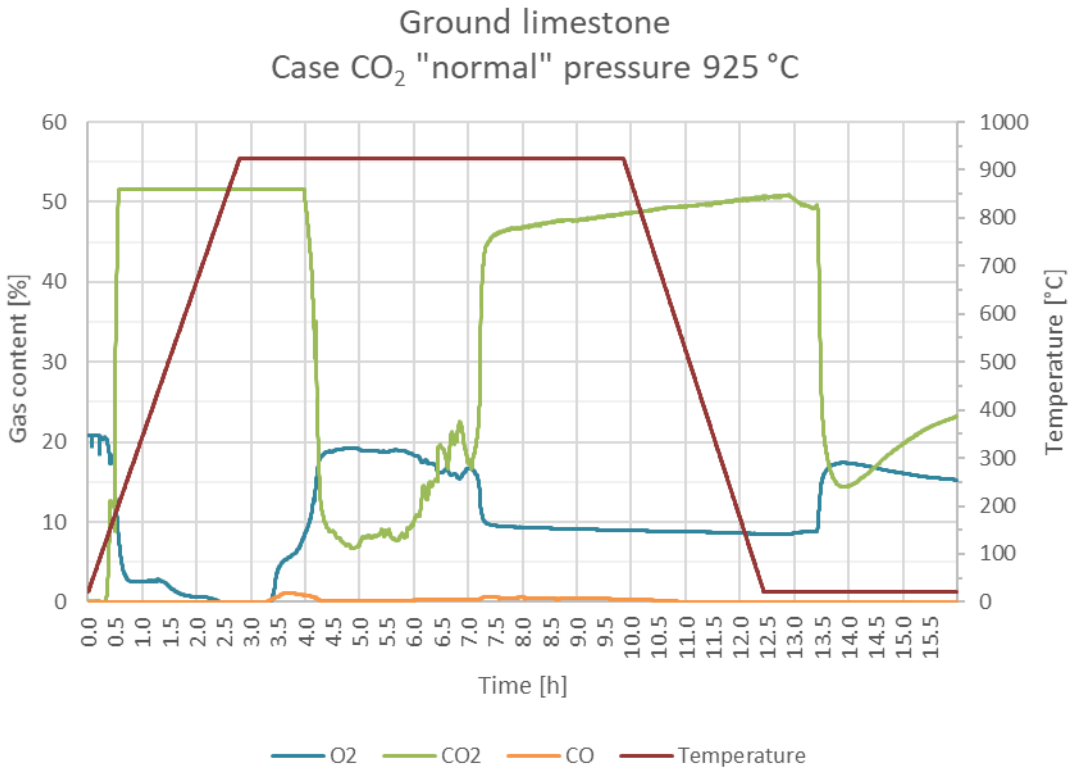

In case CO_2 “normal” pressure 925 °C of ground limestone (above) temperature was not measured with the multipoint thermocouple and no temperature data was available. Thus, temperature profile in the graph only imitates an actual temperature profile.

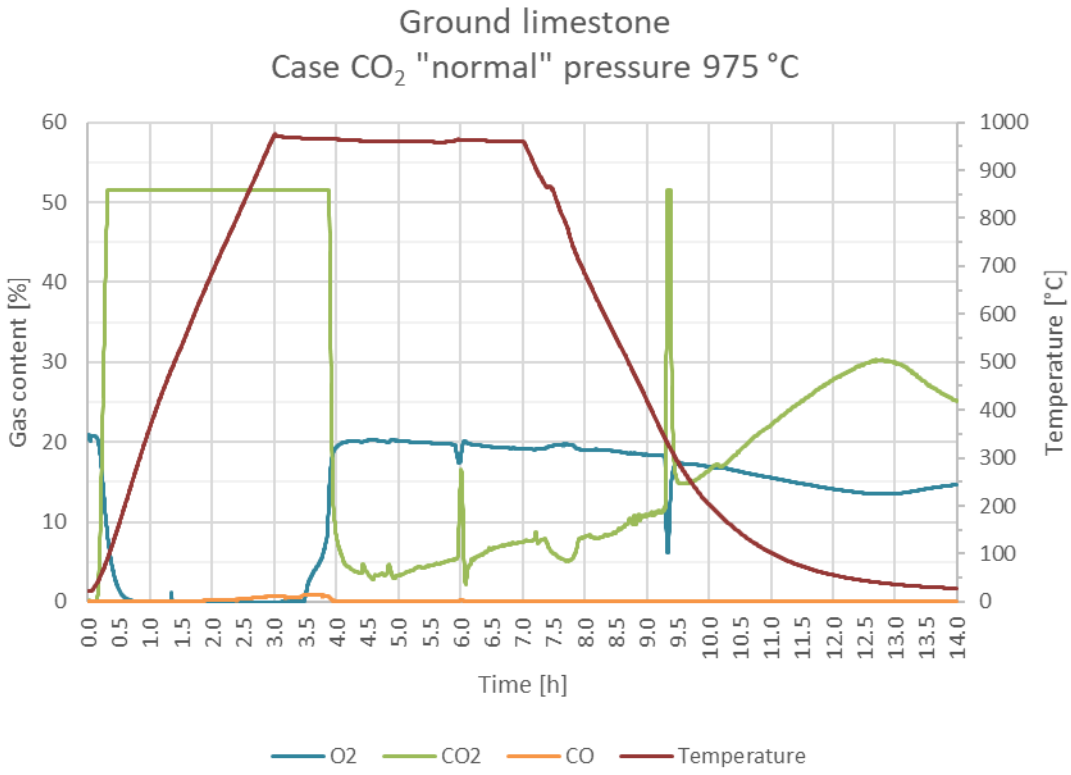
Ground limestone
Case CO_2 "normal" pressure 975 °C
Gas content [%]
Temperature [°C]
Time [h]
O2
CO2
CO
Temperature

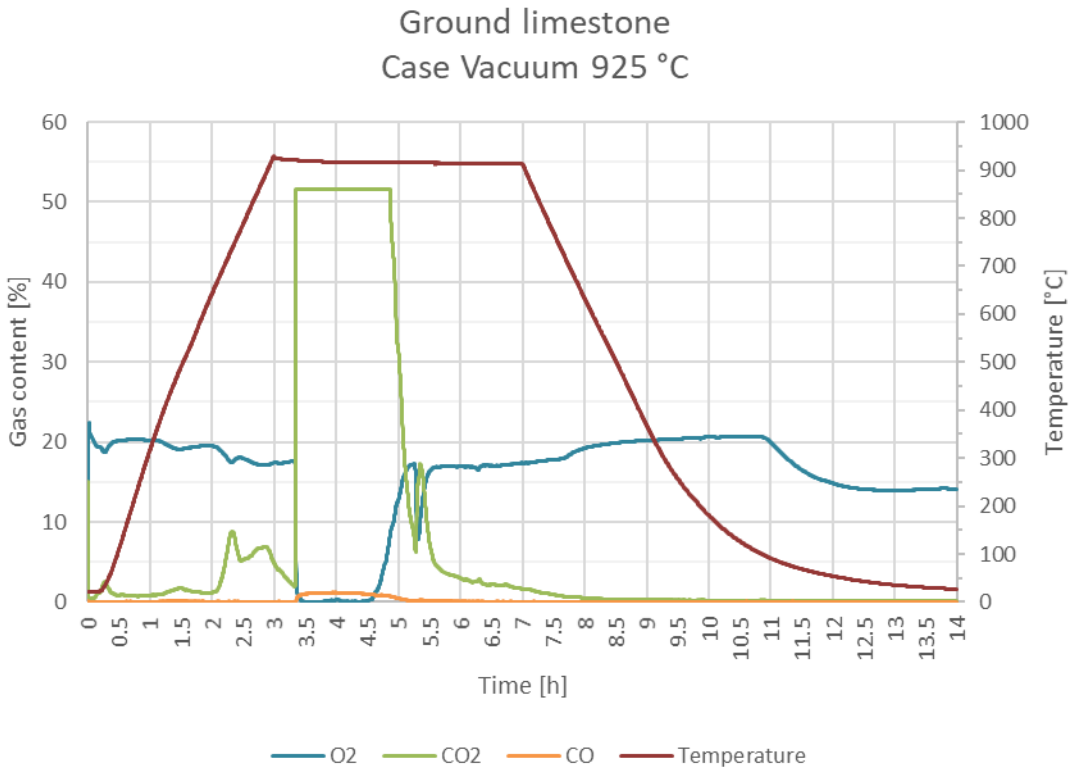
Ground limestone
Case Vacuum 925 °C
Gas content [%]
Temperature [°C]
Time [h]
O2
CO2
CO
Temperature

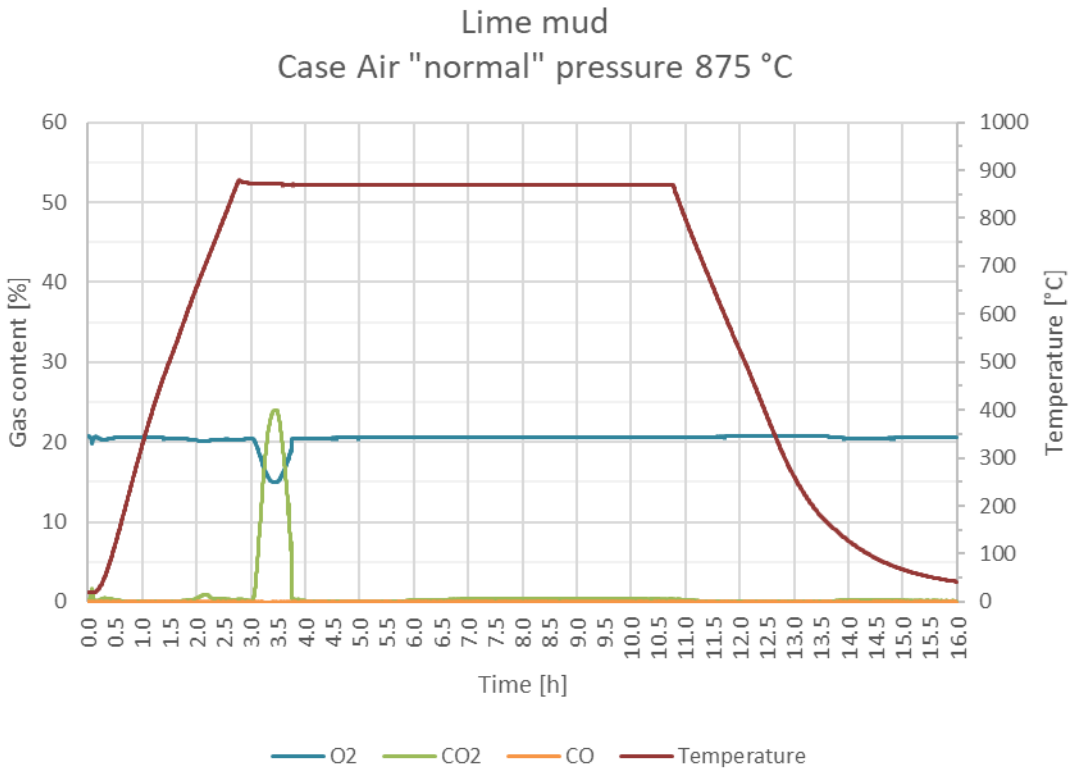
Lime mud
Case Air "normal" pressure 875 °C
Gas content [%]
Temperature [°C]
Time [h]
O2
CO2
CO
Temperature

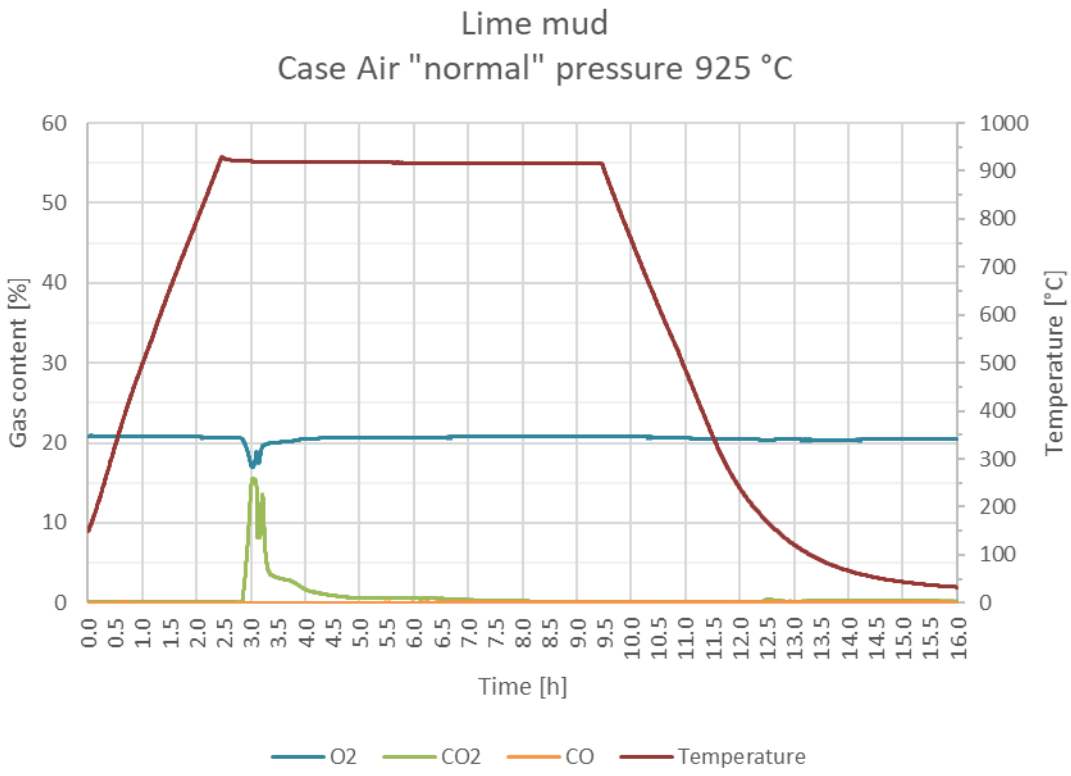
Lime mud
Case Air "normal" pressure 925 °C
Gas content [%]
Temperature [°C]
Time [h]
O2
CO2
CO
Temperature

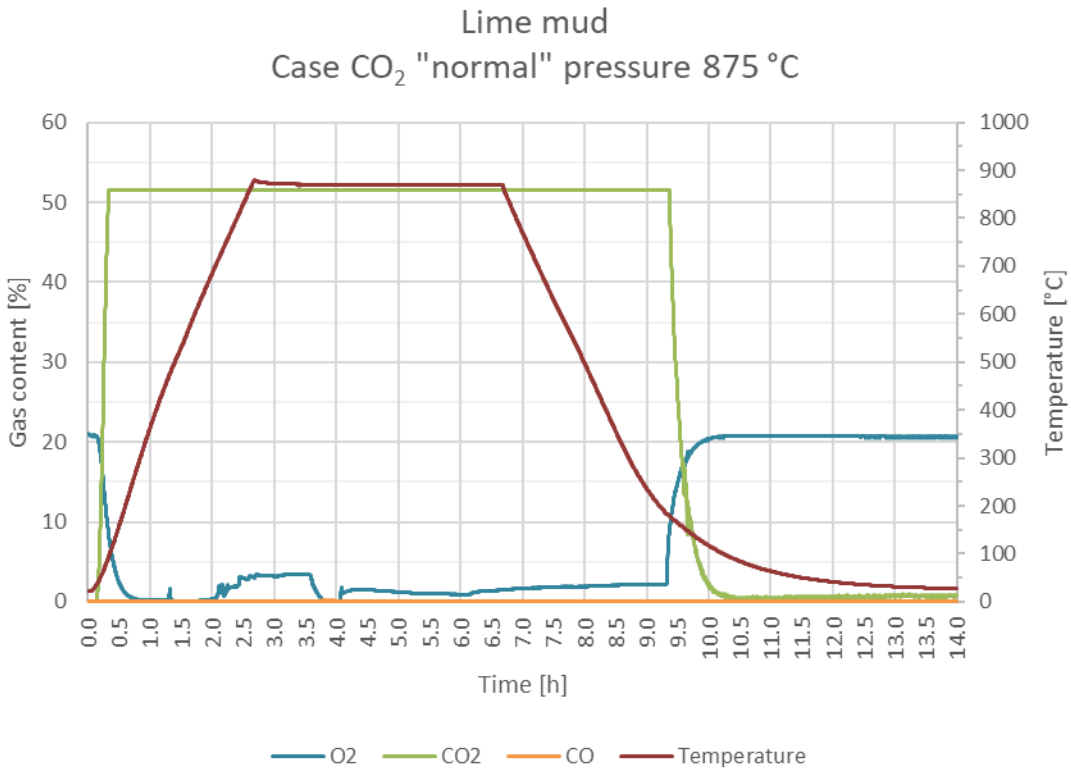
Lime mud
Case CO_2 "normal" pressure 875 °C
Gas content [%]
Temperature [°C]
Time [h]
O2
CO2
CO
Temperature

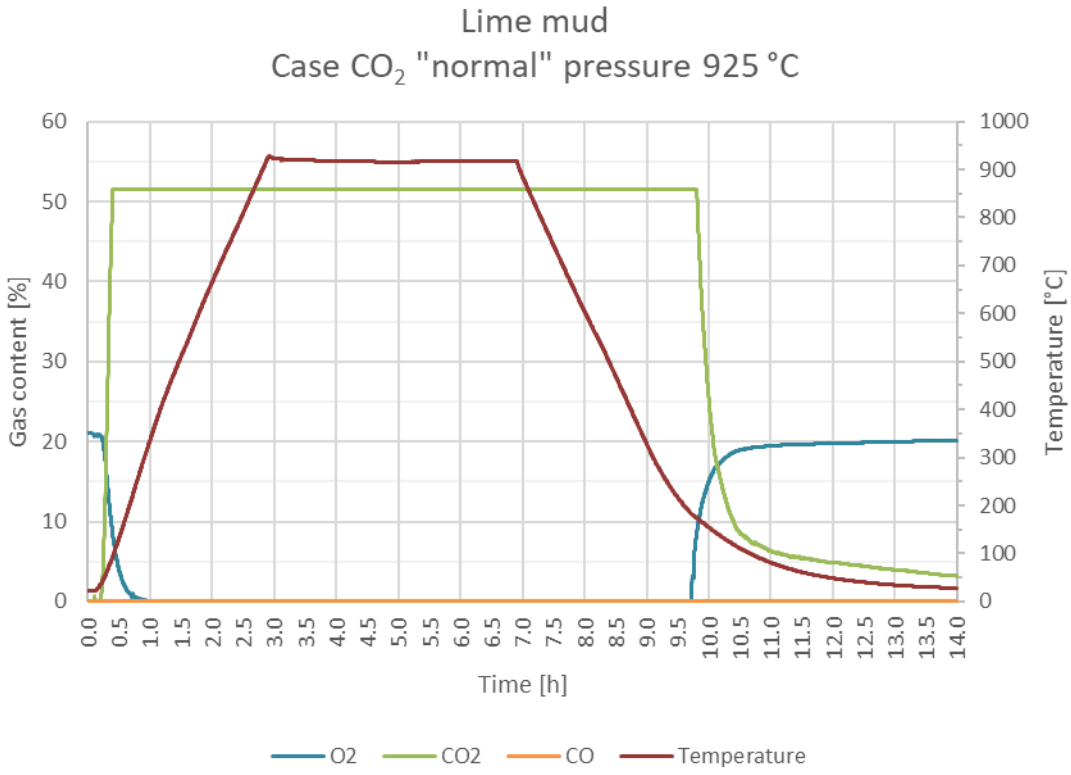
Lime mud
Case CO_2 "normal" pressure 925 °C
Gas content [%]
Temperature [°C]
Time [h]
O2
CO2
CO
Temperature

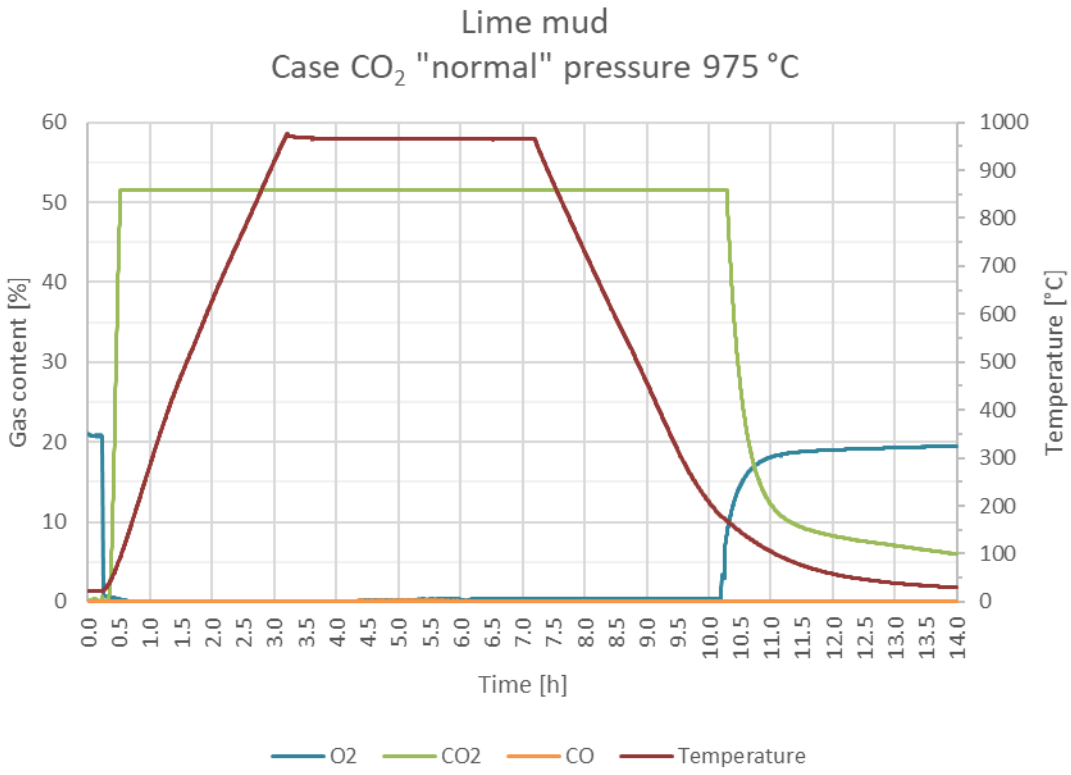
Lime mud
Case CO_2 "normal" pressure 975 °C
Gas content [%]
Temperature [°C]
Time [h]
O2
CO2
CO
Temperature

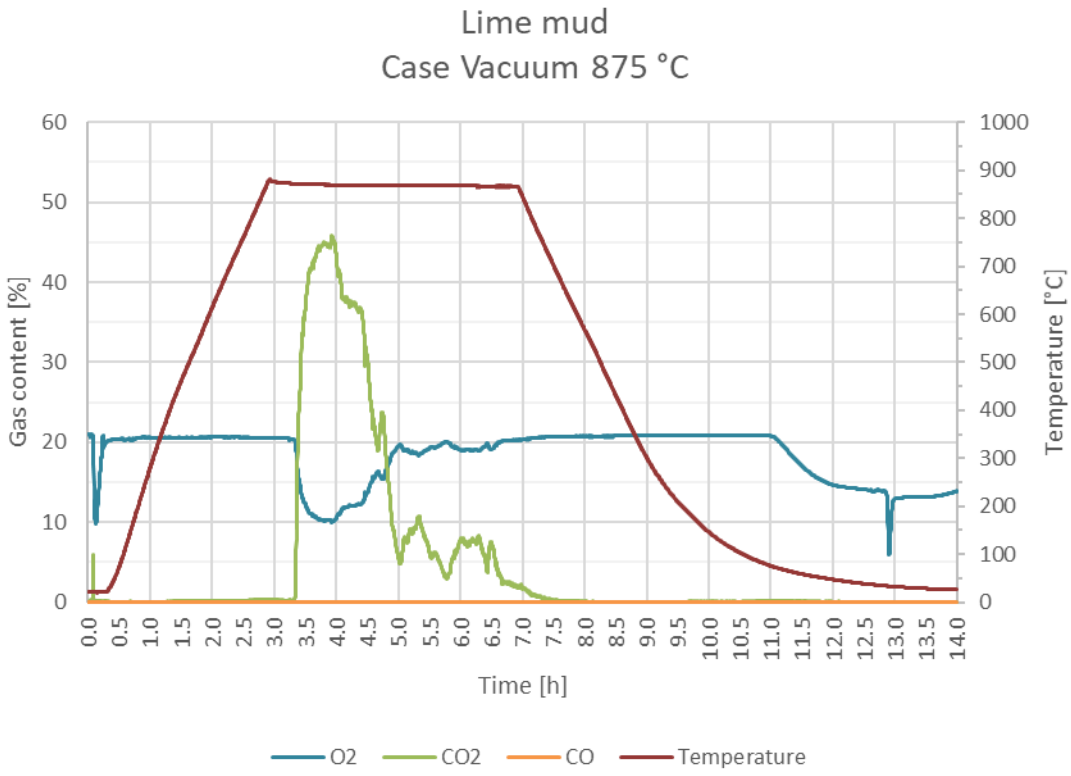
Lime mud
Case Vacuum 875 °C
Gas content [%]
Temperature [°C]
Time [h]
O2
CO2
CO
Temperature

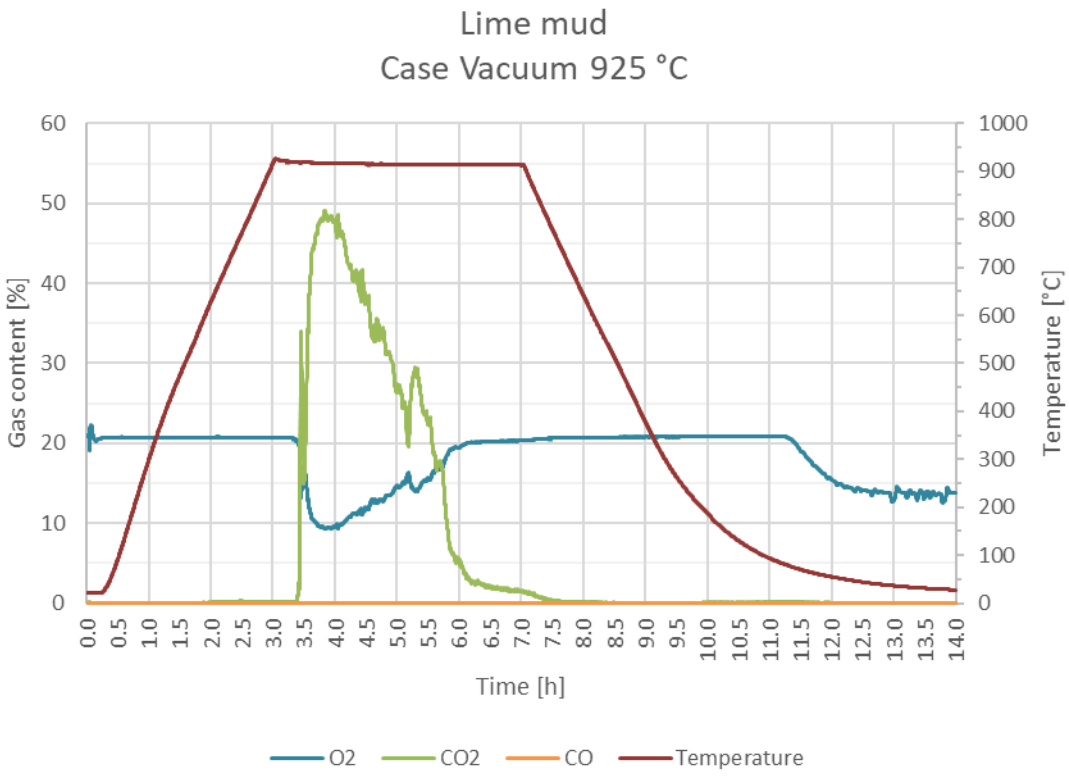
Lime mud
Case Vacuum 925 °C
Gas content [%]
Temperature [°C]
Time [h]
O2
CO2
CO
Temperature